This is an open access article published under an ACS AuthorChoice License, which permits copying and redistribution of the article or any adaptations for non-commercial purposes.

Journal of Medicinal Chemistry

Perspective

pubs.acs.org/jmc

Selective Inhibitors of Protein Methyltransferases

H. Ümit Kaniskan,[†] Kyle D. Konze,[†] and Jian Jin*[,†,‡,§]

[†]Department of Structural and Chemical Biology, [‡]Department of Oncological Sciences, [§]Department of Pharmacology and Systems Therapeutics, Icahn School of Medicine at Mount Sinai, 1425 Madison Avenue, New York, New York 10029, United States

ABSTRACT: Mounting evidence suggests that protein methyltransferases (PMTs), which catalyze methylation of histone and nonhistone proteins, play a crucial role in diverse biological processes and human diseases. In particular, PMTs have been recognized as major players in regulating gene expression and chromatin state. PMTs are divided into two categories: protein lysine methyltransferases (PKMTs) and protein arginine methyltransferases (PRMTs). There has been a steadily growing interest in these enzymes as potential therapeutic targets and therefore discovery of PMT inhibitors has also been pursued increasingly over the past decade. Here, we present a perspective on selective, small-molecule inhibitors of PMTs with an emphasis on their discovery, characterization, and applicability as chemical tools for deciphering the target PMTs' physiological functions and involvement in human diseases. We highlight the current state of PMT inhibitors and discuss future directions and opportunities for PMT inhibitor discovery.

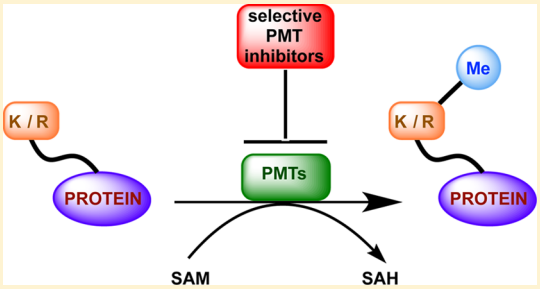

INTRODUCTION

Even though all nucleated cells contain the same genomic DNA, multicellular organisms have developed a machinery of differentiation that maintains unique biological functions of specific cell types, tissues, and organs. Growing evidence suggests that gene expression is a key component of cellular differentiation and is not only controlled by DNA sequence and transcription factors but also by epigenetic regulation.[1] Epigenetics is typically referred to as heritable changes in gene expression or phenotype without changes in DNA sequence.[2,3]

The human genome is encoded in DNA and tightly packed into 23 pairs of chromosomes that contain repeating nucleosome units. Each nucleosome consists of eight histone proteins (two copies of each of four core histones H2A, H2B, H3, and H4) and the DNA double helix that wraps around the histone octomer.[4,5] Nucleosomes are further condensed to form chromatin, which can reside in two main conformational states.[6] In the heterochromatin state, nucleosomes are tightly packed together, and gene transcription is mainly repressed. On the other hand, in the euchromatin state, nucleosomes are more loosely packed and accessible, leading to gene expression and transcription activation. Thus, epigenetic regulation of gene expression depends on the state of chromatin, which is mainly controlled by DNA methylation, noncoding RNAs, nucleosome remodeling histone variants, and post-translational modifications (PTMs) of histones.[7] Histones are small basic proteins with a flexible and charged N-terminus called histone tails, which are rich in arginine and lysine residues. PTMs of histones include, but are not limited to, methylation, acetylation, phosphorylation, sumoylation, ubiquitination, and glycosylation.[8] The histone code hypothesis[9,10] suggests that various PTMs of histones (often referred as histone marks) would promote interaction affinities for chromatin-associated proteins and may act in numerous combinations or successively on the same or different histone tails, affecting specific cellular outcomes. The proteins that are directly involved in PTMs of histones are divided into three categories: the enzymes that create these modifications (the writers), the proteins that recognize the modifications (the readers), and the enzymes that remove the modifications (the erasers).

As shown by mounting evidence, dysregulation of gene expression contributes to many human diseases including inflammation, brain disorders, metabolic diseases, and cancer, which can be caused not only by genetic mutations but also by epigenetic alterations.[2,11,12] Given the importance of epigenetic regulation in cell differentiation, proliferation, development, and maintaining cell identity, the epigenetic regulatory enzymes have been increasingly recognized as potential therapeutic targets. Hence, there is growing interest in the scientific community to discover and develop selective small-molecule inhibitors of these enzymes. Such inhibitors would be valuable chemical tools for investigating biological functions and disease associations of the target enzymes and for assessing the potential of these enzymes as therapeutic targets. Recently, small-molecule inhibitors of DNA methyltransferases (DNMTs) for the treatment of myelodysplastic syndrome[13] and histone deacetylases (HDACs) for the treatment of T-cell lymphoma[14,15] have been approved by the U.S. Food and Drug Administration (FDA) as the first epigenetic drugs, validating these epigenetic regulatory enzymes as drug targets. In this perspective, we focus on selective small-molecule inhibitors of protein methyltransferases (PMTs), also commonly referred as histone methyltransferases (HMTs). We describe past and

Received: August 12, 2014
Published: November 19, 2014

 © 2014 American Chemical Society dx.doi.org/10.1021/jm501234a | J. Med. Chem. 2015, 58, 1596−1629

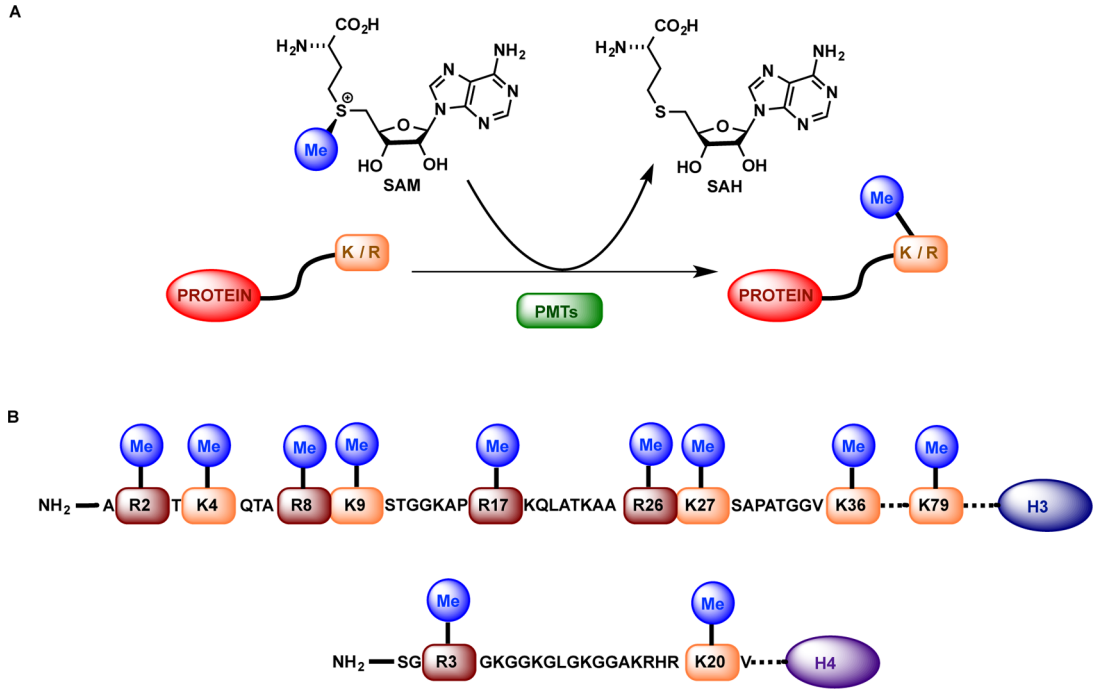

Figure 1. (A) Methylation of lysine (K) or arginine (R) residues of proteins by protein methyltransferases (PMTs). (B) Location of known methylation sites of histone 3 (H3) and histone 4 (H4). SAM, *S*-5′-adenosyl-L-methionine; SAH, *S*-5′-adenosyl-L-homocysteine.

Scheme 1. Methylation States of Lysine and Arginine Residues

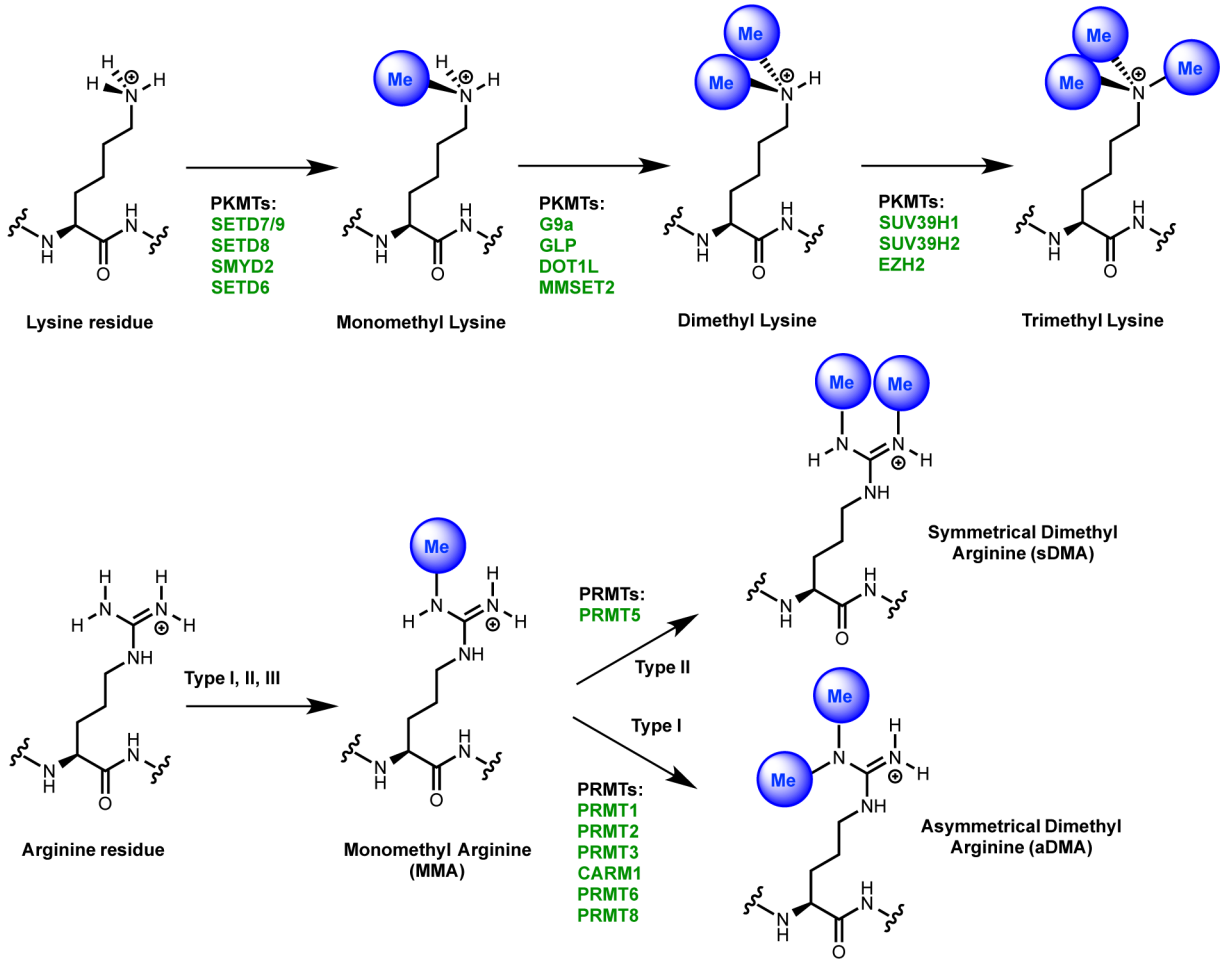

dx.doi.org/10.1021/jm501234a | J. Med. Chem. 2015, 58, 1596−1629

Table 1. Official and Alternative Gene Names[a]

PKMT (name used)	Official Name	Also Known As
SUV39H1	suppressor of variegation 3-9 homolog 1	MG44; KMT1A; SUV39H; H3-K9-HMTase 1
SUV39H2	suppressor of variegation 3-9 homolog 2	KMT1B
G9a	euchromatic histone-lysine N-methyltransferase 2	EHMT2; BAT8; GAT8; NG36; KMT1C; C6orf30
GLP	euchromatic histone-lysine N-methyltransferase 1	EHMT1; GLP1; KMT1D; FP13812; EUHMTASE1; Eu-HMTase1; bA188C12.1; RP11-188C12.1
SETDB1	SET domain, bifurcated 1	ESET; KG1T; KMT1E; TDRD21; H3-K9-HMTase4
SETDB2	SET domain, bifurcated 2	CLLD8; CLLL8; KMT1F; C13orf4
PRDM2	PR domain containing 2, with ZNF domain	RIZ; KMT8; RIZ1; RIZ2; MTB-ZF; HUMHOXY1
PRDM3	MDS1 and EVI1 complex locus	EVI1; MDS1; MECOM; MDS1-EVI1; AML1-EVI-1
PRDM16	PR domain containing 16	MEL1; LVNC8; PFM13; CMD1LL
SETD7	SET domain containing (lysine methyltransferase) 7	KMT7; SET7; SET9; SET7/9
SETD8	SET domain containing (lysine methyltransferase) 8	SET8; KMT5A; SET07; PR-Set7
EZH2	enhancer of zeste 2 polycomb repressive complex 2 subunit	WVS; ENX1; EZH1; KMT6; WVS2; ENX-1; EZH2b; KMT6A
EZH1	enhancer of zeste 1 polycomb repressive complex 2 subunit	KMT6B
SMYD2	SET and MYND domain containing 2	KMT3C; HSKM-B; ZMYND14
SMYD3	SET and MYND domain containing 3	KMT3E; ZMYND1; ZNFN3A1; bA74P14.1
MMSET	Wolf-Hirschhorn syndrome candidate 1	WHSC1; WHS; NSD2; TRX5; REIIBP
WHSC1L1	Wolf-Hirschhorn syndrome candidate 1-like 1	NSD3; pp14328
MLL1	lysine (K)-specific methyltransferase 2A	KMT2A; HRX; MLL; TRX1; ALL-1; CXXC7; HTRX1; MLL1A; WDSTS; MLL/GAS7; TET1-MLL
SETMAR	SET domain and mariner transposase fusion gene	Mar1; HsMar1; METNASE
SUV420H1	suppressor of variegation 4-20 homolog 1 (Drosophila)	CGI85; KMT5B; CGI-85
SUV420H2	suppressor of variegation 4-20 homolog 2 (Drosophila)	KMT5C
NSD1	nuclear receptor binding SET domain protein 1	STO; KMT3B; SOTOS; ARA267; SOTOS1
DOT1L	DOT1-like histone H3K79 methyltransferase	DOT1; KMT4
PRMT1	protein arginine methyltransferase 1	ANM1; HCP1; IR1B4; HRMT1L2
PRMT2	protein arginine methyltransferase 2	HRMT1L1
PRMT3	protein arginine methyltransferase 3	HRMT1L3
CARM1	coactivator-associated arginine methyltransferase 1	PRMT4
PRMT5	protein arginine methyltransferase 5	JBP1; SKB1; IBP72; SKB1Hs; HRMT1L5
PRMT6	protein arginine methyltransferase 6	HRMT1L6
PRMT7	protein arginine methyltransferase 7	-
PRMT8	protein arginine methyltransferase 8	HRMT1L3; HRMT1L4
PRMT9	protein arginine methyltransferase 9	PRMT10
ASH1L	ash1 (absent, small, or homeotic)-like (Drosophila)	ASH1; KMT2H; ASH1L1

[a]Based on HGNC (HUGO Gene Nomenclature Committee) database (http://www.ncbi.nlm.nih.gov/gene/). Red indicates the official symbol for the gene.

present advances on discovering these inhibitors and discuss future directions for PMT inhibitor discovery.[11,12,16−25]

PROTEIN METHYLATION BY PMTS

Histone methylation by PMTs is one of the most studied post-translational modifications since it is implicated in heterochromatin formation and maintenance, transcriptional regulation, DNA repair, X-chromosome inactivation, and RNA maturation.[26] In addition to histones, PMTs have been shown to target many nonhistone proteins.[27,28] PMTs (the methyl writers) catalyze the transfer of the methyl group from the cofactor *S*-5′-adenosyl-L-methionine (SAM) to either lysine or arginine residues of proteins (Figure 1A). Therefore, PMTs are further divided in two categories: protein lysine methyltransferases (PKMTs) and protein arginine methyltransferases (PRMTs). The known methylation sites for histone 3 (H3) and histone 4 (H4) tails are shown in Figure 1B. Lysine residues can be mono-, di-, and/or trimethylated by PKMTs, whereas arginine guanidinium groups can be mono and/or dimethylated.[26] Dimethylation of terminal guanidino nitrogens followed by monomethylation of arginine (MMA) could be either asymmetrical on the same nitrogen (aDMA) or symmetrical on two different guanidino nitrogens (sDMA) (Scheme 1). Methylation of lysine or arginine residues does not change the charge of these residues, but it alters the bulkiness and hydrophobicity of the protein, in turn affecting protein−protein interactions. In the case of histone lysine and arginine methylation, each methylation mark on different residues or on the same residue establishes a specific signal that is recognized by reader proteins.[11]

Both PKMTs and PRMTs have a cofactor binding site and a substrate binding site. Upon activation, these enzymes recruit lysine or arginine residues of substrate proteins to the substrate binding pocket and SAM to the cofactor binding site.[6] These two binding sites are linked by a narrow hydrophobic channel to allow the substrate and cofactor to come into close proximity to transfer the methyl group from the cofactor SAM via a S_N2 transition state to a lysine or arginine residue, releasing the

dx.doi.org/10.1021/jm501234a | J. Med. Chem. 2015, 58, 1596−1629

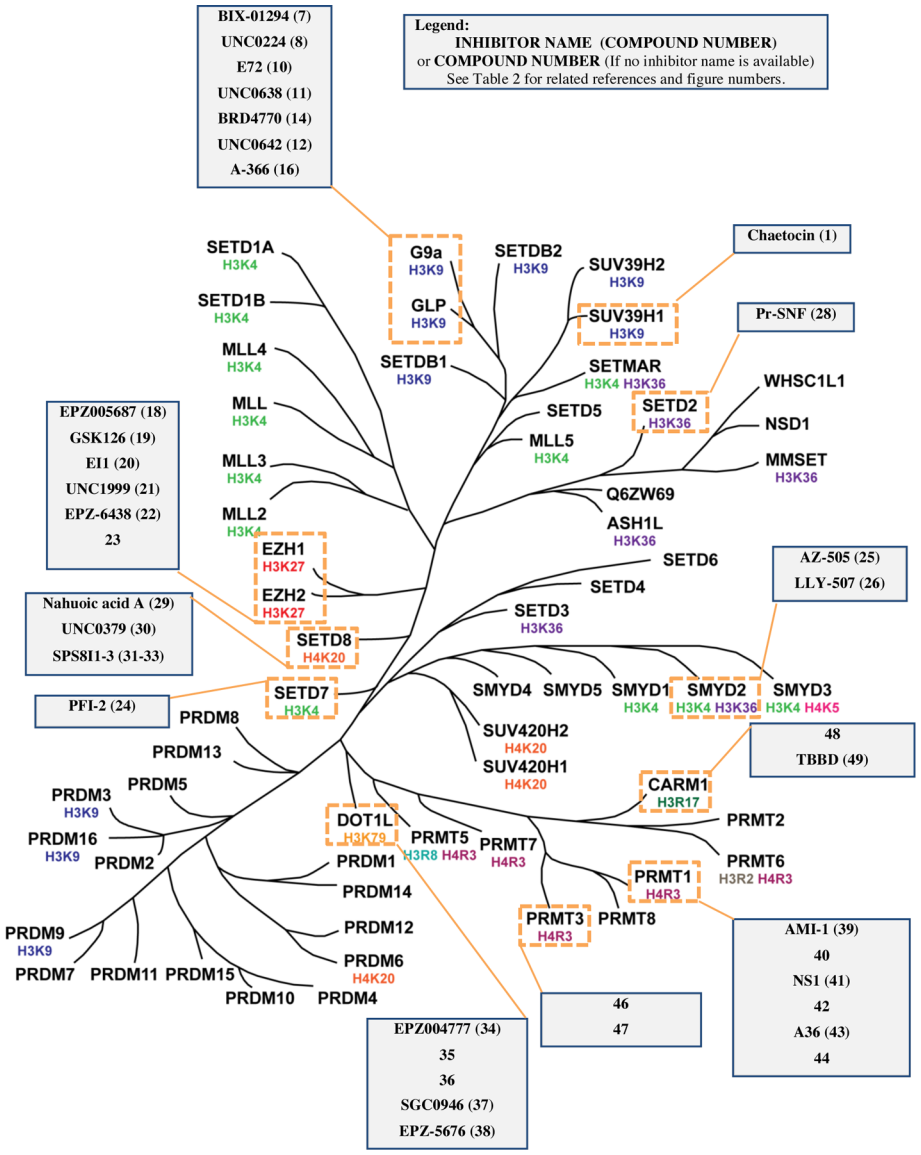

Figure 2. Phylogenetic tree of PMTs and known small-molecule inhibitors of PMTs.

cofactor product *S*-5′-adenosyl-L-homocysteine (SAH). This process can be repeated to achieve higher level of methylations of lysine or arginine residues.

■ PROTEIN LYSINE METHYLTRANSFERASES

All of the known PKMTs, with the exception of DOT1L, contain a conserved, approximately 130 amino acid long SET domain.[29−31] The SET domain was originally identified in three *Drosophila* genes: *Su(var.)3-9* (the suppressor of position-effect variegation 3-9), *En(zeste)* (an enhancer of the eye color mutant zeste), and *Trithorax* (the homeotic gene regulator).[29] Therefore, PKMTs can be divided into two classes: SET domain-containing PKMTs and non-SET domain PKMTs (DOT1L is the only member of this class). The SET domain folds into several small β-sheets that surround a knot-like structure, which brings together the two highly conserved motifs of the SET domain and forms an active site next to the SAM binding pocket.[32] SET domain-containing PKMTs are categorized according to similarities in the sequence around the SET domain and collected under five major families: SUV, SET1, SET2, EZ, and RIZ.[30,33] More recently, an alternative classification and nomenclature has been suggested[34] to give more generic names to histone modifying enzymes according to the type of their enzymatic activity and the type of residue(s) they modify, as these enzymes have also been shown to target nonhistone proteins. Therefore, PKMTs were divided into eight major groups: KMT1 (lysine methyltransferases 1) to KMT8, including SET domain-containing and non-SET enzymes (e.g., DOT1L is the only member of the KMT4 subfamily). We summarize all of the official gene names and alternative names that have been used for the enzymes discussed in this perspective in Table 1. It is worth noting that the SET domain is not limited to PKMTs. It is also found in a large number of other eukaryotic proteins and in several bacterial proteins.[35]

Histone lysine methylation catalyzed by PKMTs has been recognized as a major mechanism in regulating gene expression and transcription.[6,36] Depending on the methylation site and methylation state (e.g., mono-, di-, or trimethylation), histone lysine methylation can lead to either transcription activation or repression. For example, H3K4 (histone H3 lysine 4), H3K36, and H3K79 methylation are generally associated with tran-

dx.doi.org/10.1021/jm501234a | J. Med. Chem. 2015, 58, 1596−1629

Table 2. PMTs, Their Substrates,[a] Known Selective Small-Molecule Inhibitors, and Function(s) or Link(s) to Disease

Main Target	PMT	Non-histone Site(s)	Inhibitor(s) [ref]	Function(s) or Links to Disease(s) [ref]
H3K9	SUV39H1	-	**Chaetocin (1)** [58-64]	Genome stability during mammalian development [51]; SUV39H1-HP1 complex also plays a part in repression of euchromatic genes by retinoblastoma protein (Rb) [54]; SUV39H1 expression upregulated in glioma cell lines [57].
	G9a	p53K373	**BIX-01294 (7)** [85,86]; **UNC0224 (8)** [87]; **E72 (10)** [89]; **UNC0638 (11)** [91]; **BRD4770 (14)** [97]; **UNC0642 (12)** [95]; **A-366 (16)** [98]	Overexpressed in different cancers [45,46, 68-70]; its knockdown inhibits cancer cell growth of prostate cancer [45], leukemia [70] and lung cancer [46]; Involvement in maintenance of HIV-1 latency [47], cocaine addiction [48,73] mental retardation [74].
	GLP	p53K373		
H3K27	EZH2	-	**EPZ005687 (18)** [130]; **GSK126 (19)** [133]; **EI1 (20)** [137]; **UNC1999 (21)** [138]; **EPZ-6438 (22)** [139]; **23** [144]	Overexpression of EZH2 is associated with several human cancers [123-125], such as breast [126], prostate [127], lymphoma [128], leukemia [129].
	EZH1			
H3K4	SETD7	p53K372, p65 subunit of NF-κB, DNMT1	**PFI-2 (24)** [158]	Linked with hyperglycemia [56]; potential target for the treatment of diabetes [157].
H3K36	SMYD2	p53K370, Rb	**AZ-505 (25)** [168]; **LLY-507 (26)** [169]	Highly expressed in pediatric acute lymphoblastic leukemia [166]; overexpression of SMYD2 connected to tumor cell proliferation and results in malignant esophageal squamous cell carcinoma [167].
	SETD2	-	**Pr-SNF (28)** [175]	Associated with p53 dependent gene regulation, transcription elongation and intron-exon splicing [171-173]; tumor suppressor role of SETD2 in human breast cancer [171]; linked to leukemia development [174]; associated with hemispheric high-grade gliomas (HGGs) in older children and young adults [175].
H4K20	SETD8	p53K372, p53K382	**Nahuoic Acid (29)** [180]; **UNC0379 (30)** [181, 182] **SPS8I1-3 (31-33)** [183]	Implicated in regulating such as DNA damage response, DNA replication, and mitotic condensation
H3K79	DOT1L	-	**EPZ004777 (34)** [197]; **35** [201]; **36** [202]; **SGC0946 (37)** [199]; **EPZ-5676 (38)** [203]	DOT1L interact with MLL fusion proteins and directly involved in AML [191-195]; linked with transcriptional regulation, DNA repair, embryonic development, cell cycle regulation, hematopoiesis and cardiac function [188-190].
H4R3	PRMT1	NPL3p, MRE11, 53BP1, ASH2L	**AMI-1 (39)** [243]; **40** [249]; **NS1 (41)** [250]; **42** [251]; **A36 (43)** [253]; **44** [254]	Overexpression & aberrant splicing of PRMT1 associated with diseases such as breast, prostate, lung, colon, bladder cancer and leukemia [224-235].
	PRMT3	rpS2, PABPN1	**46**; **47** [271, 272]	Dimethylation of rpS2 results in stabilization of rpS2 and influences ribosomal biosynthesis [256-259]; interacts with tumor suppressor DAL-1 [265]; highly expressed in patients with atherosclerosis [269].
H3R17	CARM1	CBP/p300, PABP, HuR, HuD, CA150, SAP49, SmB, U1C	**48** [285-287]; **TBBD (49)** [290]	CARM1 levels elevated in castration-resistant prostate cancer [283, 284] and in aggressive breast tumors [277]

[a]Only selected nonhistone targets and function(s) and link(s) to diseases were included, not a comprehensive list.

scription activation. On the other hand, H3K9 di- and trimethylation (H3K9me2 and H3K9me3) and H3K27 trimethylation (H3K27me3) are typically associated with repression.[6,37−39] In the following section, we organize inhibitors of PKMTs according to their histone methylation site(s) (Figure 2 and Table 2).

■ INHIBITORS OF PKMTS

Inhibitors of H3K9 Methyltransferases. Methylation of H3K9 in humans is controlled by PKMTs: SUV39H1 (suppressor of variegation 3-9 homologue 1), SUV39H2, G9a (euchromatic histone-lysine *N*-methyltransferase 2 (EHMT2)), GLP (G9a-like protein 1, also known as EHMT1), SETDB1 (SET domain, bifurcated 1), SETDB2, PRDM2 (PR domain containing 2, with ZNF domain also referred as RIZ1), PRDM3, and PRDM16.[40] H3K9 dimethylation (H3K9me2) and trimethylation (H3K9me3) are repressive marks recognized by heterochromatin protein 1 (HP1), which is directly involved in the formation of transcriptionally silent chromatin.[41] Mounting evidence suggests that H3K9 methyltransferases are implicated in various human diseases.[42−48] To date, selective inhibitors of SUV39H1, G9a, and GLP have been reported. In the following section, we review the discovery and biological characterization of these inhibitors.

dx.doi.org/10.1021/jm501234a | J. Med. Chem. 2015, 58, 1596−1629

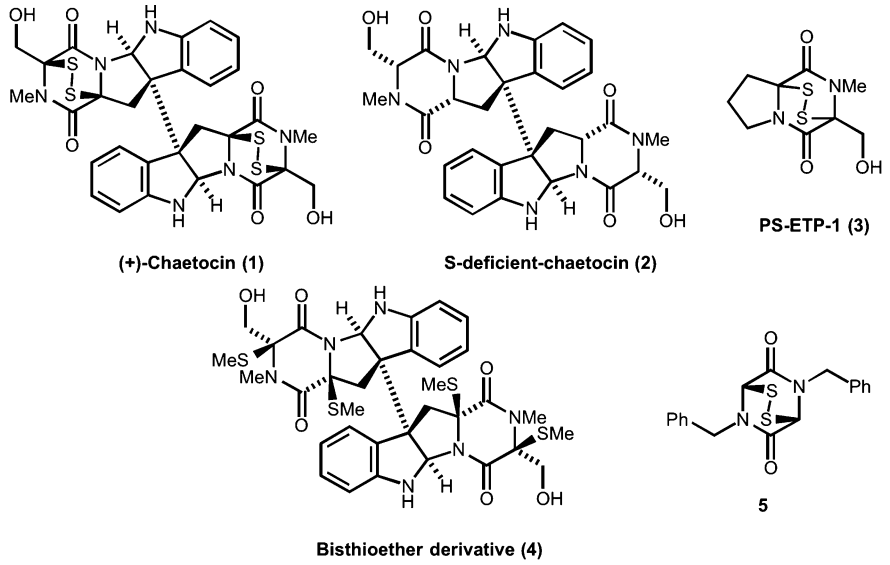

Figure 3. Structures of (+)-chaetocin and related ETP compounds.

SUV39H1 is the first identified histone lysine methyltransferase and is the human orthologue of *Drosophila* Su(var.)3-9 and *Schizosaccharomyces pombe* Clr4.[49] In this enzyme, the β-sheets of the SET domain are packed together with pre-SET and post-SET domains.[50] The latter contains three conserved cysteine residues, which are essential for the enzymatic activity. It has been clearly shown in mouse models that genome stability during mammalian development is directly related to SUV39H1/2-dependent H3K9 methylation at pericentric heterochromatin.[51] It has also been suggested that SUV39H1 and SUV39H2 play a role as tumor suppressors by maintaining H3K9 methylation at pericentric heterochromatin.[52−54] Furthermore, it has been reported that increased metastatic potential of tumor cells is linked to reduced heterochromatic accumulation of HP1α.[55] Besides heterochromatin silencing, the SUV39H1−HP1 complex plays a part in repression of euchromatic genes by retinoblastoma protein (Rb).[54] It has also been shown that the active transcriptional state of *NFκB-p65* gene is associated with reduced H3K9 methylation, in part mediated by SUV39H1.[56] Furthermore, in a recent study, SUV39H1 and SETDB1 expression was upregulated in glioma cell lines.[57]

The field of selective PKMT inhibitors was commenced by the report of the fungal mycotoxin chaetocin (**1**) (Figure 3) as the first selective inhibitor of *Drosophila* Su(var.)3-9 histone methyltransferase in 2005.[58] However, it is still a controversial subject as to whether chaetocin is a truly selective inhibitor (see below). Greiner et al. screened a library of 2976 compounds in a standard radioactive filter-binding assay and found chaetocin, which is a member in an epidithiodiketopiperazine (ETP) family of alkaloids, as the most potent inhibitor with an IC_{50} of 0.6 μM.[58] Chaetocin was characterized as a SAM-competitive inhibitor. Furthermore, inhibition assays were performed in the presence of increasing concentrations of chemical reductant dithiothreitol (DTT) to reduce the disulfide bond of chaetocin. Under these assay conditions, it was found that the inhibition was maintained and the inhibitory activity was not dependent on the disulfide functionality. It terms of selectivity, chaetocin inhibited the human SUV39H1 (IC_{50} = 0.8 μM), mouse G9a (IC_{50} = 2.5 μM), and *Neurospora crassa* DIM5 (IC_{50} = 3.0 μM), but it was less potent for *Drosophila* E(z)-complex (recombinant protein, IC_{50} = > 90 μM), SETD8, and SETD7 (bacterially expressed proteins, IC_{50} = >180 μM). Like other members of ETPs, chaetocin shows cytotoxicity depending upon initial cell density. The toxicity of other known ETPs was due to formation of mixed thiols with cellular protein.[59] Greiner et al. suggested that the toxicity of chaetocin was not caused by the inhibition of Su(var.)3-9 since the disulfide bond in chaetocin was not involved in inhibition. In addition, chaetocin reduced H3K9me2 and H3K9me3 levels in SL-2 *Drosophila* tissue culture cells at a low concentration (0.5 μM), but it did not reduce H3K4, H3K27, H3K36, and H3K79 methylation levels in these cells. However, the possibility of the *Drosophila* orthologue of mammalian G9a being responsible for the reduced H3K9me2 levels was not ruled out.

Iwasa et al. published the first total synthesis of natural (+)-chaetocin (**1**) (Figure 3) and its enantiomer and reported that both enantiomers inhibited G9a (IC_{50} = 2.5 and 1.7 μM, respectively) in 2010.[60] Interestingly, the sulfur-deficient analogue of chaetocin, **2** (Figure 3), and its enantiomer were inactive against G9a (IC_{50} > 50 μM). Thus, it was concluded that the disulfide bridge of chaetocin was crucial for the inhibitory activity and that G9a was not sensitive to absolute stereochemistry of chaetocin. More recently, Fujishiro et al. published their structure−activity relationship (SAR) studies of chaetocin[61] and reported that simple derivatives such as PS-ETP-1 (**3**) (Figure 3) were significantly less toxic but effectively inhibited G9a (IC_{50} = 5.2 μM). These results suggest that the dimeric ETP structure is not necessary for G9a inhibition.

In 2013, Cherblanc et al.[62] reported that chaetocin inhibits Su(var.)3-9 in a time-dependent and nonspecific manner via chemical modification of the enzyme by the disulfide group of chaetocin, differing from the published findings and conclusions by Greiner et al. Thus, it has been suggested that chaetocin or related natural products could not be used as selective chemical probes of PKMT function. Consistent with the results reported by Iwasa et al., Cherblanc et al. found that compound **4** (Figure 3), which does not have the bisulfide bridge, was inactive and that structurally simple ETP compound **5** (Figure 3) had an inhibitory activity with an IC_{50} of 3.2 μM. Interestingly, in their mechanism of action (MOA) studies, chaetocin was not competitive with SAM. Therefore, it was concluded that any

dx.doi.org/10.1021/jm501234a | J. Med. Chem. 2015, 58, 1596−1629

specific interaction of chaetocin with Su(var.)3-9 was due to the increased sensitivity of this enzyme to thiol-reactive compounds. These conclusions and suggestions were disputed by Greiner et al.,[63] emphasizing the 30-fold lower potency of simple ETP compound **5** as well as the differences between the assay conditions (e.g., preincubation time) of the two studies.

In their following publication, Cherblanc et al. focused on the inhibitory mechanism of chaetocin on human recombinant G9a.[64] The structurally simple ETP compound **5** (IC_{50} = 4.9 μM) showed comparable potency as that of chaetocin (IC_{50} = 2.6 μM). This result, together with the findings by Iwasa et al., demonstrated that the disulfide bridge is crucial for the activity of the inhibitor while the rest of the complex structure is not essential. Furthermore, in MOA studies, Cherblanc et al. found that inhibition of G9a by chaetocin is reversible and that activity of G9a was recovered in the presence of DTT. On the other hand, in the absence of DTT, inhibition of G9a by chaetocin was maintained. Therefore, it has been concluded that chaetocin and related ETP compounds inhibit G9a in vitro via mixed disulfide linkages formed between cysteine residues of enzyme and inhibitor. The mechanism of inhibition is dependent on the assay conditions and incubation time.

Inhibition of the G9a enzymatic activity by structurally simple ETP compounds, as shown by both Iwasa et al. and Cherblanc et al., demonstrated that the ETP core,and in turn the disulfide bridge, is essential for inhibition. These results, together with the findings from reversibility studies and denaturing mass spectrometry (MS) studies showing the involvement of different pre-SET domain cysteines,[64] support the view that chaetocin and related compounds with the thiol-reactive functionality are unlikely to be suitable for investigating biological functions of the PKMT(s) of interest as selective inhibitors. Therefore, results from cellular studies using these inhibitors should be interpreted with caution.

G9a and GLP are the main methyltransferases that catalyze mono- and dimethylation of H3K9.[65,66] They share 80% sequence identity in their respective SET domains. It has been shown that G9a and GLP can form a heterodimer.[66] In addition to H3K9, these enzymes dimethylate many nonhistone targets,[67] including the tumor suppressor p53 at lysine 373.[68] G9a is overexpressed in various cancers,[45,46,68−70] and knockdown of G9a inhibits prostate cancer,[45] leukemia[70] and lung cancer cell growth.[46] In mouse models, significant delays in acute myeloid leukemia (AML) progression and reduction of leukemia stem cell frequency were observed with loss of G9a.[71] In addition, a recent report suggested that G9a functions as a coactivator for *p21* transcription, leading cells to undergo apoptosis.[72] Involvement of G9a in maintenance of HIV-1 latency,[47] cocaine addiction,[48,73] and mental retardation[74] was also documented. In addition, G9a has been implicated in stem cell function, maintenance, differentiation, and reprogramming.[75−80] For example, G9a is critical for early mouse embryonic development and ESC (embryonic stem cell) differentiation and mediates H3K9me2 patterning during hematopoietic stem and progenitor cells (HSPCs) lineage specification.[80] Furthermore, it was recently reported that T cell-intrinsic expression of G9a was required for development of pathogenic T cells and intestinal inflammation in a colitis model.[81] GLP has been implicated in Kleefstra syndrome,[82,83] a disorder affecting intellectual ability. More recently, GLP was reported to be an essential lysine methyltransferase in the PRDM16 (PR domain containing protein 16) transcriptional complex and controls brown adipose cell fate and energy homeostasis.[84]

In 2007, Kubicek et al. reported the first selective small-molecule inhibitor of G9a and GLP.[85] The discovery of this selective inhibitor was a major advancement in the PKMT inhibitor field. High-throughput screening (HTS) of ca. 125 000 preselected compounds resulted in two confirmed hits: compound **6** (BIX-01338), which contains a 2-(*N*-acyl)-aminobenzimidazole core, and compound **7** (BIX-01294), which is a 2,4-diamino-6,7-dimethoxyquinazoline derivative (Figure 4).[85] Both compounds were tested against a panel of

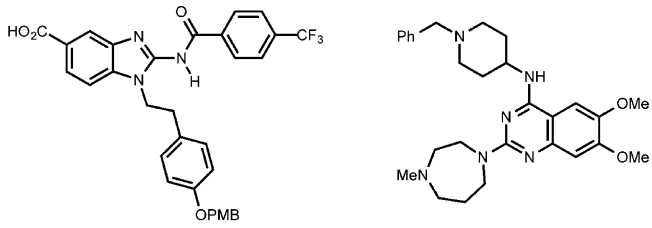

Figure 4. Structures of inhibitors **6** and **7**.

methyltransferases including G9a and GLP along with PRMT1 (protein arginine methyltransferase 1), SETD7, SETDB1, wild-type (WT) SUV39H1, and a hyperactive SUV39H1 (H320R) mutant. Compound **6** inhibited all of them in a concentration range of 5−15 μM; thus, it was not selective. On the other hand, **7** selectively inhibited G9a (IC_{50} = 1.7 μM) and GLP (IC_{50} = 38 μM) (other enzymes were not inhibited even at 45 μM). It is worth mentioning that the inhibition of GLP by **7** was measured under oversaturated reaction conditions where almost all of the substrate transformed to H3K9me3, whereas G9a inhibiton was assayed under linear reaction conditions.[86] In another study, **7** was reported to be slightly more potent for GLP (IC_{50} = 0.7 μM) than G9a (IC_{50} = 1.9 μM) when using the same linear assay conditions for both enzymes.[86] Initial mechanistic studies showed that **7** did not inhibited G9a in a SAM-competitive manner.[85] Chang et al. obtained a crystal structure of the GLP SET domain in complex with **7** and SAH, which reveals that inhibitor **7** binds to the substrate binding groove of GLP (Figure 5).[86]

Inhibitor **7** was also characterized in multiple cell-based assays. In mouse ESCs, **7** at 4.1 μM reduced global levels of

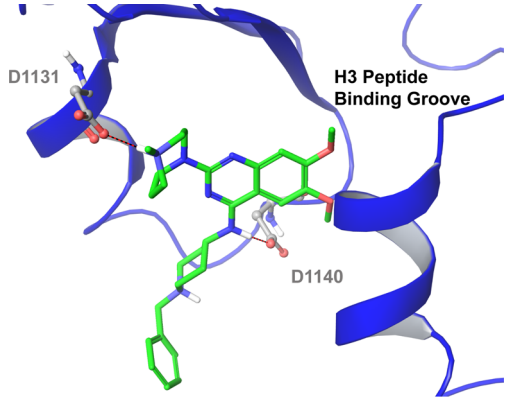

Figure 5. X-ray co-crystal structure of the GLP−**7** complex (PDB code: 3FPD). Protein residues, gray colored stick models; inhibitor, green colored stick model; and hydrogen bonds, red dashed line.

dx.doi.org/10.1021/jm501234a | *J. Med. Chem.* 2015, 58, 1596−1629

H3K9me2, increased unmodified H3K9, and did not change the H3K9me1 and H3K9me3 marks.[86] In addition, H3K27, H3K36, and H4K20 methylation marks were unaffected. Similar effects on the reduction of H3K9me2 global levels were observed in mouse embryonic fibroblast (MEF) and human HeLa cells. Furthermore, effects of **7** on the reduction of H3K9me2 at promoters of G9a target genes were investigated using chromatin immunoprecipitation (ChIP). Treatment of WT mouse ES cells (embryonic stem cells) with **7** (at 4.1 μM for 2 days) reduced the H3K9me2 mark at promoters of G9a target genes *mage-a2*, *Bmi1*, and *Serac1*. On the other hand, compound **7** did not affect the H3K9me2 mark at promoters of G9a nonresponsive genes such as *Mage-b4* and *tubulin*. It is worth noting that **7** was toxic at concentrations above 4.1 μM in cellular assays. Taken together, these results demonstrated that compound **7** is the first selective small-molecule inhibitor of G9a and GLP and that it is competitive with the peptide substrate and selectively reduces the H3K9me2 mark in cells.

In 2009, Liu et al. discovered compound **8** (UNC0224) as a potent and selective inhibitor of G9a and GLP by studying SAR of the 2,4-diaminoquinazoline scaffold represented by **7** (Figures 6 and 7).[87] After establishing initial SAR for the 2-

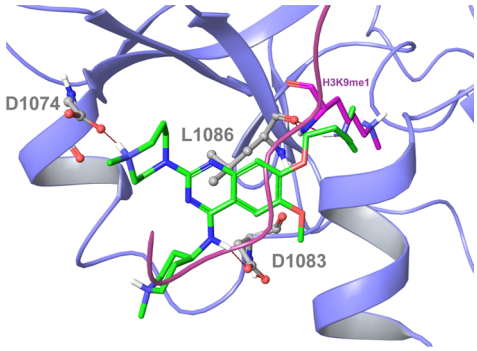

Figure 6. X-ray co-crystal structure of G9a–**8** complex (PDB code: 3K5K). Inhibitor is shown as green colored stick model, and a fragment of the histone peptide (magenta) is transposed into this crystal structure to illustrate the lysine binding channel.

and 4-amino regions, compound **8** was designed and synthesized on the basis of the crystal structure of the GLP–**7** complex.[86] In particular, the 7-dimethylaminopropoxy group of **8** was designed to occupy the lysine binding channel, which was not occupied by **7**. As expected, **8** was more potent than **7** in multiple biochemical and biophysical assays including isothermal titration calorimetry (ITC) with a K_d (dissociation constant) of 23 ± 8 nM. It was more than 1000-fold selective for G9a and GLP over SETD7 and SETD8 and also selective against a broad range of G-protein coupled receptors (GPCRs), ion channels, and transporters. A high0resolution (1.7 Å) X-ray crystal structure of the G9a–**8** complex confirmed the occupation of the G9a lysine binding channel by the 7-dimethylaminopropoxy group (Figure 6). The co-crystal structure also reveals that (1) the secondary amine at the 4-position forms a hydrogen bond with Asp1083, (2) the distal *N*-methyl group off the piperidine group is solvent-exposed, and (3) the 7-dimethylaminopropoxy group does not fully occupy the lysine channel (Figure 6). On the basis of these structural insights, Liu et al. further explored the 7-aminoalkoxy group and discovered **9** (UNC0321), which has a longer ethoxyethyl chain instead of the 3-carbon chain of **8** (Figure 7).[88] Compound **9** has been the most potent G9a inhibitor to date with a Morrison K_i of 63 pM and was 40- and 250-fold more potent than **8** and **7**, respectively. Additionally, it had high potency for GLP and showed a similar selectivity profile as that of **8**.

In 2010, Chang et al. published their G9a and GLP inhibitor **10** (E72) (Figure 8) by adding a lysine mimic to the quinazoline scaffold based on the crystal structure of the GLP–**7** complex.[89] This strategy is similar to the one used for discovering **8**. Compound **10** had a K_d of ca. 136 nM and an IC_{50} of 100 nM for GLP. It was also potent for G9a but selective over SUV39H2. Compound **10** reactivated K-ras-mediated epigenetic silencing of the proapototic Fas gene in NIH 3T3 cells with modest potency and was less cytotoxic compared to that of **7**, which could be due to its high polarity and thus low cell membrane permeability.

Similarly, the relatively high polarity and poor cell membrane permeability were likely key contributors to the poor cellular potency of **9** even though **9** was significantly more potent than **7** in biochemical assays.[90] Therefore, Liu et al. further optimized the quinazoline scaffold to simultaneously improve physicochemical properties and maintain in vitro potency.[90] From these studies, the G9a and GLP cellular chemical probe **11** (UNC0638)[91] (Figure 8), along with several back-up probes including UNC0646 and UNC0631,[90] was discovered (Figure 8). Chemical probe **11** had high in vitro potency for G9a (IC_{50} < 15 nM) and GLP (IC_{50} = 19 nM) in multiple biochemical assays.[91] In MOA studies, **11** was competitive with the peptide substrate (K_i = 3.0 ± 0.05 nM) and noncompetitive with SAM. The high binding affinity was confirmed in biophysical assays such as differential scanning fluorimetry (DSF) and surface plasmon resonance (SPR). The X-ray crystal structure of G9a in complex with **11** and SAH clearly shows that this inhibitor occupies the substrate binding groove and does not interact with the SAM binding pocket, thus confirming its mechanism of action. Major interactions of **11** in the G9a co-crystal structure are in good agreement with the ones of **8** (Figure 9).

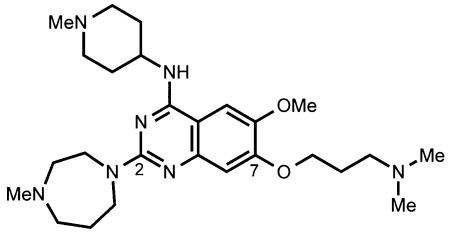

UNC0224 (8)

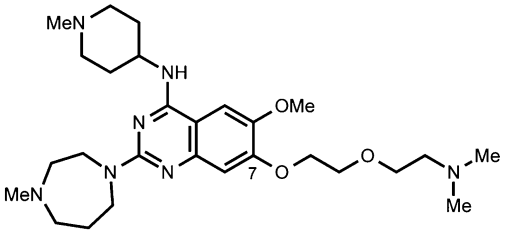

UNC0321 (9)

Figure 7. Structures of G9a and GLP inhibitors **8** and **9**.

dx.doi.org/10.1021/jm501234a | *J. Med. Chem.* 2015, 58, 1596–1629

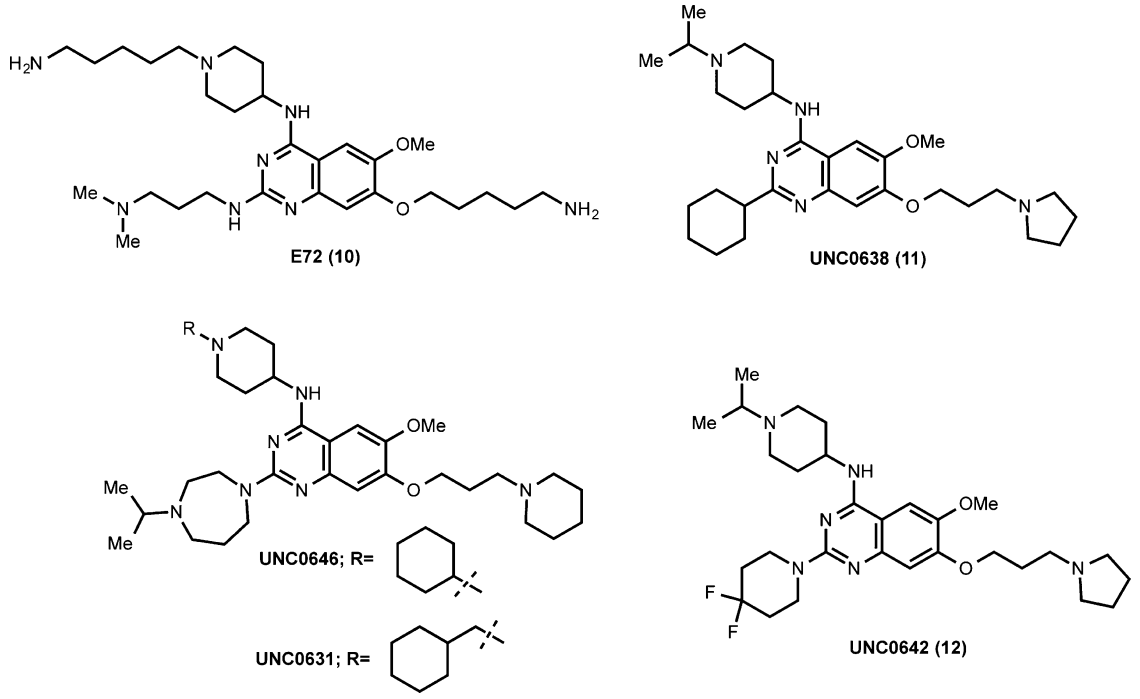

Figure 8. Structures of G9a and GLP inhibitors **10**–**12** and their analogues.

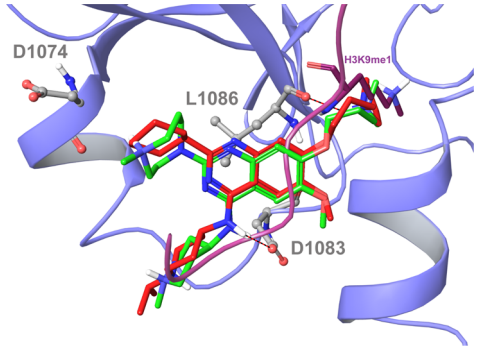

Figure 9. Overlay of the X-ray co-crystal structure of G9a–**8** complex (PDB code: 3K5K) with the one of the G9a–**11** complex (PDB code: 3RJW). Inhibitor **8**, green colored stick model; inhibitor **11**, red colored stick model. A fragment of the histone peptide (magenta) was transposed into the crystal structures to illustrate the lysine binding channel.

A high-quality chemical probe should have (1) an excellent and well-characterized selectivity profile and (2) robust on-target activities in cells.[92−94] Therefore, **11** was characterized in a broad range of epigenetic and nonepigenetic targets.[91] It was more than 200-fold selective for G9a and GLP over 16 other methyltransferases and epigenetic targets including SUV39H1, SUV39H2, EZH2, SETD7, MLL, SMYD3, SETD8, DOT1L, PRDM1, PRDM10, PRDM12, PRMT1, PRMT3, histone acetyltransferase HTATIP, Jimonji demethylase JMJD2E, and DNA methyltransferase DNMT1. It was also at least 100-fold selective over more than 80 GPCRs, kinases, ion channels, and transporters. Using an in-cell western assay, Vedadi et al. showed that **11** (IC_{50} = 81 ± 9 nM) was more potent and efficacious than **7** (IC_{50} = 500 ± 43 nM) at reducing global levels of H3K9me2 in MDA-MB-231 cells, a human breast carcinoma cell line.[91] G9a protein and mRNA levels were not affected during compound **11** treatment, suggesting that the reduction of H3K9me2 results from inhibition of enzymatic function, not from changes in protein abundance. In a standard MTT (3-(4,5-dimethylthiazol-2-yl)-2,5-diphenyl tetrazolium bromide) assay, **11** (EC_{50} = 11 000 ± 710 nM) was found to be significantly less toxic than **7** (EC_{50} = 2700 ± 76 nM) in MDA-MB-231 cells. Thus, **11** has an excellent separation of functional potency and cell toxicity with a function/toxicity ratio of 138, whereas **7** has a relatively poor separation of functional potency and cell toxicity with a function/toxicity ratio of 5.6. Compound **11** also exhibits a good separation of functional potency and cell toxicity in seven other tumor and normal cell lines. The effect of **11** on cellular levels of H3K9me2 was confirmed using quantitative MS-based proteomics. In the same study, the effect of **11** on cellular levels of other 20 common histone modifications was also assessed. With the exception of H3K14ac, **11** did not significantly change the other histone marks, suggesting that cellular actions of **11** are specific and that there is a possible cross-talk between H3K9me2 and H3K14ac. In addition, **11** reduced the H3K9me2 mark at promoters of G9a target genes *MAGEA1*, *TBC1D5*, and *MAGEA2* and had no effect on H3K9me2 at the promoter of the G9a nonresponsive gene *MAGEB4* in ChIP–chip (chromatin immunoprecipitation–DNA microarray) studies. Furthermore, **11** reactivated a silent retroviral vector and G9a target genes in mES cells. It also reduced the H3K9me2 mark at promoters of those genes and the retroviral long terminal repeat (LTR) region and indirectly induced DNA hypomethylation in mES cells. Taken together, these results demonstrated that **11** is a highly selective inhibitor of G9a and GLP and has robust on-target activities in cells.

In terms of phenotypic effects, **11** reduced clonogenecity in MCF7 cells, but it had no effect on clonogenicity in MDA-MB-231 cells, suggesting different phenotypic effects depending upon cell types and/or epigenetic states.[91] In addition, it was recently reported that **11** significantly suppressed the growth of primary human acute myeloid leukemia (AML) cells by inducing leukemia stem cell differentiation.[71] Effects of **11** phenocopied those observed in mouse AML cells that lack G9a.

dx.doi.org/10.1021/jm501234a | J. Med. Chem. 2015, 58, 1596−1629

Mechanistically, it was found that the methyltransferase activity of G9a and its interaction with the leukemogenic transcription factor HoxA9 regulate fast proliferating myeloid progenitors. These results highlight a clinical potential of G9a inhibition as a means to block the proliferation and self-renewal of AML cells by attenuating HoxA9-dependent transcription. Furthermore, it was recently reported that **11** induced differentiation of wild-type T cells into regulatory T cells and Th17 cells,[81] and adult hematopoietic stem cells continuously treated with **11** retained stem cell-like phenotypes and function better than the those that are untreated during in vitro expansion.[80]

While compound **11** is an excellent chemical probe[92,94] of G9a and GLP for cell-based studies as discussed, it displayed poor in vivo pharmacokinetic (PK) properties and consequently is not suitable for animal studies.[91] To achieve an in vivo chemical probe that is suitable for animal studies, Liu et al. further optimized compound **11** and discovered **12** (UNC0642) as the first in vivo chemical probe of G9a and GLP (Figure 8).[95] Compound **12** has high in vitro potencies for both G9a and GLP (IC_{50} < 2.5 nM) and is a substrate competitive inhibitor with a K_i of 3.7 ± 1 nM. It is 2000-fold selective for G9a and GLP over PCR2-EZH2 and >20 000-fold selective over 13 other methyltransferases (SUV39H2, MLL1, SETDB1, SETD7, SETD8, PRMT3, PRMT5, SMYD2, SMYD3, SUV420H1, SUV420H2, DOT1L, and DNMT1). It was tested against a broad panel of 50 kinases and 44 GPCRs, transporters, and ion channel. With the exception of the histamine H_3 receptor, **12** is more than 300-fold selective for G9a and GLP over these nonepigenetic targets. Similar to **11**, it displayed high potency at reducing the H3K9me2 mark and low cell toxicity in a number of tumor and normal cell lines. It also reduced clonogenicity in PANC-1 cells (a human pancreatic epithelioid carcinoma cell line). Importantly, **12** displayed much improved exposure in plasma compared to that of **11** in mouse PK studies, making it suitable for animal studies as an in vivo chemical probe of G9a and GLP. More recently, a biotinylated derivative of probe **11**, compound **13** (UNC0965) was also designed and synthesized (Figure 10).[96] This new

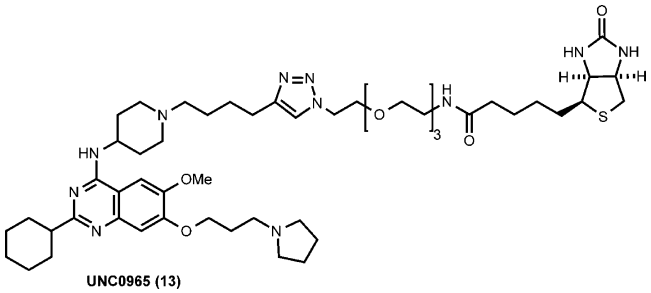

Figure 10. Structure of the biotinylated G9a inhibitor **13**.

derivative retained high in vitro potency for G9a and was active in cellular assays. Konze et al. have shown that **13** can selectively precipitate G9a from whole-cell lysates (chemipreciptation) and is an effective chemical tool for exploring the localization of G9a on chromatin both in vitro and in vivo in chem−ChIP studies.[96]

In 2012, Yuan et al. reported the discovery of **14** (BRD4770, Figure 11)[97] by synthesizing a focused library of 2-substituted benzimidazoles to mimic SAM based on compound **6** (Figure 4), a SAM-competitive but nonselective inhibitor of PKMTs.[85] Compound **14** is the methyl ester of its carboxylic acid

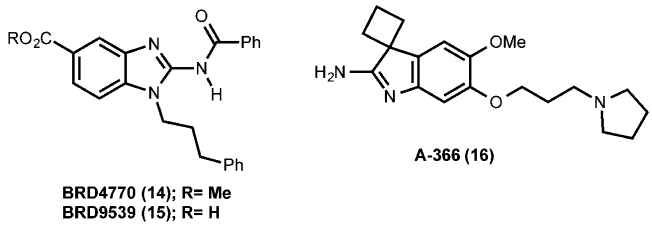

Figure 11. Structures of compounds **14**−**16**.

derivative **15** (BRD9539) for cell-based studies (Figure 11).[97] Compound **15** inhibited G9a with an IC_{50} of 6.3 μM and was selective for G9a over SUV39H1, SUV39H2, MLL1, SETD7, SETD8, PRMT1, PRMT3, PRMT5, DNMT1, and HDAC1−9. However, it also inhibited PRC2−EZH2 with a similar potency and NSD1 only at 40 μM. The potency of carboxylic acid **15** against GLP was not reported; thus, it is not clear whether **15** is a pan G9a and GLP inhibitor. Inhibition of G9a by **15** decreased with increased concentrations of SAM. Therefore, it was suggested that **15** is a SAM-competitive inhibitor.

Methyl ester **14** at 10 μM significantly reduced cellular levels of H3K9me2 and H3K9me3 and increased cellular levels of H3K9me1.[97] Interestingly, cellular levels of H3K27me3 were unaltered during compound **14** treatment, suggesting that **14** did not inhibit PRC2−EZH2 in cells. The caspase3/7 activity, as a measure of cell apoptosis, was also assessed. Methyl ester **14** did not induce caspase activity in PANC-1 cells even after 72 h treatment, whereas inhibitor **7** increased caspase activity after only 24 h, suggesting that **14** has low cell toxicity. Compound **14** treated PANC-1 cells showed enlarged and flattened cell morphology with increased senescence-associated β-galactosidase staining. The total number of cells as well as clonogenicity was reduced after 72 h of treatment with the inhibitor. Mechanistically, increase in phosphorylation of ATM (ataxia telangiectasia mutated) and nuclear translocation of phosphorylated ATM after the treatment with compound **14** were observed, whereas ATR (ataxia telangiectasia and Rad3-related) was not activated. G9a knockdown also resulted in similar effects on ATM and ATR. It was therefore suggested that **14** causes cellular senescence similar to that resulting from activation of phosphorylation of ATM by HDAC inhibitors.

In 2014, Sweis et al. reported the discovery of a potent G9a (IC_{50} = 3.3 nM) and GLP (IC_{50} = 38 nM) inhibitor **16** (A-366, Figure 11).[98] This inhibitor contains a new spiro(cyclobutane-1,3′-indol)-2′-amine core and is selective for G9a and GLP over other methyltransferases including SUV39H2, MLL1, SETDB1, SETD7, SETD8, PRMTs (1, 3, 5, 6 and 8), SMYD2, SMYD3, EZH1, EZH2, SUV420H1, SUV420H2, and DNMT1. MOA studies of **16** showed noncompetitive inhibition with respect to SAM but competitive inhibition with the peptide substrate. This finding is confirmed by the X-ray crystal structure of G9a in complex with **16**. This co-crystal structure reveals hydrogen-bonding interactions with Asp1074 and Asp1078, and the 7-aminopropoxy group interacts the lysine binding channel, similar to that of **8** and **11** interacting with G9a (Figure 12). In a human prostate cancer cell line, PC3, after treatment for 72 h with compound **16** at 3 μM, cellular levels of H3K9me2 were reduced by about 50%, whereas other histone marks, such as H3K27me3 and H3K36me2, were not affected.

Inhibitors of H3K27 Methyltransferases. Polycomb repressive complex 2 (PRC2) is the multisubunit protein complex that catalyzes methylation of H3K27.[99−104] The main biological function of PRC2 is transcriptional silencing of genes

dx.doi.org/10.1021/jm501234a | J. Med. Chem. 2015, 58, 1596−1629

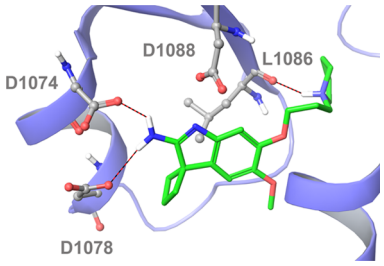

Figure 12. X-ray co-crystal structure of the G9a−**16** complex (PDB code: 4NVQ).

involved in differentiation and development via trimethylation of H3K27.[102] PRC2 is a crucial chromatin-modifying complex that is conserved from *Drosophila* to humans,[99] and the core PRC2 complex includes four subunits: EZH1 (enhancer of zeste homologue 1, also known as KMT6B) or EZH2 (enhancer of zeste 2 polycomb repressive complex 2 subunit, also known as KMT6A), SUZ12 (suppressor of zeste 12), EED (embryonic ectoderm development), and histone binding proteins RbAp46/48. EZH1 or EZH2 is the catalytic subunit of the complex, and its C-terminal SET domain is essential for the methyltransferase activity.[100,104,105] EZH1 and EZH2 are highly homologous, with 76% overall sequence identity and 96% sequence identity in their SET domains.[106] However, EZH1 and EZH2 have different expression patterns. While the former is present in both dividing and differentiated cells, the latter is found only in actively dividing cells.[102,107] Furthermore, PRC2 complex-containing EZH1 (PRC2−EZH1) has lower methyltransferase activity as compared to that of PRC2 complex-containing EZH2 (PRC2−EZH2).[107] Nevertheless, both of these complexes are involved in the maintenance of H3K27 methylation in cells.[102,107,108] Methylation of H3K27 occurs successively to give the H3K27me3 mark, which is a well-known repressive mark.[102,109]

Even though EZH2 is the catalytic subunit of PRC2−EZH2, it does not have enzymatic activity on its own and needs at least two other subunits (EED and SUZ12) to gain the methyltransferase activity.[110−112] It has recently been shown that PRC2 can contain several other protein subunits such as AEBP2, PCLs, and JARID2.[113−116] Point mutations at tyrosine 641 (Y641) in the C-terminal SET domain of EZH2 have been identified.[117] These mutants including Y641F, Y641N, Y641S, Y641H, and Y641C were observed in 7% of follicular lymphomas and 22% of germinal center B-cell (GCB) and diffuse large B-cell lymphomas (DLBCLs).[117−119] These gain-of-function Y641 mutations prefer H3K27me2 as the substrate, resulting in enhanced enzymatic activity for trimethylation of H3K27.[120,121] In contrast, wild-type EZH2 has a substrate preference for unmethylated H3K27.[120,121] Thus, wild-type EZH2 and the Y641 mutant work cooperatively, leading to increased levels of H3K27me3 in tumor tissues. Recently, a new EZH2 mutation, A677G, was identified in lymphoma cell lines and primary tumor specimens.[122] Interestingly, the A677G mutant has no substrate preference among unmethylated H3K27, H3K27me1, and H3K27me2. Overexpression of EZH2 and/or hypertrimethylation of H3K27 have been associated with a number of human cancers,[123−125] such as breast,[126] prostate,[127] lymphoma,[128] and leukemia.[129]

In 2012, Knutson et al. reported the first selective small-molecule inhibitor of EZH2.[130] This discovery was a major milestone in the PKMT inhibitor field. HTS of a 175 000-compound diversity library led to the identification of compound **17** (IC_{50} = 620 nM) as a tractable hit (Figure 13). Compound **18** (EPZ005687, Figure 13) (IC_{50} = 54 ± 5

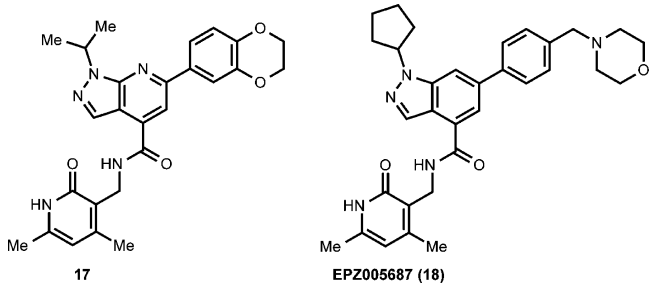

Figure 13. Structures of EZH2 inhibitors **17** and **18**.

nM) was discovered by optimization of this hit including (1) addition of an amine functionality at the 4-position of the phenyl ring, (2) change of the 5,6-fused pyrrazolapyridine to the indozole, and (3) introduction of a larger lipophilic group at the indazole nitrogen (Figure 13).[130]

Michaelis−Menten kinetic studies indicated that this inhibitor was competitive with SAM with a K_i of 24 ± 7 nM and noncompetitive with the peptide substrate.[130] It was previously reported that the cofactor product SAH inhibited EZH2 in a SAM-competitive manner.[131] Yonetani−Theorell analysis[132] displayed that **18** and SAH were mutually exclusive inhibitors of PRC2. Therefore, with this indirect evidence, binding of **18** in the EZH2 SAM pocket has been suggested. Compound **18** was more than 500-fold selective for PRC2−EZH2 over 14 other methyltransferases, including G9a, GLP, SETD7, SMYD2, SMYD3, WHSC1L1, MMSET, PRMTs (1, 3, 4, 5, 6, and 8), and DOT1L. Interestingly, **18** was about 50-fold selective for PRC2−EZH2 over PRC2−EZH1. It also displayed similar potencies for EZH2 Y641 mutants (Y641N, F, S, H, and C) compared to that for wild-type EZH2. On the other hand, **18** was approximately 5-fold more potent for the A677G mutant than that for wild-type EZH2. In addition, **18** showed no significant inhibition at 10 μM against most of the 77 GPCRs and ion channels tested (hit only 4 targets with the lowest extrapolated IC_{50} of 1.5 μM, corresponding to more than 60-fold selectivity).

In OCI-LY19 cells, a wild-type EZH2 lymphoma cell line, **18** reduced H3K27me3 levels with an IC_{50} of 80 ± 30 nM.[130] H3K27me3 and H3K27me2 were the only major PTMs that were significantly changed (a slight increase in H3K27Ac was also observed). Similarly, this inhibitor significantly reduced the H3K27me3 mark in WSU-DLCL2 cells, a lymphoma cell line harboring the Y641F mutant. Although **18** did not affect the growth of OCI-LY19 cells (with wild-type EZH2), it significantly inhibited the growth of WSU-DLCL2 (with $EZH2^{Y641F}$ mutant) and Pfeiffer (with $EZH2^{A677G}$ mutant) cells with a delayed onset of activity. These results suggest that hypertrimethylation of H3K27 is essential for proliferation and survival of lymphoma cells harboring EZH2 mutants. In addition, gene set enrichment analysis (GSEA) studies showed that inhibition of EZH2 by **18** in WSU-DLCL2 cells resulted in derepression of known EZH2 target genes. Taken together, these results have demonstrated that **18** is a potent and selective inhibitor of EZH2 and that it is competitive with SAM and engages in the target in cells.

dx.doi.org/10.1021/jm501234a | *J. Med. Chem.* 2015, 58, 1596−1629

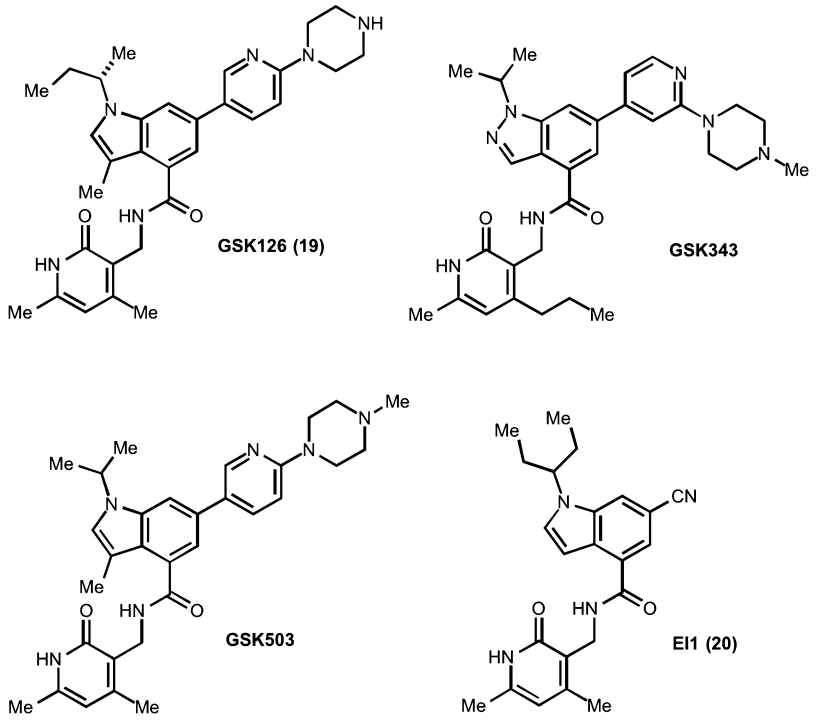

Figure 14. Structures of EZH2 inhibitors **19** and **20** and their analogues.

Shortly after the publication of inhibitor **18**, McCabe et al. reported another selective EZH2 inhibitor, **19** (GSK126, Figure 14),[133] which shares the core scaffold with **18**. HTS of the corporate compound collection resulted in the identification of a small-molecule inhibitor (K_i^{app} = 700 nM) as a hit.[134] Optimization of this hit led to the discovery of **19**[133] along with several other potent EZH2 inhibitors including GSK343[106] and GSK503[135] (Figure 14) with the same core template. Compound **19** contains the same pyridone group as **18** but has an indole group instead of the indazole group of **18** (Figure 13).

Compound **19** potently inhibited both wild-type and mutant EZH2 with K_i^{app} of 0.5−3 nM.[133] It was competitive with the cofactor SAM and noncompetitive with peptide substrates. It was more than 1000-fold selective for EZH2 over 20 other methyltransferases including G9a, SUV39H1, SUV39H2, MLL1−4, SETD8, SETD7, SMYD2, MMSET, SETMAR, PRMTs (1, 3, 4, 5, and 6), DOT1L, DNMT3a, and DNMT3b. It was also more than 150-fold selective for EZH2 over EZH1. Additionally, **19** showed no significant inhibition against a broad panel of kinases, GPCRs, ion channels, and transporters as well as other chromatin-modifying enzymes such as HDAC1−11, JMJD2d, JMJD3, and LSD1.

McCabe et al. also investigated the effect of **19** on cell proliferation in a panel of B-cell lymphoma cell lines and found that six of the seven most sensitive DLBCL cell lines harbored Y641N, Y641F, or A677G mutations, whereas most of the insensitive DLBCL cells in the panel had no mutations.[133] These results suggest that the growth of DLBCL cells harboring the gain-of-function mutations is dependent on PRC2−EZH2 methyltransferase activity. The timing of **19**-induced effects on the proliferation and cell death was also studied in two of the most sensitive DLBCL cell lines: Pfeiffer (with A677G mutation) and KARPAS-422 (with Y641N mutation). In Pfeiffer cells, **19** displayed a relatively fast onset of activity. Inhibition of cell proliferation by **19** was started after 2 days, and a clear decrease in cell number was observed after 3 days. The observed cell death was attributed to caspase-mediated apoptosis. On the other hand, **19** exhibited a delayed onset of activity in KARPAS-422 cells. Six to seven days were required to reach the maximal potency in inhibiting the growth of these cells. Mechanistically, a mainly cytostatic effect was observed in KARPAS-422 cells with minimal caspase activity. In addition, the effect of **19** on gene expression in DLBCL cell lines was examined. The treatment with **19** led to clear transcriptional activation in the most sensitive DLBCL cell lines. The gene expression changes caused by EZH2 inhibition via **19** versus EZH2 knockdown via shRNA were very similar in both Pfeiffer and KARPAS-422 cell lines, suggesting that the observed effects were due to on-target activity of the inhibitor. The ChIP-seq (chromatin immunoprecipitation followed by sequencing) analysis for the three most sensitive cell lines, Pfeiffer, WSU-DLCL2 (harboring Y641F), and KARPAS-422, showed that the genes upregulated in response to compound **19** treatment displayed enrichment in H3K27me3 before treatment, suggesting that the EZH2 target genes are transcriptionally repressed by the H3K27me3 mark.

Furthermore, **19** was efficacious in KARPAS-422 and Pfeiffer tumor xenograft mouse models.[133] In particular, intraperitoneal (IP) administration of **19** at 50 mg/kg once daily, 150 mg/kg once daily, or 300 mg/kg twice per week for 35 days resulted in a drastic reduction in tumor volume and a marked improvement in survival in the more aggressive KARPAS-422 xenograft model. After the treatment with **19** was stopped, tumor stasis was seen in the 50 mg/kg once daily group, whereas complete tumor eradication had been observed in the 150 mg/kg once daily and 300 mg/kg twice per week groups for 25 days. A dose-dependent decrease in the H3K27me3 mark and an increase in expression of EZH2 target genes were observed in both xenograft mouse models. Compound **19** was well-tolerated at the doses and schedules used in these mouse models. In summary, **19** is a highly potent and selective EZH2

dx.doi.org/10.1021/jm501234a | J. Med. Chem. 2015, 58, 1596−1629

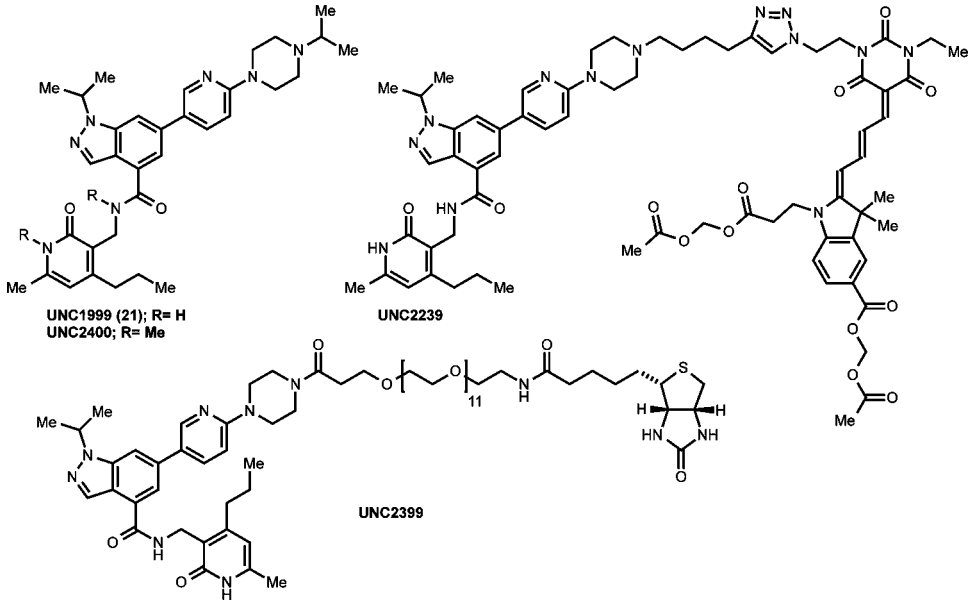

Figure 15. Structures of EZH2 and EZH1 inhibitor **21** and **21**-based tool compounds.

inhibitor, has robust on-target activity in cells, and is efficacious in multiple cell-based and in vivo models. Importantly, **19** has been advanced into phase 1 clinical trials for the treatment of GCB-DLBCL.[136]

Shortly after inhibitors **18** and **19** were published, Qi et al. reported **20** (EI1, Figure 14),[137] a selective EZH2 inhibitor, which shares the same pyridone and indole/indazole core with inhibitors **18** and **19**. Compound **20** potently inhibited the wild-type EZH2 and Y641F mutant with IC_{50}'s of 15 ± 2 and 13 ± 3 nM, respectively. It was competitive with the cofactor SAM with a K_i of 13 ± 3 nM calculated by using Cheng–Prusoff equation. Compound **20** was more than 10 000-fold selective for EZH2 over 10 other PMTs including G9a, SUV39H2, MLL, SETD2, SETD7, SETD8, SMYD2, WHSC1L1, CARM1, and DOT1L and was also about 90-fold selective for EZH2 over EZH1.

The effect of **20** on DLBCL cell lines harboring EZH2 gain-of-function mutations (Y641F and Y641N) and a rhabdoid tumor cell line G4001 (with wild-type EZH2) was investigated.[137] **20** concentration-dependently decreased cellular levels of H3K27me3 and H3K27me2, but it did not affect H3K27me1 and other di- and trimethylation marks on H3K4, H3K9, H3K36, and H3K79, suggesting that the cellular action of **20** is specific. This inhibitor activated *p16*, a well-characterized target gene of EZH2. The expression levels of *p16* were increased 20-fold after 5 days of treatment with **20**. Furthermore, ChIP experiments revealed that both H3K27me3 and EZH2 were enriched at the *p16* promoter, but upon the treatment with **20**, the H3K27me3 mark was drastically reduced at the *p16* promoter, whereas EZH2 levels were not changed, suggesting that *p16* expression was activated by the suppression of the H3K27me3 mark but not by EZH2 occupancy at the promoter. Moreover, similar to **18** and **19**, compound **20** strongly inhibited the proliferation of DLBCL cell lines (WSU-DLCL2, SU-DHL6, KARPAS-422, DB, SU-DHL4) harboring EZH2 gain-of-function mutants. On the other hand, the proliferation of DLBCL cell lines (OCI-LY19, GA10, and Toledo) with wild-type EZH2 was not or was only weakly inhibited by **20**. In addition, Qi et al. found that inhibition of EZH2 by **20** significantly blocked cell cycle progression and induced apoptosis in DLBCL cell lines harboring EZH2 mutants. The time-dependent gene expression changes in KARPAS-422 ($EZH2^{Y641N}$) cells suggest that the reduction of H3K27me3 at the gene promoters is associated with **20**-dependent transcriptional upregulation.

In 2013, Konze et al. reported an orally bioavailable chemical probe of EZH2 and EZH1, **21** (UNC1999, Figure 15).[138] Docking of **18** into an EZH2 homology model built on the basis of the X-ray crystal structure of GLP suggested that the morpholinomethyl group was solvent-exposed. Konze et al. therefore explored this region to improve physicochemical properties of this chemical series. From this study, **21** was discovered as a chemical probe of EZH2 and EZH1. It displayed high in vitro potency for EZH2 (IC_{50} < 10 nM) and possessed more desirable lipophilicity (clogP = 3.1) compared with that of **18** and **19**. In MOA studies, **21** was competitive with SAM with a K_i of 4.6 ± 0.8 nM and noncompetitive with the peptide substrate. It was also highly potent for Y641 mutants (F and N). Importantly, **21** was more than 10 000-fold selective for EZH2 over 15 other methyltransferases including G9a, GLP, SUV39H2, SUV420H1, SUV420H2, MLL1, SETDB1, SETD7, SETD8, SMYD2, PRMTs (1, 3, and 5), DOT1L, and DNMT1. Interestingly, unlike the EZH2 inhibitors discussed earlier, **21** was only about 10–15-fold selective for EZH2 over EZH1. Thus, it would be a useful tool in cellular and disease settings where the H3K27 methylation by PRC2–EZH2 is compensated by PRC2–EZH1. In addition, **21** was highly selective over a broad panel of more than 90 kinases, GPCRs, transporters, and ion channels, with the exception of sigma2. Inhibitor **21** reduced H3K27me3 levels with an IC_{50} of 124 ± 11 nM in MCF10A cells and exhibited low cell toxicity (EC_{50} = 19 200 ± 1200 nM).[138] Thus, **21** had an excellent separation of cellular potency and toxicity, with a function-to-toxicity ratio of more than 150. In addition, **21** at 5000 nM for 72 h did not significantly change EZH2 protein levels in MCF7 cells even though the H3K27me3 mark was completely removed. Furthermore, **21** concentration-dependently inhibited the proliferation of DB cells, a DLBCL cell line harboring the $EZH2^{Y641N}$ mutant. DB cells were killed completely by the treatment with 5000 nM **21**. Consistent

dx.doi.org/10.1021/jm501234a | J. Med. Chem. 2015, 58, 1596–1629

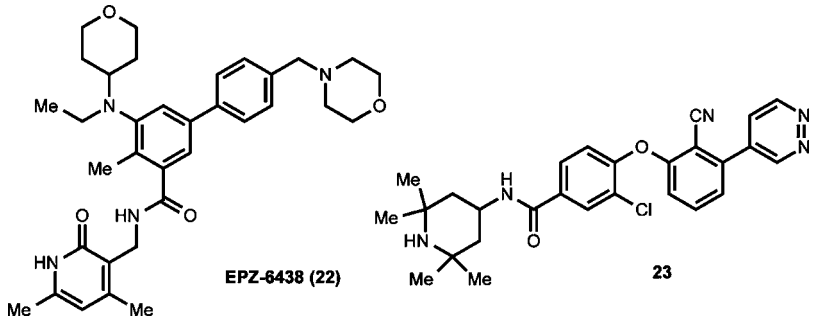

Figure 16. Structures of EZH2 and EZH1 inhibitors **22** and **23**.

with the results generated in MCF7 cells, **21** at 3000 nM for 72 h significantly reduced H3K27me3 levels in DB cells and did not affect EZH2 protein levels. Importantly, **21** was orally bioavailable, likely due to its improved physicochemical properties. A single 50 mg/kg oral dose of **21** attained good plasma exposure levels and high C_{max} of 4700 nM in Swiss albino mice. In summary, compound **21** is a potent and selective inhibitor of EZH2 and EZH1, is competitive with SAM, has robust on-target activity in cells, and is orally bioavailable, making it a valuable tool for assessing in vivo efficacy and potential toxicity of dual inhibition of EZH2 and EZH1 in chronic animal studies.

Konze et al. also developed a number of inhibitor **21**-based tool compounds.[138] First, UNC2400 (Figure 15), which is a dimethylated analogue, was designed and synthesized as a negative control for cell-based studies.[138] Even though this dimethylated derivative is structurally very similar to **21**, it was more than 1000-fold less potent for EZH2 than **21** in biochemical assays, did not affect H3K27me3 levels in cells, and displayed similar (low) cell toxicity as that of **21**. Second, UNC2399 (Figure 15), a biotinylated derivative of **21**, was designed and synthesized for chem−ChIP and chemoproteomics studies.[96] This tool compound displayed high in vitro potency for EZH2 (IC_{50} = 17 ± 2 nM) and can selectively pull down EZH2 from whole-cell lysates. Third, UNC2239 (Figure 15), a cell-penetrant dye conjugate of **21**, was developed for live cell imaging studies.[138] This conjugate also exhibited high in vitro potency for EZH2 (IC_{50} = 21 ± 1 nM) and has been used for nuclear colocalization studies in live cells.

Shortly after the publication of inhibitor **21**, Knutson et al. reported an orally active EZH2 inhibitor, **22** (EPZ-6438, Figure 16), which has better potency and pharmacokinetic properties than that of their early compound **18**.[139] Inhibitor **22** contains the same pyridone core as other EZH2 inhibitors discussed earlier, but it does not have the indole/indazole motif. It displayed high in vitro potency for wild-type EZH2 (K_i = 2.5 ± 0.5 nM) as well as EZH2 Y641F, C, H, N, and S and A677G mutants. In MOA studies, **22** was competitive with SAM and noncompetitive with the peptide substrate. It was around 35-fold selective for EZH2 over EZH1 and more than 4500-fold selective for EZH2 over 14 other PTMs including G9a, GLP, SETD7, SMYD2, SMYD3, MMSET, WHSC1L1, PRMTs (1, 3, 4, 5, 6, and 8), and DOT1L.

Specific inactivating mutations in subunits of the chromatin remodeling complex SWI/SNF (switch/sucrose nonfermentable) have been found in human cancers.[140] One of such example is the SMARCB1 subunit that is inactivated in nearly all malignant rhabdoid tumors (MRTs), one of the most common malignancies in pediatric oncology. It has been shown that EZH2 expression is higher in SMARCB1-deficient tumors.[139,141] Inhibitor **22** showed a concentration-dependent reduction of global levels of H3K27me3 as well as H3K27me2 and H3K27me1, but it did not affect other H3 PTMs (K4me3, K9me3, K36me2, K79me2, and K27ac) in SMARCB1-deficient MRT cells (G401).[139] The treatment of G401 cells with **22** caused antiproliferative effects with nanomolar potency and reached the maximal activity at day 14. On the other hand, **22** did not suppress proliferation of RD cells, which contain wild-type SMARCB1. Furthermore, the treatment of G401 cells with **22** induced G1 arrest at day 7 and apoptosis at day 11, whereas this inhibitor did not affect cell cycle or induce apoptosis in RD cells. These results suggest that the proliferation of SMARCB1-deficient MRT cells such as G401 cells is dependent on overexpression of EZH2 and hypertrimethylation of H3K27 and that EZH2 inhibitors are effective at blocking the proliferation of these aggressive tumor cells. Importantly, **22** (twice daily oral dosing at 250 or 500 mg/kg for 28 days) completely eliminated G401 xenografts in SCID (severe combined immunodeficiency) mice. The complete tumor regression was sustained for 32 days after the cessation of compound **22** treatment. In the tumors that were harvested from a subset of the animals treated with **22** for 21 days, a strong correlation was observed between inhibition of H3K27me3 levels and antitumor activity. In addition, **22** was well-tolerated in all treatment groups. In June 2013, compound **22** became the first EZH2 inhibitor that entered human clinical trials. It is being evaluated for the treatment of advanced solid tumors or B-cell lymphomas.[142]

In 2013, Garapaty-Rao et al. reported an EZH2 small-molecule inhibitor containing a new scaffold that differs from that of previously reported pyridone indole/indazole-based EZH2 inhibitors.[143] HTS of a 150 000-compound corporate collection led to the identification of a hit containing a tetramethylpiperidinyl benzamide scaffold. Optimization of this hit resulted in the discovery of compound **23** (Figure 16), which displayed good in vitro potency for wild-type EZH2 (IC_{50} = 21 ± 4 nM) and $EZH2^{Y641N}$ mutant (IC_{50} = 197 ± 14 nM).[144] This inhibitor was also competitive with SAM, similar to other known EZH2 inhibitors. It was selective for EZH2 over five other PKMTs including G9a, SETD7, SETD8, WHSC1, and DOT1L and was about 10-fold selective for EZH2 over EZH1 (IC_{50} = 213 ± 70 nM).

Compound **23** reduced global levels of H3K27me3 and H3K27me2 levels with a modest potency (EC_{50} = 7 μM) and did not affect H3K27me1, H3K4me3, H3K9me3, and H3K36me3 levels in HeLa cells.[143] This inhibitor did not reduce protein levels of EZH2, EZH1, SUZ12, and EED. The effect of compound **23** on 46 common histone modifications

dx.doi.org/10.1021/jm501234a | J. Med. Chem. 2015, 58, 1596−1629

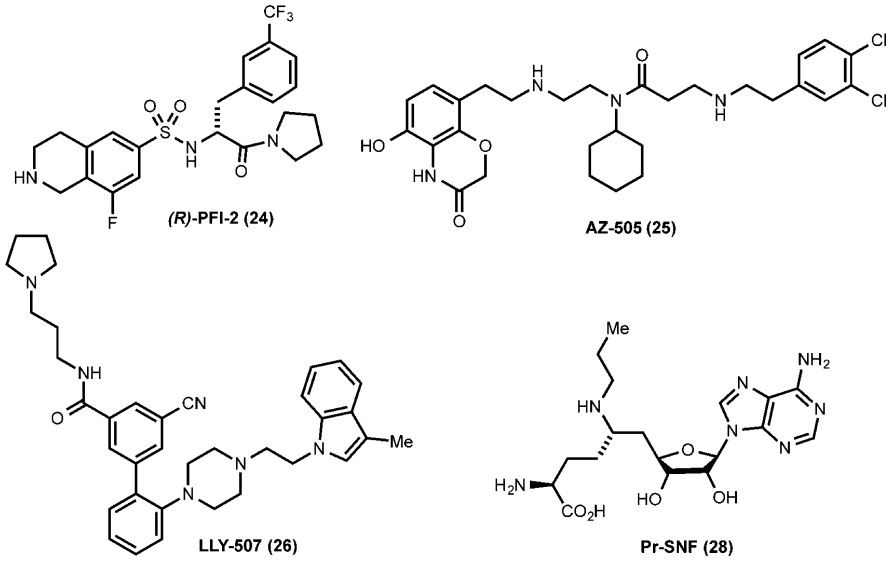

Figure 17. Structures of inhibitors of H3K4 and H3K36 methyltransferases.

was studied using mass spectrometry in two germinal center B cell-like (GCB) DLBCL cell lines: HT (with wild-type EZH2) and SUDHL6 (with mutant EZH2). This study confirmed the effect of compound **23** on reducing H3K27me3 and H3K27me2 marks. In addition, compound **23** inhibited the growth of Pfeiffer (with $EZH2^{A677G}$) cells with a delayed onset of activity but did not affect the growth of OCI-LY19 (with wild-type EZH2) cells, even though H3K27me3 levels were reduced in both cell lines. Transcription levels of previously known EZH2-regulated genes including *ABAT*, *EPB41L1*, *APOL1*, *CEACAM1*, *PIGZ*, *SESN3*, and *SOX9* were increased in a concentration-dependent manner in Pfeiffer cells. On the other hand, genes that are important for cell cycle progression were either not affected (*CDKN2A*, *CDKN1A*, and *CDKN2B*) or were downregulated (*CDKN1C* and *CDKN2D*). It was also found that compound **23** did not inhibit the growth of prostate cancer cell lines PC3 and DU145 even though it significantly reduced H3K27me3 levels in both cell lines, suggesting that the proliferation of these prostate cancer cell lines is independent of EZH2 activity and H3K27 hypertrimethylation.

Inhibitors of H3K4 and H3K36 Methyltransferases. Methylation of H3K4 in humans is controlled by PKMTs: SETD1A, SETD1B, and SETD7 as well as the MLL family proteins MLL1−5, SETMAR, and SMDY1, 2, and 3.[18,145,146] H3K4 trimethylation is a hallmark of transcriptional activation.[11]

MLL (also known as lysine (K)-specific methyltransferase 2A (KMT2A), TRX1, and MLL1) is a large multidomain (several N-terminal DNA domains and a C-terminal SET domain with an essential post-SET region) protein[147] that is specific for H3K4 mono-, di-, and trimethylation.[148−150] Chromosomal rearrangements associated with MLL have been shown to cause acute myeloid leukemia (AML), acute lymphoblastic leukemia (ALL), or mixed lineage leukemia (MLL).[151] More than 50 functionally diverse MLL fusion proteins have been identified in human leukemias.[149,152] AF4, AF9, AF10, AF6, and ENL are the most commonly seen MLL fusion partners in MLL-rearranged leukemias.[149] MLL has also been shown to be essential for homeotic gene regulation and embryonic development via regulation of *Hox* gene expression in mice.[153] Although peptide- or peptidomimetic-based inhibitors of MLL are known,[154] selective small-molecule inhibitors of MLLs have not been reported. It is worth noting that small-molecule inhibitors of WDR5 (WD repeat-containing protein 5), as an indirect way of disrupting MLL activity, have been reported.[155]

SETD7 (SET domain containing (lysine methyltransferase) 7, also known as KMT7, SET7, SET9, and SET7/9) monomethylates H3K4 and many nonhistone proteins including p53 and DNMT1.[156] It has recently been linked with hyperglycemia via its contribution to upregulation of the gene encoding p65 subunit of NF-κB in response to glucose.[56] It has been suggested that SETD7 is a potential target for the treatment of diabetes.[157]

Compound **24** ((*R*)-PFI-2), the first chemical probe of SETD7, was very recently reported by Barsyte-Lovejoy et al. (Figure 17).[158] An initial hit (IC_{50} = 2.1 μM) was discovered by HTS of a 150 000-compound collection. Optimization of this initial hit resulted in the discovery of **24**, which was highly potent for SETD7 (IC_{50} = 2.0 ± 0.2 nM, K_i^{app} = 0.33 ± 0.04 nM). Interestingly, its enantiomer was about 500-fold less potent and is an excellent negative control for cell-based studies. Chemical probe **24** was more than 1000-fold selective for SETD7 over 18 other methyltransferases including G9a, GLP, EZH2, EZH1, SUV39H2, SUV420H1, SUV420H2, SETD2, SETD8, SMYD2, MLL, WHSC1, PRMT1, PRMT3, PRMT5, PRMT8, and DOT1L as well as DNMT1. It was also selective for SETD7 over 134 GPCRs, ion channels, and other enzyme targets (less than 35% inhibition at 10 μM).

Inhibitor **24** exhibited an unusual cofactor-dependent and substrate-competitive MOA. It occupied the substrate binding groove in the X-ray crystal structure of the SETD7−**24** complex (PDB code: 4JLG). However, **24** bound to SETD7 only in the presence of SAM in SPR experiments. Therefore, inhibition of SETD7 by **24** was not purely substrate competitive, and SAM had a significant role in the binding of **24** to SETD7. The direct binding of **24** to SETD7 in cells was demonstrated by the pull-down studies using a biotinylated derivative of **24** as well as by compound **24** increasing the stability of SETD7 in a cellular thermal shift assay (CETSA). Furthermore, inhibitor **24** increased nuclear localization of the transcriptional coactivator yes-associated protein (YAP) in a

dx.doi.org/10.1021/jm501234a | J. Med. Chem. 2015, 58, 1596−1629

concentration-dependent manner and induced expression of YAP-silenced genes in cells. The effect of **24** matched genetic deletion of SETD7. Therefore, **24** is a well-characterized chemical probe and will be a valuable tool for elucidating the role of SETD7 in various human diseases.

The SMYD (SET and MYND domain containing) family of proteins is uniquely defined by a SET domain that is split into two fragments by a zinc ion binding domain MYND (myeloid translocation protein-8, Nervy, and DEAF-1) and followed by a cysteine-rich post-SET domain.[49] The SMYD family of proteins might be important in developmental regulation, as the disruption of the *Smyd1* gene results in impaired cardiomyocyte maturation, flawed cardiac morphogenesis, and embryonic lethality in mice.[159] SMYD1 (also known as KMT3D) and SMYD3 (also known as KMT3E) modify chromatin structure through their H3K4-specific enzymatic methylation activity. SMYD3 has been shown to be involved in cancer cell proliferation and is overexpressed in most hepatocellular and colorectal carcinomas as well as breast cancer.[160,161] A recent report showed that the methylation of MAP3K2 by SMYD3 increases MAP kinase signaling and promotes the formation of Ras-driven carcinomas.[162] SMYD2 (also known as KMT3C) was reported to methylate H3K4 as well as H3K36.[146,163]

H3K36 methylation is another hallmark that is associated with transcriptional activation and in humans is controlled by PKMTs: NSD1, MMSET, WHSC1L1, SETD2, ASH1L, and SMYD2. SMYD2 has been shown to methylate the tumor suppressors p53[164] and Rb[165] in addition to histone H3. Very recently, SMYD2 has been demonstrated to be highly expressed in pediatric acute lymphoblastic leukemia and consitutes a poor prognostic indicator.[166] Overexpression of SMYD2 was also connected to tumor cell proliferation and resulted in malignant esophageal squamous cell carcinoma.[167]

In 2011, Ferguson et al. reported the discovery of **25** (AZ-505), a potent and selective inhibitor of SMYD2 (Figure 17).[168] HTS of a 1 230 000-compound collection resulted in the discovery of **25** with an IC_{50} of 0.12 μM and a K_d of 0.5 μM (by ITC). This inhibitor was around 700-fold selective for SMYD2 over six other PKMTs including closely related SMYD3 as well as G9a, GLP, SETD7, EZH2, and DOT1L. Michaelis–Menten kinetics studies revealed that **25** was competitive with a peptide substrate (361–380 of the C-terminal regulatory domain of p53) and noncompetitive with SAM. As mentioned previously, SMYD proteins comprise a unique split SET domain. The S-sequence and the core SET domain combine to form the catalytically active SET domain of SMYD2, and the MYND, I-SET, and post-SET domains surround the core SET domain.[168] To understand the structural basis of p53 recognition and inhibitor binding, a series of X-ray crystal structures of SMYD2 in complex with the cofactor SAM, a peptide substrate (366–378 of the C-terminal regulatory domain of p53), and/or **25** were obtained. There were no significant conformational changes observed on binding with the p53 peptide substrate or the inhibitor. The two residues that are highly conserved in SMYD proteins, Y240 and Y258, are very important for activity. While Y258 positions the amino group of the substrate lysine in the lysine binding channel, the hydroxyl group of Y240 is essential for the catalytic activity, as the mutation of this residue eradicates the catalytic activity of SMYD2, as shown by Brown et al.[146] Inhibitor **25** features three different functional groups: benzooxazinone, cyclohexyl, and dichlorophenethyl moieties (Figure 17). The benzooxazinone moiety lies deep in the lysine binding channel, interacting with Y258 as well as SAM. The cyclohexyl group is placed in the interface of the core SET and I-SET domains. The dichlorophenethyl moiety extends across the peptide binding groove and interacts with a secondary hydrophobic pocket. The X-ray co-crystal structures confirm that compound **25** is a substrate-competitive inhibitor (Figure 18). Cellular activities of **25** were not reported.

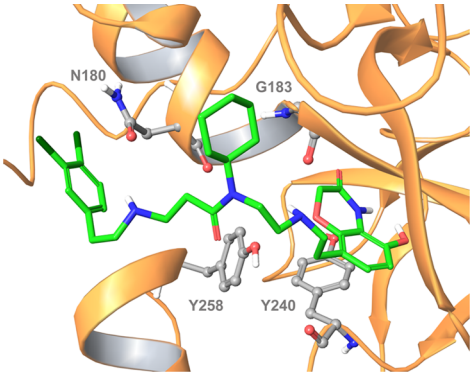

Figure 18. X-ray co-crystal structure of the SMYD2–**25** complex (PDB code: 3S7B).

More recently, **26** (LLY-507, Figure 17), a chemical probe of SMYD2, was discovered.[169] Compound **26**, which does not share a common scaffold with **25**, inhibited SMYD2 with an IC_{50} of less than 15 nM and was more than 100-fold selective over other methyltransferases and nonepigenetic targets. Importantly, inhibitor **26** is active in cells. It inhibited monomethylation of p53 K370 in cells with an IC_{50} of about 600 nM. Details of this SMYD2 chemical probe have not been reported.

Human SETD2 (SET domain containing 2, also known as KMT3A and SET2) has been shown to be a tumor suppressor associated with p53-dependent gene regulation, transcription elongation, and intron–exon splicing.[170−172] A recent study suggests that the disruption of SETD2 H3K36 trimethylation pathway is a distinct mechanism for leukemia development.[173] Evidence for the tumor suppressor role of SETD2 in human breast cancer was also provided.[171] The disruption of H3K36 trimethylation by loss-of-function SETD2 mutations has been suggested to be central to the genesis of hemispheric high-grade gliomas (HGGs) in older children and young adults.[174]

Zheng et al. designed and synthesized *N*-alkyl derivatives of sinefugin (**27**) (Figure 19), which is a close analogue of the

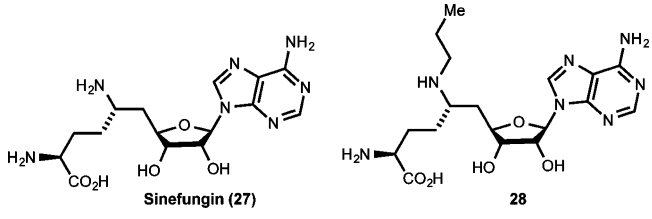

Figure 19. Structures of inhibitors **27** and **28**.

cofactor SAM and nonselective inhibitor of PMTs,[12] and tested them against various methyltransferases.[175] From this study, *n*-propyl sinefungin (**28**) (Pr-SNF) (Figures 17 and 19) was discovered as a selective inhibitor of SETD2 (IC_{50} = 0.8 ± 0.02 μM). **28** was highly selective for SETD2 over G9a, GLP, SETD8, EZH2, MLL, SUV39H2, SUV420H1, SUV420H2, PRMT3, DOT1L, and DNMT1.[175] It displayed modest

dx.doi.org/10.1021/jm501234a | J. Med. Chem. 2015, 58, 1596–1629

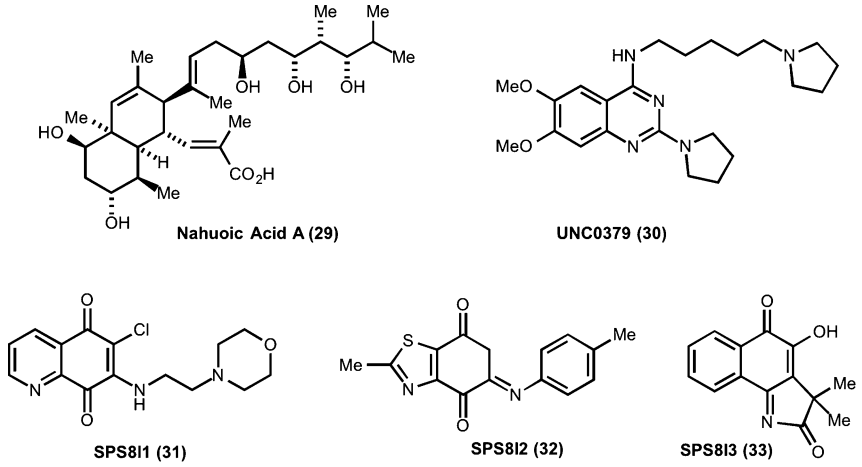

Figure 20. Structures of SETD8 inhibitors.

potency for SETD7 (IC_{50} = 2.2 ± 0.4 μM), CARM1 (IC_{50} = 3.0 ± 0.3 μM), and PRMT1 (IC_{50} = 9.5 ± 0.4 μM). The X-ray crystal structure of SETD2 in complex with **28** suggests that this inhibitor forms hydrogen bonds with the two backbone carbonyl groups in the SETD2 active open conformer, resulting in the observed selectivity for SETD2 over other methyltransferases. Findings from SAR studies also suggest that the lysine binding pocket of SETD2 is flexible enough to accommodate a large group such as the *n*-propyl group. Inhibitor **28** was further characterized using enzyme kinetics studies. The kinetic data obtained from these studies together with structural information revealed by the co-crystals suggest that the SETD2-catalyzed methylation goes through a random sequential mechanism and that inhibition occurs via either a **28**−SETD2 binary complex or a **28**−SETD2−substrate ternary complex. Cellular activities of compound **28** were not reported.

Inhibitors of H4K20 Methyltransferases. Methylation of H4K20, which is considered to be a transcriptionally repressive mark, is catalyzed by PKMTs: SUV420H1, SUV420H2, and SETD8 (SET domain containing (lysine methyltransferase) 8) in humans.[176] The latter, also known as SET8, PR-SET7, or KMT5A, is the sole methyltransferase that catalyzes monomethylation of H4K20.[176−178] SETD8 and H4K20me1 (H4K20 monomethylation) have been implicated in regulating a diverse set of biological processes including the DNA damage response, DNA replication, and mitotic condensation. In addition to H4K20, SETD8 methylates many nonhistone substrates including the tumor suppressor p53[27] and proliferating cell nuclear antigen (PCNA).[179] The monomethylation of p53 lysine 382 by SETD8 represses p53 target genes.[27] The monomethylation of PCNA by SETD8 at lysine 248 stabilizes PCNA protein and increases the interaction between PCNA and the flap endonuclease FEN1, which promotes the proliferation of cancer cells.[179]

The first selective inhibitor of SETD8 is a marine natural product nahuoic acid A (**29**) (Figure 20).[180] **29** inhibited SETD8 with an IC_{50} of 6.5 ± 0.5 μM and was competitive with the cofactor SAM (K_i = 2.0 ± 0.3 μM) and noncompetitive with the peptide substrate. It was selective for SETD8 over 10 other methyltransferases including G9a, GLP, SETD7, SUV39H2, SUV420H1, SUV420H2, PRMT3, PRMT5, CARM1, DOT1L, PRC2-EZH2, DNMT1, and MLL.

Very recently, Ma et al. reported the first substrate-competitive inhibitor of SETD8, **30** (UNC0379, Figure 20).[181,182] This small-molecule inhibitor was discovered by cross-screening of about 150 quinazoline-based compounds against SETD8. Compound **30** displayed inhibitory activity against SETD8 with micromolar potency in multiple biochemical assays. Binding of this inhibitor to SETD8 was confirmed by biophysical studies such as ITC and SPR. Importantly, **30** was selective for SETD8 over 15 other methyltransferases including G9a, GLP, SETDB1, SETD7, SUV39H2, SUV420H1, SUV420H2, PRC2−EZH2, MLL1, SMYD2, PRMT1, PRMT3, PRMT5, DOT1L, and DNMT1. In MOA studies, inhibitor **30** was competitive with the peptide substrate and noncompetitive with SAM. This MOA finding was confirmed using a peptide displacement assay.

However, in vitro potencies of **29** and **30** are modest, and cellular activities of these inhibitors have not been reported. In addition, selective inhibitors of SUV420H1 and SUV420H2, the other two H4K20 PKMTs, have not been published.

Most recently, another report on small-molecule inhibitors of SETD8 was published by Blum et al.[183] Screening of more than 5000 commercial compounds resulted in the discovery of three SETD8 inhibitors: **31** (SPS8I1, also known as NSC663284, IC_{50} = 0.21 ± 0.03 μM), **32** (SPS8I2, also as known as BVT948, IC_{50} = 0.50 ± 0.20 μM), and **33** (SPS8I3, as known as ryuvidine, IC_{50} = 0.70 ± 0.20 μM) (Figure 20).[183] The selectivity of these inhibitors was evaluated against other PMTs including SETD2, GLP, G9a, SMYD2, and SETD7 as well as PRMT1, PRMT3, and CARM1. Inhibitor **31** was only 2.5-fold selective over SMYD2 and >6-fold selective over other PMTs tested. Similarly, **32** showed modest selectivity over SETD2, G9a, SMYD2, CARM1, and PRMT3, whereas **33** was less selective. Further mechanistic studies suggested that **31** (substrate dependent), **32** (no substrate or SAM dependence), and **33** (both substrate and SAM dependent) inhibited SETD8 via distinct modes of action. Since structures of these three inhibitors shared a common quinonic motif, which could react with active cysteine residues, further mechanistic studies were performed. From these studies, it was concluded that **31**−**33** inhibited SETD8 via an irreversible slow-onset process. It is worth noting that other commercially available compounds containing a simple and related quinonic motif did not inhibit SETD8, suggesting that the full structures of these inhibitors are necessary for the inhibition. Cys270 of SETD8 was identified as the reactive residue for **31** and **32**, whereas **33** targeted cysteine residues in a nonspecific manner. In

dx.doi.org/10.1021/jm501234a | J. Med. Chem. 2015, 58, 1596−1629

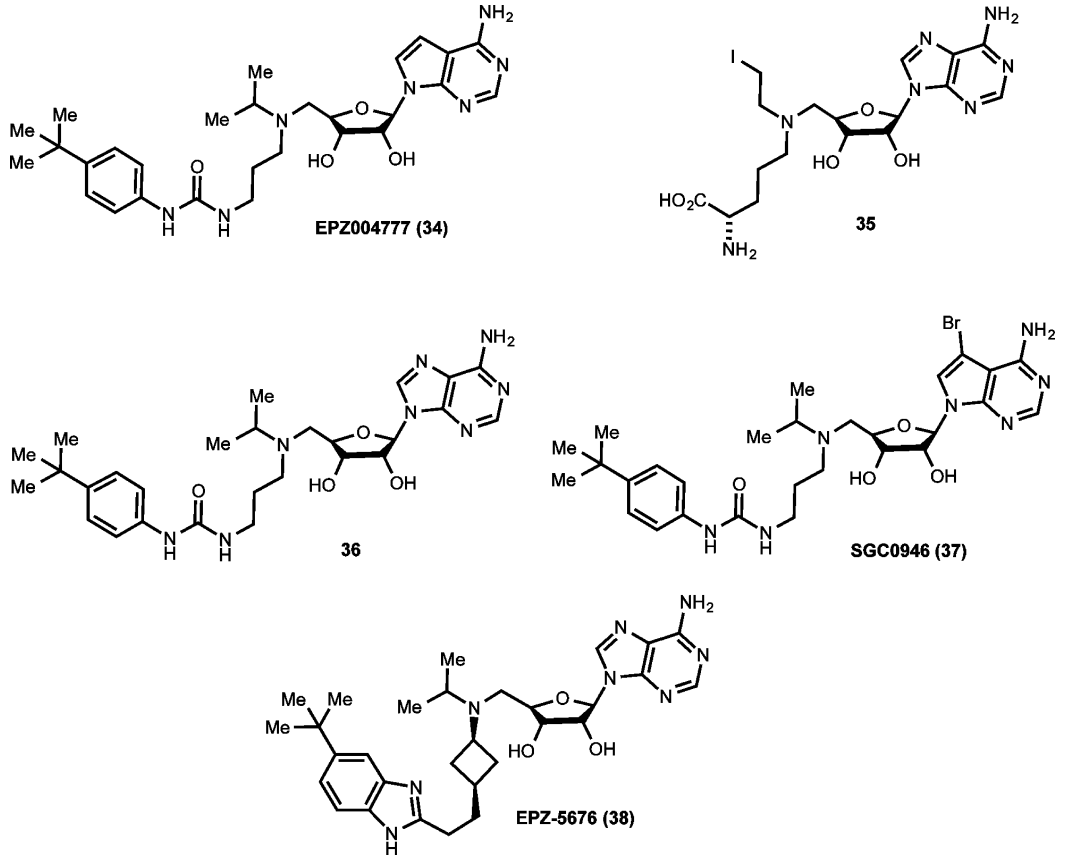

Figure 21. Structures of DOT1L inhibitors.

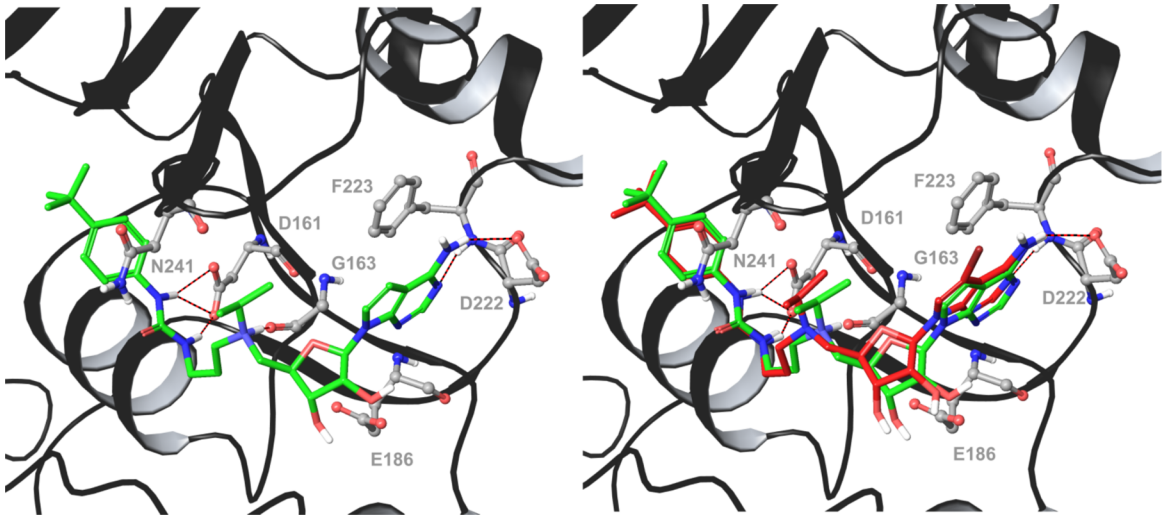

Figure 22. Co-crystal structure of DOT1L–**34** complex (PDB code: 4ER3) (left). Overlay of DOT1L–**34** and DOT1L–**37** complexes (PDB code: 4ER6) (right).

HEK293T cells, the H4K20me1 mark was reduced within 24 h of treatment with the inhibitors, whereas other histone marks (e.g., H4K20me2/3, H3K9me) were not affected. In addition, these inhibitors at 1–5 μM produced a cell cycle arrest phenotype, similar to that of SETD8 knockdown. However, off-target effects on other PMTs (**31** for SMYD2 and **33** for PRMT3 and SETD2) and other cellular targets (**31**, inhibition of Cdc25; **32**, inhibition of cyclin-dependent kinase 4 and 2 (CDK4/2); and **33**, inhibition of protein tyrosine phosphatase PTB1B) were observed and documented. Overall, compounds **31**–**33** are small-molecule irreversible inhibitors of SETD8. They exhibited modest selectivity and were active in cells.

Inhibitors of H3K79 Methyltransferases. DOT1L (disruptor of telomeric silencing 1-like) is the only PKMT identified in humans that does not contain the SET domain.[184] DOT1L, also known as KMT4, has a non-SET catalytic domain, which adopts a folding topology that is also observed in PRMTs and DNMTs.[185,186] It has been shown that DOT1L is responsible for mono-, di-, and trimethylation of H3K79.[184,187] Methylation of H3K79, which is generally

dx.doi.org/10.1021/jm501234a | J. Med. Chem. 2015, 58, 1596–1629

associated with transcriptional activation, has been linked with transcriptional regulation, DNA repair, embryonic development, cell cycle regulation, hematopoiesis, and cardiac function.[188−190] Importantly, DOT1L has been shown to interact with AF4, AF9, AF10, AF6, and ENL, the most commonly seen MLL fusion proteins in MLL-rearranged leukemias.[191−195] DOT1L interacts with these MLL fusion proteins and is recruited to their target genes including leukemogenic genes such as *HOXA9* and *MEIS1*.[188] These interactions result in abnormal methylation that drives leukemogenesis. Therefore, DOT1L has been considered as a potential therapeutic target for the treatment of MLL-rearranged leukemia.[12,196]

In 2011, Daigle et al. reported the first selective DOT1L inhibitor, **34** (EPZ004777), which was designed and synthesized based on the cofactor SAM and the crystal structure of the enzyme active site (Figure 21).[197] Inhibitor **34** displayed very high in vitro potency (IC_{50} = 400 ± 100 pM) and was remarkably selective (more than 1000-fold) for DOT1L over nine other PMTs including G9a, SETD7, WHSC1, EZH1, EZH2, PRMT1, PRMT5, PRMT8, and CARM1, despite being structurally close to SAM, the universal methyl donor for all methyltransferases. As expected, **34** was competitive with SAM and noncompetitive with the peptide substrate in MOA studies.[198] The very high binding affinity (K_i = 300 pM) of **34** was mainly driven by its slow off rate, leading to a very long residence time. The X-ray crystal structure of DOT1L−**34** published in 2012 (Figure 22) not only confirmed that **34** was a cofactor-competitive inhibitor[199] but also revealed that the high affinity and long residence time of **34** was driven by a ligand-induced conformational adaptation of DOT1L.[198]

A global reduction in H3K79me2 levels was observed in cell lines MOLM-13, MLL-AF9 (derived from human MLL-rearranged AML cell line), MV4-11, MLL-AF4 (MLL-rearranged biphenotypic leukemia), and Jurkat (non-MLL-rearranged T-cell acute leukemia) after the treatment with **34**.[197] The full effect on the reduction of H3K79me2 levels was observed in 4−5 days. H3K79me1 levels were also reduced by the inhibitor, whereas trimethylation levels could not be measured. In addition, no significant reduction of other histone methylation marks (e.g., H3K4me3, H3K9me3, H3K27me2, H3K27me3, H3K36me2, H4K20me2, H3R17me2a, H4R3me2s) was observed, suggesting that the cellular action of **34** is specific.

Compound **34** concentration-dependently inhibited the expression of *HOXA9* and *MEIS1*, the overexpression of which is the hallmark of MLL-rearranged leukemia.[197] The maximum reduction of *HOXA9* and *MEIS1* mRNA levels in MOLM-13 and MV4-11 cells was observed after 6−8 days of inhibitor treatment. In these cell lines, **34** exhibited a drastic antiproliferative effect, whereas Jurkat control cells were unaffected. It is worth mentioning that a significant delay (6−8 days) was observed for the antiproliferative effect, consistent with the time course of this inhibitor's effect on *HOXA9* and *MEIS1*. Furthermore, **34** displayed an antiproliferative effect against six other MLL-rearranged leukemia cell lines with low micromolar potencies, but it was largely ineffective in six non-MLL-rearranged leukemia cell lines (IC_{50} > 10 μM). In addition, GSEA of the genes up- and downregulated in the treated MV4-11 and MOLM-13 cells suggests that DOT1L inhibition by **34** reverses the MLL-rearranged leukemia gene signature. Taken together, these results suggest that the DOT1L methyltransferase activity is essential for the proliferation of MLL-rearranged leukemia cells and MLL fusion mediated transformation but is nonessential for the proliferation of non-MLL-rearranged leukemia cells.

Importantly, continuous infusion of **34** via an implanted osmotic minipump for 14 days dose-dependently increased survival in NSG (NOD scid gamma) mice after intravenous injection of MV4-11 cells. The H3K79me2 levels in subcutaneous MV4-11 tumors derived from **34**-treated animals were significantly reduced. Thus, it was demonstrated for the first time that selective inhibition of DOT1L's methyltransferase activity had antitumor activity in animal models of MLL-rearranged leukemia.[197,200] These results highlight a clinical potential of selective DOT1L inhibition as a means for treating MLL-rearranged leukemia.

Shortly after the publication of inhibitor **34**, Yao et al. reported the discovery of compound **35** (Figure 21), a selective, mechanism-based inhibitor of DOT1L.[201] This inhibitor displayed high in vitro potency for DOT1L (IC_{50} = 38 nM) and was more than 29-fold selective for DOT1L over other methyltransferases tested: CARM1, PRMT1, G9a, and SUV39H1. It was suggested that compound **35** would undergo an intramolecular cyclization to form a reactive aziridinium intermediate, which would further react with the ε-NH_2 group of the lysine 79 to covalently link to H3K79. In addition, Yao et al. noticed that the 6-NH_2 group of SAM (adenosine moiety NH_2 group) forms only one hydrogen bond with the enzyme and that there is a relatively large hydrophobic pocket available in the co-crystal structure of the DOT1L−SAM complex. On the other hand, SET domain-containing PKMTs such as G9a form two hydrogen bonds with the 6-NH_2 group. Therefore, Yao et al. designed and synthesized 6-*N*-methyl SAH and found that it was indeed highly selective for DOT1L (K_i = 290 nM) over CARM1, PRMT1, G9a, and SUV39H1 (K_i > 20 000 nM). The X-ray crystal structure of DOT1L in complex with 6-*N*-methyl SAH confirms that the *N*-methyl group sits in the hydrophobic pocket. Activities of these DOT1L inhibitors in cell-based assays were not reported.

In a continuation of this work, Anglin et al. reported extensive SAR studies, which led to the discovery of compound **36** (Figure 21).[202] Compound **36** had high in vitro potency (K_i = 0.46 nM) and was more than 4500-fold selective for DOT1L over CARM1, PRMT1, and SUV39H1. An alkyl group such as methyl, ally, and benzyl on the 6-amino group was well-tolerated (DOTL1L K_i of 0.76, 12, and 22 nM, respectively) and led to high selectivity for DOT1L. Compound **36** inhibited the proliferation of MV4-11 cells with a slow onset of activity, but it did not affect the proliferation of NB4 cells, which harbor wild-type MLL.

Yu et al., in December 2012, reported a chemical probe of DOT1L with improved in vitro and cellular potencies.[199] The co-crystal structure of DOT1L−**34** that they obtained revealed remodeling of the catalytic site (Figure 22),[199] consistent with the ligand-induced conformational adaptation reported by Basavapathruni et al.[198] It was noticed that a hydrophobic cleft near the 7-position of the deazaadenosine moiety was not exploited. Therefore, a focused set of analogues aimed at exploiting this hydrophobic pocket was synthesized, resulting in the discovery of **37** (SGC0946), which has a bromo substitution at the 7-position of the deazaadenosine ring (Figure 21).[199] This inhibitor was more potent than **34** in biochemical and biophysical assays (e.g., K_d = 0.06 nM versus 0.25 nM in SPR).[199] Similar to **34**, compound **37** was highly selective for DOT1L over 13 other methyltransferases including

G9a, GLP, SUV39H2, SUV420H1, SUV420H2, MLL, SETDB1, SETD7, SETD8, PRC2−EZH2, PRMT3, PRMT5, and DNMT1. **37** was also almost 10-fold more potent at reducing H3K79 methylation levels in MCF10A cells, with an IC_{50} of 8.8 ± 1.6 nM, than that of **34** (IC_{50} = 84 ± 20 nM). Furthermore, **37** (at 1 μM) was more effective than **34** at killing human cord blood cells transformed with an MLL−AF9 fusion oncogene, whereas it (at 1 and 5 μM) did not affect viability of cord blood cells transformed with an unrelated oncogene, TLS-ERG.

In 2013, Daigle et al. reported a new DOT1L inhibitor, **38** (EPZ-5676), as a result of their structure-guided design and optimization of the compound **34** series (Figure 21).[203] The X-ray co-crystal structure of **38** in complex with DOT1L clearly showed that the inhibitor occupied the SAM binding pocket and induced conformational changes in DOT1L (PDB code: 4HRA). Compound **38** inhibited DOT1L with a Morrison K_i of 0.08 ± 0.03 nM, which is more potent than that of **34** (Morrison K_i = 0.3 ± 0.02 nM). It was more than 37 000-fold selective for DOT1L over 16 other PMTs including G9a, GLP, SETD7, SMYD2, SMYD3, MMSET, WHSC1L1, PRMTs (1, 3, 4, 5, 6, and 8), EZH1, and EZH2.

Inhibitor **38** reduced H3K79me2 levels in MV4-11 cells (a MLL-AF4 expressing acute leukemia cell line) with an IC_{50} of 3 nM and in HL-60 cells (a non-MLL-rearranged cell line) with a similar potency.[203] More than 90% reduction of H3K79me2 was observed in 3−4 days. H3K79me1 levels were also reduced. On the other hand, no significant reduction of other histone methylation marks (H3K4me3, H3K9me3, H3K27me2, H3K27me3, H3K36me2, H4K20me2, H3R17me2a, and H4R3me2s) was observed. This finding is consistent with the high in vitro selectivity of compound **38**. Additionally, **38** concentration-dependently inhibited *HOXA9* and *MEIS1* mRNA levels in MV4-11 cells. The maximum reduction was observed after 8 days of treatment.

The proliferation of MV4-11 cells treated with **38** for 14 days was inhibited with an IC_{50} of 3.5 nM. The antiproliferative activity was observed as early as 4 days, but it reached a maximum at day 7. This delayed onset of activity is likely due to a cascade of epigenetic events including the depletion of the H3K79me2 mark, inhibition of MLL fusion target gene expression, and a reversal in leukemogenic gene expression.[197,204,205] In addition, **38** exhibited nanomolar antiproliferative activity against most of other MLL-rearranged cell lines tested but weaker potencies against non-MLL-rearranged cell lines. Importantly, continuous intravenous (IV) infusion of **38** at 70 mg/kg per day for 21 days resulted in complete elimination of the established subcutaneous (SC) MV4-11 tumors in immunocompromised rats. The tumor regression was sustained for more than 30 days after the cessation of compound **38** treatment. All doses were well-tolerated by the test animals, and no significant body weight loss was observed. Furthermore, H3K79me2 levels and *HOXA9* and *MEIS1* mRNA levels were significantly reduced in MV4-11 SC xenograft tissue harvested from rats dosed by continuous IV infusion for 14 days. Inhibition of H3K79 methylation was also observed in bone marrow cells and PBMCs isolated from the same rats. Taken together, these results suggest that **38** displays on-target activity in vivo and has a potential to be an effective therapeutics for the treatment of MLL-rearranged leukemia. In 2013, compound **38** became the first PMT inhibitor advanced to the clinic, a watershed event in the PMT inhibitor field. It is currently being evaluated in phase 1 clinical trials for the treatment of AML and ALL.[206,207]

PROTEIN ARGININE METHYLTRANSFERASES

Protein arginine methylation catalyzed by PRMTs is another important and common type of PTM in eukaryotic cells.[208−210] Arginine is unique among amino acids with its ability to form interactions via its five potential hydrogen-bond donors with surrounding hydrogen-bond acceptors. Every methylation of arginine would take away a potential hydrogen bond as well as create steric bulkiness and increased hydrophobicity. Importantly, methylation does not neutralize the cationic charge of arginine residues, and it was suggested that methylation could enhance their interactions toward aromatic rings via cation−π interactions.[211] Thus, methylation of arginine residues in proteins can change their recognition and in turn affect their physiological functions.[212]

Nine PRMTs have been identified to date, and they are responsible for mono- and/or dimethylation of the guanidino group of arginine.[208] As we mentioned earlier, there are two possible ways for dimethylation to occur after monomethylation of arginine (MMA): either by methylating the same nitrogen, yielding asymmetrical dimethyl arginine (aDMA), or by methylating another nitrogen to give symmetrical dimethyl arginine (sDMA) (Scheme 1). On the basis of their methylation functions, PRMTs are divided into three categories: type I, type II, and type III.[213] Type I PRMTs, which include PRMT1 (protein arginine methyltransferase 1), PRMT2, PRMT3, CARM1 (coactivator-associated arginine methyltransferase 1, also known as PRMT4), PRMT6, and PRMT8, catalyze monomethylation and asymmetric dimethylation of arginine. On the other hand, PRMT5 is a type II PRMT that catalyzes monomethylation and symmetrical dimethylation of arginine. PRMT7 is categorized as a type III PRMT, as it catalyzes monomethylation of arginine only. PRMT9 (also known as F-box only protein 11 (FBXO11)) has not been classified yet because its activity has not been fully characterized.

All PRMTs contain a conserved core region of about 310 amino acids.[214] They typically have additions to the N-terminus with the exception of CARM1, which also has C-terminal additions.[31] The monomeric structure of the PRMT core comprises a MTase domain, a β-barrel[214] that is unique to PRMTs, and a dimerization arm. A homodimeric structure was observed in PRMT1 and PRMT3, and it has been suggested that dimer formation is a conserved feature for PRMTs.[214,215] PRMTs generally methylate glycine and arginine-rich (GAR) motifs in their substrates[210] with the exception of CARM1, which specifically methylates proline, glycine, and methionine-rich (PGM) motifs.[216,217] PRMT5, on the other hand, can symmetrically dimethylate both of these motifs.[218] In addition to histones, PRMTs methylate nonhistone proteins.[208,212,219] Dysregulation of PRMTs and arginine methylation have been implicated in cancer and other diseases.[208,213]

INHIBITORS OF PRMTS

Inhibitors of PRMT1/PRMTs. PRMT1 was the first mammalian protein arginine methyltransferase identified.[220] It has been shown that PRMT1 is responsible for most of the type I arginine methyltransferase activity in mammalian cells.[221] PRMT1 catalyzes asymmetrical dimethylation of H4R3 (H4R3me2a), which is associated with transcriptional activa-

dx.doi.org/10.1021/jm501234a | J. Med. Chem. 2015, 58, 1596−1629

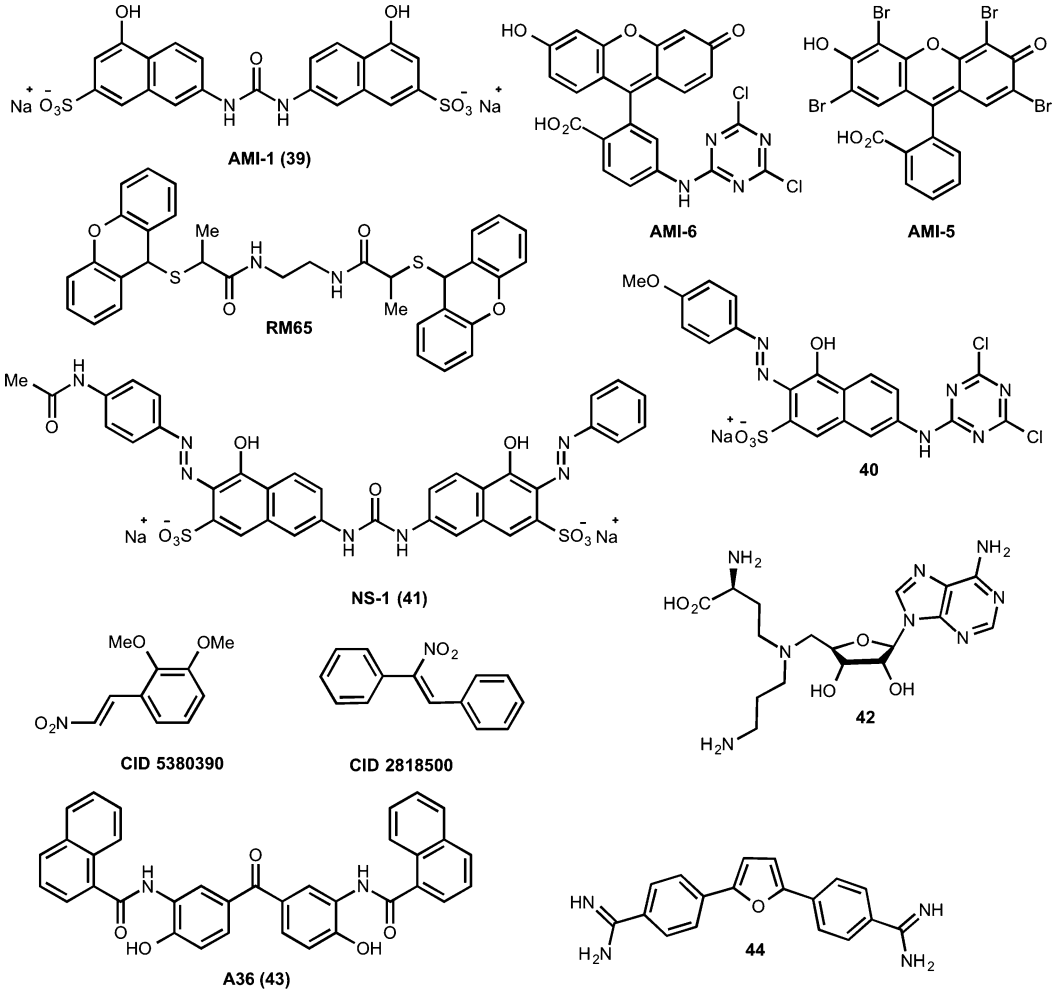

Figure 23. Structures of small-molecule inhibitors of PRMT1/PRMTs.

tion.[222,223] Overexpression as well as aberrant splicing of PRMT1 has been implicated in diseases such as breast, prostate, lung, colon, and bladder cancers and leukemia.[224−235] Additionally, PRMT1 has been associated with human telomeres[236] and shown to directly regulate the AKT signaling pathway.[237,238] Large numbers of nonhistone substrates such as DNA repair proteins MRE11,[239] p53 binding protein 1 (53BP1),[240] ASH2L,[241] and the tumor suppressor BRCA1[242] have been identified for PRMT1.

Even though there has been continuous interest in the discovery of selective PRMT1 inhibitors over the past decade, most of the reported PRMT1 inhibitors (Figure 2 and Table 2) lack sufficient potency and selectivity against a broad panel of PMTs, thus limiting their potential use in functional studies.

In 2004, Cheng et al. reported the discovery of the first small-molecule inhibitors of PRMTs, named AMIs (arginine methyltransferase inhibitors), by HTS of a 9000-compound library.[243] Among the nine hits identified, only **39** (AMI-1), a symmetrical sulfonated urea salt, and AMI-6 (Figure 23) showed specificity for PRMTs over PKMTs.[243] Compound **39** inhibited PRMT1 with an IC_{50} of 8.8 μM. Further studies demonstrated that it was not competitive with SAM. Therefore, it was suggested that this inhibitor binds in the substrate binding pocket. It was reported that **39** inhibited the methylation of Npl3p in HeLA cells in a concentration-dependent manner. In 2007, Ragno et al. published their structure- and ligand-based modeling studies on AMIs and their close analogues, and, although AMI-5 was confirmed to be a PRMT1 inhibitor (IC_{50} = 1.4 μM), selectivity of these inhibitors was not reported (Figure 23).[244] In the same year, a target-based approach[245] to discover inhibitors of PRMTs by Spannhoff et al. resulted in PRMT inhibitors Stilbamidine and Allantodapsone with IC_{50}'s of 57 ± 6.2 and 1.7 ± 3 μM for PRMT1, respectively.[246] Spannhoff et al. also reported the PRMT1 inhibitor RM65 (IC_{50} = 55 ± 3.4 μM) (Figure 23), which was identified via virtual screening.[247] Again, no selectivity data was shown for these inhibitors. A similar virtual screening approach was also reported by Heinke et al.[248]

In an effort to develop more potent inhibitors of PRMTs, Bonham et al. discovered compound **40**, which inhibited PRMT1 (IC_{50} = 4.2 ± 1.6 μM) and CARM1 (IC_{50} = 2.6 ± 0.6 μM).[249] However, **40** (Figure 23) also inhibited PRMT5, PRMT6, and PRMT8 even though it was selective against SETD7. In the same year (2010), Feng et al. reported the discovery of compound **41**, named NS1 (naphthalene-sulfo derivative 1), via virtual screening of 400 000 compounds (Figure 23).[250] Compound **41** inhibited PRMT1 with an IC_{50} of 13 ± 0.1 μM. MOA studies suggested that this inhibitor was competitive with the substrate with a K_i of 1.7 ± 0.54 μM. However, even though **41** did not inhibit CARM1, it inhibited PRMT3 and PRMT6 with similar potencies.

dx.doi.org/10.1021/jm501234a | J. Med. Chem. 2015, 58, 1596−1629

In 2011, Dowden et al. reported a SAM derivative as a PRMT1 inhibitor. Compound **42** inhibited PRMT1 with an IC_{50} of 3.9 ± 1.8 μM and was inactive against CARM1 and SETD7 (Figure 23).[251] In 2012, Dillon et al. reported the discovery of two mechanism-based inhibitors, CID 5380390 and CID 2818500 (Figure 23), which inhibited PRMT1 and PRMT8, the only two PRMTs that contain a reactive cysteine in their active sites.[252] These inhibitors were inactive against CARM1 and SETD7. In the same year, Wang et al. reported the discovery of PRMT1 inhibitor **43** (A36) via pharmacophore-based virtual screening (Figure 23).[253] Compound **43** inhibited PRMT1 with an IC_{50} of 12 ± 0.2 μM. It was about 7-fold more potent for PRMT1 over CARM1, but it was only 2-fold more potent over PRMT5. It was suggested that **43** was a substrate-competitive inhibitor. In 2014, Yan et al. reported compound **44**, a diamidine containing PRMT1 inhibitor (Figure 23).[254] It inhibited PRMT1 with an IC_{50} of 9.4 ± 1.1 μM and was selective for PRMT1 over CARM1 (more than 42-fold), PRMT5 (around 18-fold), and PRMT6 (around 30-fold). Compound **44** inhibited the proliferation of several leukemia cell lines. It was also found that cell lines derived from Down syndrome patients and MLL-AF9 patients (CMY, CHRF-288-1, and MOLM-13 cells) were more sensitive to compound **44** treatment than other cell lines tested (HEL, Jurkat, and HL-60).

Inhibitors of PRMT3. PRMT3 (protein arginine methyltransferase 3) was first reported in 1998.[255] This type I PRMT is located mainly in cytosol and has a zinc finger domain at its N-terminus. The primary substrate of PRMT3 is 40S ribosomal protein S2 (rpS2).[256,257] Asymmetric dimethylation of rpS2 by PRMT3 results in stabilization of rpS2 and influences ribosomal biosynthesis.[256−259] PRMT3 has also been reported to methylate the recombinant mammalian nuclear poly(A)-binding protein (PABPN1)[260−262] and a histone peptide (H4 1−24) in vitro.[263] The protein complex consisting of PRMT3, the von Hippel-Lindau (VHL) tumor suppressor, and ARF (alternative reading frame) has been shown to methylate the tumor suppressor p53.[264] In addition, the tumor suppressor DAL-1 (differentially expressed in adenocarcinoma of the lung-1) inhibits the methyltransferase activity of PRMT3 by interacting with it, suggesting that DAL-1 may affect tumor growth by regulating PRMT3 function.[265] Epigenetic down-regulation of DAL-1 has been associated with a number of cancers.[266−268] Furthermore, PRMT3 expression levels are elevated in myocardial tissues from patients with atherosclerosis,[269] potentially implicating the involvement of PRMT3. Additionally, PRMT3 function has been reported to be essential for dendritic spine maturation in rats.[270]

In 2012, Siarheyeva et al. reported the discovery of the first selective PRMT3 inhibitor, compound **45** (Figure 24), via screening a library of 16 000 diversity compounds.[271]

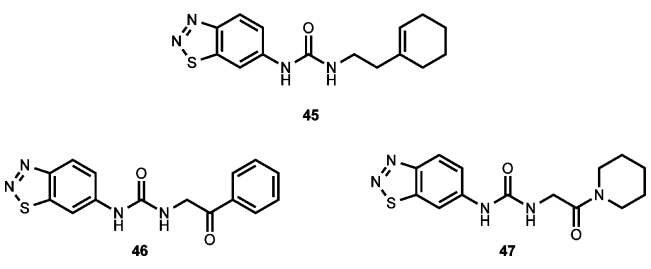

Figure 24. Structures of PRMT3 inhibitors.

Compound **45** inhibited PRMT3 with an IC_{50} of 1.6 ± 0.3 μM and was selective for PRMT3 over other methyltransferases including G9a, GLP, SUV39H2, SETD7, SETD8, PRMT1, CARM1, PRMT5, and PRMT8. This inhibitor displayed rapid on and off rates with K_d of 9.5 ± 0.5 μM. Interestingly, in MOA studies, this inhibitor was noncompetitive with both SAM and the peptide substrate. The X-ray crystal structure of the PRMT3−inhibitor **45** complex reveals that it occupies a novel allosteric binding site located at the interface of the two subunits of the PRMT3 homodimer (Figure 25). The cyclohexenyl moiety interacts with the alpha-Y segment of the activation helix of the opposite subunit. This interaction most likely leads to the alpha-X segment becoming disordered. It has been shown that the proper folding of the alpha-X segment is crucial for both cofactor and substrate binding. Thus, it is most likely that the binding of **45** to the allosteric site prevents the proper positioning/folding of the alpha-X segment, which in turn inhibits the enzymatic activity of PRMT3. Other key ligand−protein interactions revealed by the co-crystal structure include (1) a hydrogen bond between the middle nitrogen of the tightly fit benzothiadiazole moiety with the hydroxyl group of T466, (2) two hydrogen bonds between the two nitrogens of the central urea moiety and the carboxylate group of E422, (3) and a hydrogen bond between the oxygen of the urea moiety with the guanidinium group of R396 (Figure 25). The key hydrogen-bond interactions were confirmed by SAR studies in addition to site-directed mutagenesis studies.

Subsequent SAR studies by Liu et al. resulted in the discovery of more potent inhibitors compounds **46** (IC_{50} = 0.48 μM) and **47** (IC_{50} = 0.23 μM) (Figure 24).[272] These inhibitors possess the same benzothiodiazole and urea moieties but differ in the right-hand side functional group. Compound **46** contains a benzoyl group, whereas compound **47** has a piperidinyl amide. Similar to **45**, compound **46** showed excellent selectivity for PRMT3 over other methyltransferases including G9a, GLP, SUV39H2, PRMT5, SETD7, PRC2, SETD8, SETDB1, SUV420H1, SUV420H2, MLL1, SMYD3, SMYD2, DOT1L, and DNMT1. The crystal structure of the PRMT3−**46** complex confirmed that this inhibitor occupies the same allosteric binding site. Cellular activities of compounds **46** and **47** were not reported. Taken together, these results suggest that the allosteric binding site of PRMT3 can be exploited to yield potent and selective inhibitors.

Inhibitors of CARM1 (PRMT4). Co-activator-associated arginine methyltransferase 1 (CARM1, also known as PRMT4) activates the transcription by asymmetric dimethylation of H3R17.[273,274] It was first identified as a steroid receptor coactivator and was the first member of the PRMTs to be associated with transcriptional regulation.[273] The loss of CARM1 results in neonatal lethality, evidenced by the death of newborn knockout mice shortly after birth.[275] CARM1 has been shown to be involved in mRNA splicing,[276] RNA processing and stability,[275] cell cycle progression,[277] and DNA damage response.[278] In addition to histones, CARM1 methylates a variety of proteins such as CBP/p300, PABP, HuR, HuD, CA150, SAP49, SmB, and U1C.[276,279−282] CARM1 levels have shown to be elevated in castration-resistant prostate cancer[283,284] and aggressive breast tumors.[277] Because of the involvement of CARM1 in a wide variety of biological processes and diseases,[213] it has been pursued as a potential therapeutic target.

dx.doi.org/10.1021/jm501234a | J. Med. Chem. 2015, 58, 1596−1629

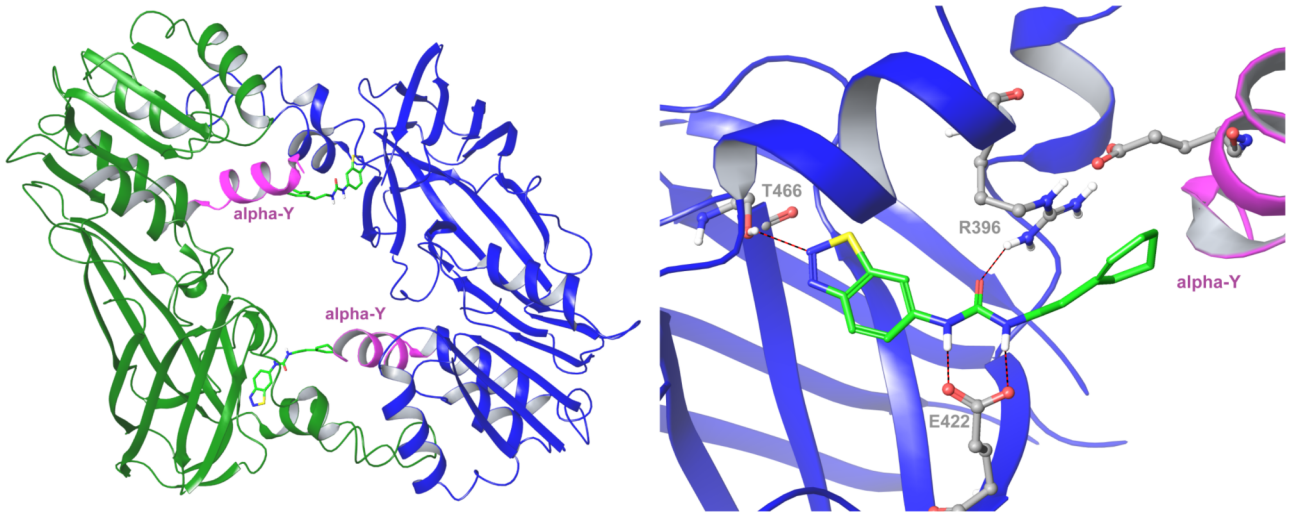

Figure 25. Co-crystal structure of the dimeric PRMT3−**45** complex (PDB code: 3SMQ) (left). Allosteric binding pocket and key interactions of **45** with PRMT3 (right).

Huynh et al. reported the discovery of the CARM1 inhibitor compound **48** (Figure 26) via optimization of a pyrrazole

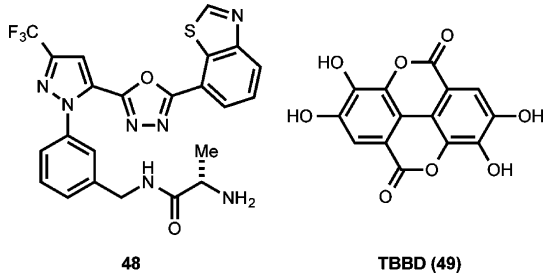

Figure 26. Structures of selected inhibitors of CARM1 (PRMT4).

containing hit, which was identified by a HTS campaign.[285−287] This inhibitor was potent with an IC_{50} of 40 nM and more than 600-fold selective for CARM1 over PRMT1 and PRMT3. However, additional selectivity, MOA, and cellular activity data were not reported. Therrien et al. also reported the discovery of potent CARM1 inhibitors, which were based on the reported pyrrazole core.[288,289] However, these inhibitors lack significant cellular activity.

In 2010, Selvi et al. identified a CARM1 inhibitor, TBBD (ellagic acid, **49**), which was isolated from pomegranate crude extract (Figure 26).[290] Compound **49** concentration-dependently inhibited CARM1, but it did not inhibit G9a and histone acetyltransferase CBP/p300. It was demonstrated by using Lineweaver−Burk plots that **49** was noncompetitive with both H3 and SAM. However, ITC experiments showed minimal interaction between **49** and CARM1 alone. It was suggested that the partial inhibition of CARM1 by **49** could be mediated via its interaction with the enzyme−substrate complex. Inhibitor **49** at 5 μM reduced more than 50% of H3R17 methylation. In addition, **49** significantly reduced expression levels of *p21* in H1299 and HEK293T cells but not in HeLa cells.

■ CONCLUSIONS AND FUTURE DIRECTIONS

As we discussed throughout this perspective, a growing body of evidence suggests that protein methyltransferases play a key role in the regulation of transcriptional activity and are implicated in cancer and many other human diseases. Due to these key functions, there has been a steadily growing interest in pursuing these enzymes as potential therapeutic targets. Therefore, discovery of selective, small-molecule inhibitors of these methyltransferases has become a very active area of research over the past decade. There has been tremendous progress in the PMT inhibitor field as a result of collective advances made in assay development, high-throughput screening, structural biology, and medicinal chemistry. This research area was kicked off by the reports of the first PKMT inhibitor chaetocin in 2005 and the first PRMT inhibitor **39** in 2004 and culminated by the initiations of human clinical trials for the DOT1L inhibitor **38** in 2012 and the EZH2 inhibitors **22** in 2013 and **19** in 2014. Highly potent, selective, well-characterized chemical probes with robust on-target activities in cells have been developed. These chemical probes including **11**, **12**, **18**, **19**, **20**, **21**, **22**, **34**, **37**, and **38** are valuable tools for further investigating the biological functions of the targeted enzymes and assessing the potential of these proteins as therapeutic targets. The discoveries of substrate-competitive inhibitors of G9a/GLP (e.g., **6**, **11**, **12**, **16**), SMYD2 (**25** and **26**), SETD8 (**30**), and SETD7 (**24**) suggest that the substrate binding groove of PKMTs can be targeted to yield potent and selective inhibitors. Similarly, the discoveries of highly potent, selective, and SAM-competitive inhibitors of DOT1L (e.g., **34**, **37**, **38**) and EZH2 (e.g., **18**, **19**, **20**, **21**, **22**) provided experimental evidence that extremely high selectivity can be achieved by targeting the SAM binding site of PKMTs, which is analogous to targeting the ATP binding site of protein kinases. In addition, the discovery of the PRMT3 allosteric inhibitors (e.g., **46** and **47**) suggests that the allosteric binding site of PRMT3 and potentially other PRMTs can be exploited to create potent and selective inhibitors.

Despite the significant progress that has been made over last 10 years, there is much to be done in the PMT inhibitor field. We highlight a few challenges and opportunities in this area. First and foremost, a systematical coverage of PMTs as a protein family with potent and selective inhibitors is needed. Currently, many individual targets and subgroups of targets on the PMT phylogenetic tree lack selective inhibitors (Figure 2). For example, there are no selective inhibitors reported for SMYD3, MMSET (NSD2), and PRMT5, which are potentially

dx.doi.org/10.1021/jm501234a | J. Med. Chem. 2015, 58, 1596−1629

important therapeutic targets. Potent, selective, and cell-penetrant inhibitors of these PMTs would be invaluable tools for therapeutic hypothesis testing and target validation. On the other hand, there is limited understanding of biological functions and potential disease implications for many PMTs on the phylogenetic tree, and no selective inhibitors have been reported for many of these targets (e.g., PRDMs). Chemical probes of these proteins that have sufficient potency, selectivity, and cell permeability would be extremely valuable for investigating and understanding their biological functions. Second, thorough characterization in biochemical, biophysical, and cellular assays is needed for some of the existing inhibitors and future inhibitors. While the chemical probes discussed earlier were well-characterized, a number of other inhibitors need to be thoroughly characterized. For the inhibitors to be used in in vitro studies, in addition to activities in biochemical assays, a direct interaction between the target and the small-molecule inhibitor should be demonstrated by a biophysical method (e.g., ITC, SPR) or by a NMR solution or X-ray crystal structure of the protein−ligand complex. Selectivity of these inhibitors for the target PMT(s) over a broad panel of other methyltransferases should also be assessed and achieved. For the inhibitors to be used in cellular studies, sufficient cell permeability and target engagement in cells should be demonstrated in addition to the in vitro target engagement and selectivity described above. These characterizations are necessary for associating the observed biological effects with the inhibition of the target PMT(s) by the ligands. Third, it has been challenging to discover potent, selective, and cell-penetrant inhibitors of PRMTs. A breakthrough in this area will be truly exciting and is keenly awaited. Fourth, understanding of the molecular basis for high subtype selectivity is needed. While the ligand-induced DOT1L conformation adaptation provides an excellent explanation for the extremely high selectivity observed for DOT1L inhibitors **34** and **37**,[198,199] there is no satisfactory explanation for the high selectivity (>150-fold) of **19** for EZH2 over EZH1, as EZH2 and EZH1 share 96% sequence identity in their SET domains. High-resolution structures of the EZH2−inhibitor and EZH1−inhibitor complexes would likely shed light on how such high subtype selectivity is achieved. It would also be valuable to demonstrate that this level of high selectivity can be achieved for other closely related PKMTs. For example, G9a and GLP share 80% sequence identity in their SET domains, and all reported inhibitors have similar potencies for both G9a and GLP. A highly selective G9a or GLP inhibitor would be a useful tool for dissecting the role of G9a or GLP in biological systems. Fifth, improvement on PK properties of several in vivo probes would be beneficial. As described earlier, the development of inhibitor **38**, the first PKMT clinical candidate, was a watershed event in the field. However, continuous intravenous infusion of this DOT1L inhibitor via an osmotic minipump was required to achieve sustained tumor regression. The next generation of DOT1L inhibitors that are orally bioavailable would be beneficial for patients. It would be interesting to see whether good oral bioavailability can be achieved for the inhibitors derived from the SAM scaffold. Similarly, improvement on plasma exposure and therapeutic window of **12**, the first in vivo chemical probe of G9a and GLP, would make it more suitable for chronic animal studies. Sixth, there are opportunities to generate chemical tools such as biotinylated ligands of PMTs by exploiting recently developed high-affinity inhibitors. These tools would be very useful in chemical biology studies such as chemoproteomics, chem−ChIP, and Chem−Seq.

In this perspective, we highlight the key progress on the discovery, characterization, and application of selective PMT inhibitors for investigating physiological functions and disease implications of the target PMTs. We also discuss challenges and future directions and opportunities in the PMT inhibitor field. It is our hope that this perspective will inspire new and original discoveries. Over the last 10 years, we have witnessed amazing progress in this emerging research field, culminated by three PKMT inhibitors entering clinical trials in 2012−2014. It is anticipated that the next 10 years will be even more exciting for this now very active area. The biomedical community eagerly awaits the clinical successes of selective PMT inhibitors and discoveries of many potent, selective, cell-penetrant, first-in-class PMT inhibitors.

AUTHOR INFORMATION

Corresponding Author

*Phone: 212-659-8699. E-mail: jian.jin@mssm.edu.

Notes

The authors declare no competing financial interest.

Biographies

H. Ümit Kaniskan earned his Ph.D. in organic chemistry at Case Western Reserve University under the supervision of Dr. Philip Garner. During his doctoral study, he completed the formal total synthesis of Bioxalomycin β2 and Cyanocycline A. He then pursued his postdoctoral studies in Dr. Movassaghi's group at Massachusetts Institute of Technology, while working on synthesis of Myrmicarin alkaloids. In January 2013, Dr. Kaniskan joined Dr. Jin's laboratory at the Center for Integrative Chemical Biology and Drug Discovery and later at the Icahn School of Medicine at Mount Sinai as a postdoctoral research associate in the Structural and Chemical Biology department. He is currently focusing his research on discovering functionally selective ligands of G protein-coupled receptors and chemical probes of histone methyltransferases.

Kyle D. Konze received a Bachelor of Biomedical Engineering from the University of Minnesota in 2011. He conducted undergraduate research in computer-aided drug design in the laboratory of Dr. Yuk Sham. He is currently a graduate student in the division of Chemical Biology and Medicinal Chemistry at the University of North Carolina at Chapel Hill and pursuing his Ph.D. in the laboratory of Dr. Jian Jin. His dissertation research is focused on the discovery and design of small-molecule chemical probes for protein lysine methyltransferases. His research has resulted in two first-author publications to date. Most recently, he has been awarded with a prestigious predoctoral fellowship from the Medicinal Chemistry Division of the American Chemical Society.

Jian Jin received a Ph.D. degree in synthetic organic chemistry from Pennsylvania State University and completed postdoctoral training at The Ohio State University. He joined GlaxoSmithKline in 1998 and was a manager of medicinal chemistry from 2003 to 2008. In 2008, Dr. Jin joined the University of North Carolina at Chapel Hill as a faculty member and served as an associate director of medicinal chemistry in the Center for Integrative Chemical Biology and Drug Discovery. In 2014, Dr. Jin joined Icahn School of Medicine at Mount Sinai as a Professor of Structural and Chemical Biology, Oncological Sciences, and Pharmacology. Over the last 6 years, Dr. Jin's laboratory has focused on discovering chemical probes of protein methyltransferases and functionally selective ligands of G protein-coupled receptors.

■ ACKNOWLEDGMENTS

This work was supported by grant R01GM103893 (to J.J.) from the National Institute of General Medical Sciences of the U.S. National Institutes of Health. H.Ü.K. was supported by a postdoctoral fellowship from the Structural Genomics Consortium. K.D.K. was supported by a predoctoral fellowship from the Medicinal Chemistry Division of the American Chemical Society.

■ ABBREVIATIONS USED

PTMs, post-translational modifications; DNMTs, DNA methyltransferases; HDACs, histone deacetylases; FDA, Food and Drug Administration; PMTs, protein methyltransferases; HMTs, histone methyltransferases; SAM, *S*-5′-adenosyl-L-methionine; SAH, *S*-5′-adenosyl-L-homocysteine; PKMTs, protein lysine methyltransferases; PRMTs, protein arginine methyltransferases; H3, histone 3; H4, histone 4; MMA, monomethylation of arginine; sDMA, symmetrical monomethylation of arginine; aDMA, asymmetrical monomethylation of arginine; H3K4, histone 3, lysine 4; SUV39H1, suppressor of variegation 3-9 homologue 1; EHMT2, euchromatic histone-lysine *N*-methyltransferase 2; GLP, G9a-like protein 1; SETDB1, SET domain, bifurcated 1; PRDM2, PR domain containing 2, with ZNF domain; ETP, epidithiodiketopiperazine; DTT, dithiothreitol; mES, mouse embryonic stem; ES cell, embryonic stem cell; HSPCs, hematopoietic stem and progenitor cells; AML, acute myeloid leukemia; HTS, high-throughput screening; PRMT1, protein arginine methyltransferase 1; MEFs, mouse embryonic fibroblasts; ChIP, chromatin immunoprecipitation; WT, wild type; ITC, isothermal titration calorimetry; DSF, differential scanning fluorimetry; GPCRs, G-protein coupled receptors; SPR, surface plasmon resonance; PRC2, polycomb repressive complex 2; EZH1, enhancer of zeste homologue 1; EZH2, enhancer of zeste 2 polycomb repressive complex 2 subunit; SUZ12, suppressor of zeste 12; EED, embryonic ectoderm development; DLBCLs, diffuse large B-cell lymphomas; SWI/SNF, switch/sucrose nonfermentable; MLL, mixed lineage leukemia; ALL, acute lymphoblastic leukemia; SETD7, SET domain containing (lysine methyltransferase) 7; SMYD, SET and MYND domain containing; MYND, myeloid translocation protein-8, Nervy, and DEAF-1; SMYD2, SET and MYND domain containing 2; SETD2, SET domain containing 2; HGGs, hemispheric high-grade gliomas; SETD8, SET domain containing (lysine methyltransferase) 8; H4K20me, H4K20 monomethylation; PCNA, proliferating cell nuclear antigen; DOT1L, disruptor of telomeric silencing 1-like; CARM1, coactivator-associated arginine methyltransferase 1; GAR, glycine and arginine rich; PGM, proline, glycine, and methionine rich; AMIs, arginine methyltransferase inhibitors; PRMT3, protein arginine methyltransferase 3; PABPN1, mammalian nuclear poly(A)-binding protein; VHL, von Hippel–Lindau; ARF, alternative reading frame; DAL-1, differentially expressed in adenocarcinoma of the lung-1; ELISA, enzyme-linked immunosorbent assay; MS, mass spectrometry; mESC, mouse embryonic stem cells; SAHH, SAH hydrolase; SPA, scintillation proximity assay; HP1, heterochromatin protein 1; GSEA, gene set enrichment analysis; MTT, 3-(4,5-dimethylthiazol-2-yl)-2,5-diphenyl tetrazolium bromide; ChIP–chip, chromatin immunoprecipitation–DNA microarray; LTR, long terminal repeat; PK, pharmacokinetic; ATM, ataxia telangiectasia mutated; ATR, ataxia telangiectasia and Rad3-related; SC, subcutaneous; IV, intravenous; WDR5, WD repeat-containing protein 5

■ REFERENCES

(1) Bernstein, B. E.; Meissner, A.; Lander, E. S. The mammalian epigenome. *Cell* **2007**, *128*, 669–681.
(2) Jones, P. A.; Baylin, S. B. The epigenomics of cancer. *Cell* **2007**, *128*, 683–692.
(3) Berger, S. L.; Kouzarides, T.; Shiekhattar, R.; Shilatifard, A. An operational definition of epigenetics. *Genes Dev.* **2009**, *23*, 781–783.
(4) Luger, K.; Mader, A. W.; Richmond, R. K.; Sargent, D. F.; Richmond, T. J. Crystal structure of the nucleosome core particle at 2.8 Å resolution. *Nature* **1997**, *389*, 251–260.
(5) Khorasanizadeh, S. The nucleosome: from genomic organization to genomic regulation. *Cell* **2004**, *116*, 259–272.
(6) Kouzarides, T. Chromatin modifications and their function. *Cell* **2007**, *128*, 693–705.
(7) Allis, C. D.; Jenuwein, T.; Reinberg, D. *Epigenetics*; Cold Spring Harbor Laboratory Press: Cold Spring Harbor, NY, 2007; p 502.
(8) Gelato, K. A.; Fischle, W. Role of histone modifications in defining chromatin structure and function. *Biol. Chem.* **2008**, *389*, 353–363.
(9) Strahl, B. D.; Allis, C. D. The language of covalent histone modifications. *Nature* **2000**, *403*, 41–45.
(10) Jenuwein, T.; Allis, C. D. Translating the histone code. *Science* **2001**, *293*, 1074–1080.
(11) Arrowsmith, C. H.; Bountra, C.; Fish, P. V.; Lee, K.; Schapira, M. Epigenetic protein families: a new frontier for drug discovery. *Nat. Rev. Drug Discovery* **2012**, *11*, 384–400.
(12) Copeland, R. A.; Solomon, M. E.; Richon, V. M. Protein methyltransferases as a target class for drug discovery. *Nat. Rev. Drug Discovery* **2009**, *8*, 724–732.
(13) Lyko, F.; Brown, R. DNA methyltransferase inhibitors and the development of epigenetic cancer therapies. *J. Natl. Cancer Inst.* **2005**, *97*, 1498–1506.
(14) Duvic, M.; Vu, J. Vorinostat: a new oral histone deacetylase inhibitor approved for cutaneous T-cell lymphoma. *Expert Opin. Invest. Drugs* **2007**, *16*, 1111–1120.
(15) Szyf, M. Epigenetics, DNA methylation, and chromatin modifying drugs. *Annu. Rev. Pharmacol. Toxicol.* **2009**, *49*, 243–263.
(16) Liu, Y.; Liu, K.; Qin, S.; Xu, C.; Min, J. Epigenetic targets and drug discovery: Part 1: Histone methylation. *Pharmacol. Ther.* **2014**, *143*, 275–294.
(17) Sweis, R. F.; Michaelides, M. R. Recent advances in small-molecule modulation of epigenetic targets: discovery and development of histone methyltransferase and bromodomain inhibitors. *Annu. Rep. Med. Chem.* **2013**, *48*, 185–203.
(18) Wang, Z.; Patel, D. J. Small molecule epigenetic inhibitors targeted to histone lysine methyltransferases and demethylases. *Q. Rev. Biophys.* **2013**, *46*, 349–373.
(19) Zagni, C.; Chiacchio, U.; Rescifina, A. Histone methyltransferase inhibitors: novel epigenetic agents for cancer treatment. *Curr. Med. Chem.* **2013**, *20*, 167–185.
(20) Helin, K.; Dhanak, D. Chromatin proteins and modifications as drug targets. *Nature* **2013**, *502*, 480–488.
(21) He, Y.; Korboukh, I.; Jin, J.; Huang, J. Targeting protein lysine methylation and demethylation in cancers. *Acta Biochim. Biophys. Sin.* **2012**, *44*, 70–79.
(22) Yost, J. M.; Korboukh, I.; Liu, F.; Gao, C.; Jin, J. Targets in epigenetics: inhibiting the methyl writers of the histone code. *Curr. Chem. Genomics* **2011**, *5*, 72–84.
(23) Bissinger, E.-M.; Heinke, R.; Sippl, W.; Jung, M. Targeting epigenetic modifiers: inhibitors of histone methyltransferases. *MedChemComm* **2010**, *1*, 114–124.
(24) Spannhoff, A.; Sippl, W.; Jung, M. Cancer treatment of the future: inhibitors of histone methyltransferases. *Int. J. Biochem. Cell Biol.* **2009**, *41*, 4–11.

(25) Spannhoff, A.; Hauser, A. T.; Heinke, R.; Sippl, W.; Jung, M. The emerging therapeutic potential of histone methyltransferase and demethylase inhibitors. *ChemMedChem.* **2009**, *4*, 1568−1582.
(26) Martin, C.; Zhang, Y. The diverse functions of histone lysine methylation. *Nat. Rev. Mol. Cell Biol.* **2005**, *6*, 838−849.
(27) Shi, X.; Kachirskaia, I.; Yamaguchi, H.; West, L. E.; Wen, H.; Wang, E. W.; Dutta, S.; Appella, E.; Gozani, O. Modulation of p53 function by SET8-mediated methylation at lysine 382. *Mol. Cell* **2007**, *27*, 636−646.
(28) Chuikov, S.; Kurash, J. K.; Wilson, J. R.; Xiao, B.; Justin, N.; Ivanov, G. S.; McKinney, K.; Tempst, P.; Prives, C.; Gamblin, S. J.; Barlev, N. A.; Reinberg, D. Regulation of p53 activity through lysine methylation. *Nature* **2004**, *432*, 353−360.
(29) Jenuwein, T.; Laible, G.; Dorn, R.; Reuter, G. SET domain proteins modulate chromatin domains in eu- and heterochromatin. *Cell. Mol. Life Sci.* **1998**, *54*, 80−93.
(30) Baumbusch, L. O.; Thorstensen, T.; Krauss, V.; Fischer, A.; Naumann, K.; Assalkhou, R.; Schulz, I.; Reuter, G.; Aalen, R. B. The *Arabidopsis thaliana* genome contains at least 29 active genes encoding SET domain proteins that can be assigned to four evolutionarily conserved classes. *Nucleic Acids Res.* **2001**, *29*, 4319−4333.
(31) Cheng, X.; Collins, R. E.; Zhang, X. Structural and sequence motifs of protein (histone) methylation enzymes. *Annu. Rev. Biophys. Biomol. Struct.* **2005**, *34*, 267−294.
(32) Jacobs, S. A.; Harp, J. M.; Devarakonda, S.; Kim, Y.; Rastinejad, F.; Khorasanizadeh, S. The active site of the SET domain is constructed on a knot. *Nat. Struct. Biol.* **2002**, *9*, 833−838.
(33) Kouzarides, T. Histone methylation in transcriptional control. *Curr. Opin. Genet. Dev.* **2002**, *12*, 198−209.
(34) Allis, C. D.; Berger, S. L.; Cote, J.; Dent, S.; Jenuwien, T.; Kouzarides, T.; Pillus, L.; Reinberg, D.; Shi, Y.; Shiekhattar, R.; Shilatifard, A.; Workman, J.; Zhang, Y. New nomenclature for chromatin-modifying enzymes. *Cell* **2007**, *131*, 633−636.
(35) Zhang, X.; Tamaru, H.; Khan, S. I.; Horton, J. R.; Keefe, L. J.; Selker, E. U.; Cheng, X. Structure of the neurospora SET domain protein DIM-5, a histone H3 lysine methyltransferase. *Cell* **2002**, *111*, 117−127.
(36) Taverna, S. D.; Li, H.; Ruthenburg, A. J.; Allis, C. D.; Patel, D. J. How chromatin-binding modules interpret histone modifications: lessons from professional pocket pickers. *Nat. Struct. Mol. Biol.* **2007**, *14*, 1025−1040.
(37) Bannister, A. J.; Kouzarides, T. Regulation of chromatin by histone modifications. *Cell Res.* **2011**, *21*, 381−395.
(38) Barski, A.; Cuddapah, S.; Cui, K.; Roh, T. Y.; Schones, D. E.; Wang, Z.; Wei, G.; Chepelev, I.; Zhao, K. High-resolution profiling of histone methylations in the human genome. *Cell* **2007**, *129*, 823−837.
(39) Zhang, Z.; Pugh, B. F. High-resolution genome-wide mapping of the primary structure of chromatin. *Cell* **2011**, *144*, 175−186.
(40) Krauss, V. Glimpses of evolution: heterochromatic histone H3K9 methyltransferases left its marks behind. *Genetica* **2008**, *133*, 93−106.
(41) Bannister, A. J.; Zegerman, P.; Partridge, J. F.; Miska, E. A.; Thomas, J. O.; Allshire, R. C.; Kouzarides, T. Selective recognition of methylated lysine 9 on histone H3 by the HP1 chromo domain. *Nature* **2001**, *410*, 120−124.
(42) Chen, M. W.; Hua, K. T.; Kao, H. J.; Chi, C. C.; Wei, L. H.; Johansson, G.; Shiah, S. G.; Chen, P. S.; Jeng, Y. M.; Cheng, T. Y.; Lai, T. C.; Chang, J. S.; Jan, Y. H.; Chien, M. H.; Yang, C. J.; Huang, M. S.; Hsiao, M.; Kuo, M. L. H3K9 histone methyltransferase G9a promotes lung cancer invasion and metastasis by silencing the cell adhesion molecule Ep-CAM. *Cancer Res.* **2010**, *70*, 7830−7840.
(43) Wen, B.; Wu, H.; Shinkai, Y.; Irizarry, R. A.; Feinberg, A. P. Large histone H3 lysine 9 dimethylated chromatin blocks distinguish differentiated from embryonic stem cells. *Nat. Genet.* **2009**, *41*, 246−250.
(44) Kang, M. Y.; Lee, B. B.; Kim, Y. H.; Chang, D. K.; Kyu Park, S.; Chun, H. K.; Song, S. Y.; Park, J.; Kim, D. H. Association of the SUV39H1 histone methyltransferase with the DNA methyltransferase 1 at mRNA expression level in primary colorectal cancer. *Int. J. Cancer* **2007**, *121*, 2192−2197.
(45) Kondo, Y.; Shen, L.; Ahmed, S.; Boumber, Y.; Sekido, Y.; Haddad, B. R.; Issa, J. P. Downregulation of histone H3 lysine 9 methyltransferase G9a induces centrosome disruption and chromosome instability in cancer cells. *PLoS One* **2008**, *3*, e2037.
(46) Watanabe, H.; Soejima, K.; Yasuda, H.; Kawada, I.; Nakachi, I.; Yoda, S.; Naoki, K.; Ishizaka, A. Deregulation of histone lysine methyltransferases contributes to oncogenic transformation of human bronchoepithelial cells. *Cancer Cell Int.* **2008**, *8*, 15.
(47) Imai, K.; Togami, H.; Okamoto, T. Involvement of histone H3 lysine 9 (H3K9) methyl transferase G9a in the maintenance of HIV-1 latency and its reactivation by BIX01294. *J. Biol. Chem.* **2010**, *285*, 16538−16545.
(48) Maze, I.; Covington, H. E., III; Dietz, D. M.; LaPlant, Q.; Renthal, W.; Russo, S. J.; Mechanic, M.; Mouzon, E.; Neve, R. L.; Haggarty, S. J.; Ren, Y.; Sampath, S. C.; Hurd, Y. L.; Greengard, P.; Tarakhovsky, A.; Schaefer, A.; Nestler, E. J. Essential role of the histone methyltransferase G9a in cocaine-induced plasticity. *Science* **2010**, *327*, 213−216.
(49) Rea, S.; Eisenhaber, F.; O'Carroll, D.; Strahl, B. D.; Sun, Z. W.; Schmid, M.; Opravil, S.; Mechtler, K.; Ponting, C. P.; Allis, C. D.; Jenuwein, T. Regulation of chromatin structure by site-specific histone H3 methyltransferases. *Nature* **2000**, *406*, 593−599.
(50) Aagaard, L.; Laible, G.; Selenko, P.; Schmid, M.; Dorn, R.; Schotta, G.; Kuhfittig, S.; Wolf, A.; Lebersorger, A.; Singh, P. B.; Reuter, G.; Jenuwein, T. Functional mammalian homologues of the *Drosophila* PEV-modifier Su(var)3-9 encode centromere-associated proteins which complex with the heterochromatin component M31. *EMBO J.* **1999**, *18*, 1923−1938.
(51) Peters, A. H.; O'Carroll, D.; Scherthan, H.; Mechtler, K.; Sauer, S.; Schofer, C.; Weipoltshammer, K.; Pagani, M.; Lachner, M.; Kohlmaier, A.; Opravil, S.; Doyle, M.; Sibilia, M.; Jenuwein, T. Loss of the Suv39h histone methyltransferases impairs mammalian heterochromatin and genome stability. *Cell* **2001**, *107*, 323−337.
(52) Brasher, S. V.; Smith, B. O.; Fogh, R. H.; Nietlispach, D.; Thiru, A.; Nielsen, P. R.; Broadhurst, R. W.; Ball, L. J.; Murzina, N. V.; Laue, E. D. The structure of mouse HP1 suggests a unique mode of single peptide recognition by the shadow chromo domain dimer. *EMBO J.* **2000**, *19*, 1587−1597.
(53) Muramatsu, D.; Singh, P. B.; Kimura, H.; Tachibana, M.; Shinkai, Y. Pericentric heterochromatin generated by HP1 protein interaction-defective histone methyltransferase Suv39h1. *J. Biol. Chem.* **2013**, *288*, 25285−25296.
(54) Nielsen, S. J.; Schneider, R.; Bauer, U. M.; Bannister, A. J.; Morrison, A.; O'Carroll, D.; Firestein, R.; Cleary, M.; Jenuwein, T.; Herrera, R. E.; Kouzarides, T. Rb targets histone H3 methylation and HP1 to promoters. *Nature* **2001**, *412*, 561−565.
(55) Kirschmann, D. A.; Lininger, R. A.; Gardner, L. M.; Seftor, E. A.; Odero, V. A.; Ainsztein, A. M.; Earnshaw, W. C.; Wallrath, L. L.; Hendrix, M. J. Down-regulation of HP1Hsalpha expression is associated with the metastatic phenotype in breast cancer. *Cancer Res.* **2000**, *60*, 3359−3363.
(56) Brasacchio, D.; Okabe, J.; Tikellis, C.; Balcerczyk, A.; George, P.; Baker, E. K.; Calkin, A. C.; Brownlee, M.; Cooper, M. E.; El-Osta, A. Hyperglycemia induces a dynamic cooperativity of histone methylase and demethylase enzymes associated with gene-activating epigenetic marks that coexist on the lysine tail. *Diabetes* **2009**, *58*, 1229−1236.
(57) Spyropoulou, A.; Gargalionis, A.; Dalagiorgou, G.; Adamopoulos, C.; Papavassiliou, K. A.; Lea, R. W.; Piperi, C.; Papavassiliou, A. G. Role of histone lysine methyltransferases SUV39H1 and SETDB1 in gliomagenesis: modulation of cell proliferation, migration, and colony formation. *NeuroMol. Med.* **2014**, *16*, 70−82.
(58) Greiner, D.; Bonaldi, T.; Eskeland, R.; Roemer, E.; Imhof, A. Identification of a specific inhibitor of the histone methyltransferase SU(VAR)3-9. *Nat. Chem. Biol.* **2005**, *1*, 143−145.
(59) Gardiner, D. M.; Waring, P.; Howlett, B. J. The epipolythiodioxopiperazine (ETP) class of fungal toxins: distribution,

mode of action, functions and biosynthesis. *Microbiology* **2005**, *151*, 1021−1032.
(60) Iwasa, E.; Hamashima, Y.; Fujishiro, S.; Higuchi, E.; Ito, A.; Yoshida, M.; Sodeoka, M. Total synthesis of (+)-chaetocin and its analogues: their histone methyltransferase G9a inhibitory activity. *J. Am. Chem. Soc.* **2010**, *132*, 4078−4079.
(61) Fujishiro, S.; Dodo, K.; Iwasa, E.; Teng, Y.; Sohtome, Y.; Hamashima, Y.; Ito, A.; Yoshida, M.; Sodeoka, M. Epidithiodiketopiperazine as a pharmacophore for protein lysine methyltransferase G9a inhibitors: reducing cytotoxicity by structural simplification. *Bioorg. Med. Chem. Lett.* **2013**, *23*, 733−736.
(62) Cherblanc, F. L.; Chapman, K. L.; Brown, R.; Fuchter, M. J. Chaetocin is a nonspecific inhibitor of histone lysine methyltransferases. *Nat. Chem. Biol.* **2013**, *9*, 136−137.
(63) Greiner, D.; Bonaldi, T.; Eskeland, R.; Roemer, E.; Imhof, A. Reply to "Chaetocin is a nonspecific inhibitor of histone lysine methyltransferases". *Nat. Chem. Biol.* **2013**, *9*, 137.
(64) Cherblanc, F. L.; Chapman, K. L.; Reid, J.; Borg, A. J.; Sundriyal, S.; Alcazar-Fuoli, L.; Bignell, E.; Demetriades, M.; Schofield, C. J.; DiMaggio, P. A., Jr.; Brown, R.; Fuchter, M. J. On the histone lysine methyltransferase activity of fungal metabolite chaetocin. *J. Med. Chem.* **2013**, *56*, 8616−8625.
(65) Tachibana, M.; Sugimoto, K.; Nozaki, M.; Ueda, J.; Ohta, T.; Ohki, M.; Fukuda, M.; Takeda, N.; Niida, H.; Kato, H.; Shinkai, Y. G9a histone methyltransferase plays a dominant role in euchromatic histone H3 lysine 9 methylation and is essential for early embryogenesis. *Genes Dev.* **2002**, *16*, 1779−1791.
(66) Tachibana, M.; Ueda, J.; Fukuda, M.; Takeda, N.; Ohta, T.; Iwanari, H.; Sakihama, T.; Kodama, T.; Hamakubo, T.; Shinkai, Y. Histone methyltransferases G9a and GLP form heteromeric complexes and are both crucial for methylation of euchromatin at H3-K9. *Genes Dev.* **2005**, *19*, 815−826.
(67) Rathert, P.; Dhayalan, A.; Murakami, M.; Zhang, X.; Tamas, R.; Jurkowska, R.; Komatsu, Y.; Shinkai, Y.; Cheng, X.; Jeltsch, A. Protein lysine methyltransferase G9a acts on non-histone targets. *Nat. Chem. Biol.* **2008**, *4*, 344−346.
(68) Huang, J.; Dorsey, J.; Chuikov, S.; Zhang, X.; Jenuwein, T.; Reinberg, D.; Berger, S. L. G9A and GLP methylate lysine 373 in the tumor suppressor p53. *J. Biol. Chem.* **2010**, *285*, 9636−9641.
(69) Kondo, Y.; Shen, L.; Suzuki, S.; Kurokawa, T.; Masuko, K.; Tanaka, Y.; Kato, H.; Mizuno, Y.; Yokoe, M.; Sugauchi, F.; Hirashima, N.; Orito, E.; Osada, H.; Ueda, R.; Guo, Y.; Chen, X.; Issa, J. P.; Sekido, Y. Alterations of DNA methylation and histone modifications contribute to gene silencing in hepatocellular carcinomas. *Hepatol. Res.* **2007**, *37*, 974−983.
(70) Goyama, S.; Nitta, E.; Yoshino, T.; Kako, S.; Watanabe-Okochi, N.; Shimabe, M.; Imai, Y.; Takahashi, K.; Kurokawa, M. EVI-1 interacts with histone methyltransferases SUV39H1 and G9a for transcriptional repression and bone marrow immortalization. *Leukemia* **2010**, *24*, 81−88.
(71) Lehnertz, B.; Pabst, C.; Su, L.; Miller, M.; Liu, F.; Yi, L.; Zhang, R.; Krosl, J.; Yung, E.; Kirschner, J.; Rosten, P.; Underhill, T. M.; Jin, J.; Hebert, J.; Sauvageau, G.; Humphries, R. K.; Rossi, F. M. The methyltransferase G9a regulates HoxA9-dependent transcription in AML. *Genes Dev.* **2014**, *28*, 317−327.
(72) Oh, S. T.; Kim, K. B.; Chae, Y. C.; Kang, J. Y.; Hahn, Y.; Seo, S. B. H3K9 histone methyltransferase G9a-mediated transcriptional activation of p21. *FEBS Lett.* **2014**, *588*, 685−691.
(73) Covington, H. E., III; Maze, I.; Sun, H.; Bomze, H. M.; DeMaio, K. D.; Wu, E. Y.; Dietz, D. M.; Lobo, M. K.; Ghose, S.; Mouzon, E.; Neve, R. L.; Tamminga, C. A.; Nestler, E. J. A role for repressive histone methylation in cocaine-induced vulnerability to stress. *Neuron* **2011**, *71*, 656−670.
(74) Schaefer, A.; Sampath, S. C.; Intrator, A.; Min, A.; Gertler, T. S.; Surmeier, D. J.; Tarakhovsky, A.; Greengard, P. Control of cognition and adaptive behavior by the GLP/G9a epigenetic suppressor complex. *Neuron* **2009**, *64*, 678−691.
(75) Link, P. A.; Gangisetty, O.; James, S. R.; Woloszynska-Read, A.; Tachibana, M.; Shinkai, Y.; Karpf, A. R. Distinct roles for histone methyltransferases G9a and GLP in cancer germ-line antigen gene regulation in human cancer cells and murine embryonic stem cells. *Mol. Cancer Res.* **2009**, *7*, 851−862.
(76) Tachibana, M.; Matsumura, Y.; Fukuda, M.; Kimura, H.; Shinkai, Y. G9a/GLP complexes independently mediate H3K9 and DNA methylation to silence transcription. *EMBO J.* **2008**, *27*, 2681−2690.
(77) Dong, K. B.; Maksakova, I. A.; Mohn, F.; Leung, D.; Appanah, R.; Lee, S.; Yang, H. W.; Lam, L. L.; Mager, D. L.; Schubeler, D.; Tachibana, M.; Shinkai, Y.; Lorincz, M. C. DNA methylation in ES cells requires the lysine methyltransferase G9a but not its catalytic activity. *EMBO J.* **2008**, *27*, 2691−2701.
(78) Shi, Y.; Desponts, C.; Do, J. T.; Hahm, H. S.; Scholer, H. R.; Ding, S. Induction of pluripotent stem cells from mouse embryonic fibroblasts by Oct4 and Klf4 with small-molecule compounds. *Cell Stem Cell* **2008**, *3*, 568−574.
(79) Shi, Y.; Do, J. T.; Desponts, C.; Hahm, H. S.; Scholer, H. R.; Ding, S. A combined chemical and genetic approach for the generation of induced pluripotent stem cells. *Cell Stem Cell* **2008**, *2*, 525−528.
(80) Chen, X.; Skutt-Kakaria, K.; Davison, J.; Ou, Y. L.; Choi, E.; Malik, P.; Loeb, K.; Wood, B.; Georges, G.; Torok-Storb, B.; Paddison, P. J. G9a/GLP-dependent histone H3K9me2 patterning during human hematopoietic stem cell lineage commitment. *Genes Dev.* **2012**, *26*, 2499−2511.
(81) Antignano, F.; Burrows, K.; Hughes, M. R.; Han, J. M.; Kron, K. J.; Penrod, N. M.; Oudhoff, M. J.; Wang, S. K.; Min, P. H.; Gold, M. J.; Chenery, A. L.; Braam, M. J.; Fung, T. C.; Rossi, F. M.; McNagny, K. M.; Arrowsmith, C. H.; Lupien, M.; Levings, M. K.; Zaph, C. Methyltransferase G9A regulates T cell differentiation during murine intestinal inflammation. *J. Clin. Invest.* **2014**, *124*, 1945−1955.
(82) Kleefstra, T.; Brunner, H. G.; Amiel, J.; Oudakker, A. R.; Nillesen, W. M.; Magee, A.; Genevieve, D.; Cormier-Daire, V.; van Esch, H.; Fryns, J. P.; Hamel, B. C.; Sistermans, E. A.; de Vries, B. B.; van Bokhoven, H. Loss-of-function mutations in euchromatin histone methyl transferase 1 (EHMT1) cause the 9q34 subtelomeric deletion syndrome. *Am. J. Hum. Genet.* **2006**, *79*, 370−377.
(83) Kleefstra, T.; van Zelst-Stams, W. A.; Nillesen, W. M.; Cormier-Daire, V.; Houge, G.; Foulds, N.; van Dooren, M.; Willemsen, M. H.; Pfundt, R.; Turner, A.; Wilson, M.; McGaughran, J.; Rauch, A.; Zenker, M.; Adam, M. P.; Innes, M.; Davies, C.; Lopez, A. G.; Casalone, R.; Weber, A.; Brueton, L. A.; Navarro, A. D.; Bralo, M. P.; Venselaar, H.; Stegmann, S. P.; Yntema, H. G.; van Bokhoven, H.; Brunner, H. G. Further clinical and molecular delineation of the 9q subtelomeric deletion syndrome supports a major contribution of EHMT1 haploinsufficiency to the core phenotype. *J. Med. Genet.* **2009**, *46*, 598−606.
(84) Ohno, H.; Shinoda, K.; Ohyama, K.; Sharp, L. Z.; Kajimura, S. EHMT1 controls brown adipose cell fate and thermogenesis through the PRDM16 complex. *Nature* **2013**, *504*, 163−167.
(85) Kubicek, S.; O'Sullivan, R. J.; August, E. M.; Hickey, E. R.; Zhang, Q.; Teodoro, M. L.; Rea, S.; Mechtler, K.; Kowalski, J. A.; Homon, C. A.; Kelly, T. A.; Jenuwein, T. Reversal of H3K9me2 by a small-molecule inhibitor for the G9a histone methyltransferase. *Mol. Cell* **2007**, *25*, 473−481.
(86) Chang, Y.; Zhang, X.; Horton, J. R.; Upadhyay, A. K.; Spannhoff, A.; Liu, J.; Snyder, J. P.; Bedford, M. T.; Cheng, X. Structural basis for G9a-like protein lysine methyltransferase inhibition by BIX-01294. *Nat. Struct. Mol. Biol.* **2009**, *16*, 312−317.
(87) Liu, F.; Chen, X.; Allali-Hassani, A.; Quinn, A. M.; Wasney, G. A.; Dong, A.; Barsyte, D.; Kozieradzki, I.; Senisterra, G.; Chau, I.; Siarheyeva, A.; Kireev, D. B.; Jadhav, A.; Herold, J. M.; Frye, S. V.; Arrowsmith, C. H.; Brown, P. J.; Simeonov, A.; Vedadi, M.; Jin, J. Discovery of a 2,4-diamino-7-aminoalkoxyquinazoline as a potent and selective inhibitor of histone lysine methyltransferase G9a. *J. Med. Chem.* **2009**, *52*, 7950−7953.
(88) Liu, F.; Chen, X.; Allali-Hassani, A.; Quinn, A. M.; Wigle, T. J.; Wasney, G. A.; Dong, A.; Senisterra, G.; Chau, I.; Siarheyeva, A.; Norris, J. L.; Kireev, D. B.; Jadhav, A.; Herold, J. M.; Janzen, W. P.; Arrowsmith, C. H.; Frye, S. V.; Brown, P. J.; Simeonov, A.; Vedadi, M.;

Jin, J. Protein lysine methyltransferase G9a inhibitors: design, synthesis, and structure activity relationships of 2,4-diamino-7-aminoalkoxy-quinazolines. *J. Med. Chem.* **2010**, *53*, 5844−5857.
(89) Chang, Y.; Ganesh, T.; Horton, J. R.; Spannhoff, A.; Liu, J.; Sun, A.; Zhang, X.; Bedford, M. T.; Shinkai, Y.; Snyder, J. P.; Cheng, X. Adding a lysine mimic in the design of potent inhibitors of histone lysine methyltransferases. *J. Mol. Biol.* **2010**, *400*, 1−7.
(90) Liu, F.; Barsyte-Lovejoy, D.; Allali-Hassani, A.; He, Y.; Herold, J. M.; Chen, X.; Yates, C. M.; Frye, S. V.; Brown, P. J.; Huang, J.; Vedadi, M.; Arrowsmith, C. H.; Jin, J. Optimization of cellular activity of G9a inhibitors 7-aminoalkoxy-quinazolines. *J. Med. Chem.* **2011**, *54*, 6139−6150.
(91) Vedadi, M.; Barsyte-Lovejoy, D.; Liu, F.; Rival-Gervier, S.; Allali-Hassani, A.; Labrie, V.; Wigle, T. J.; Dimaggio, P. A.; Wasney, G. A.; Siarheyeva, A.; Dong, A.; Tempel, W.; Wang, S. C.; Chen, X.; Chau, I.; Mangano, T. J.; Huang, X. P.; Simpson, C. D.; Pattenden, S. G.; Norris, J. L.; Kireev, D. B.; Tripathy, A.; Edwards, A.; Roth, B. L.; Janzen, W. P.; Garcia, B. A.; Petronis, A.; Ellis, J.; Brown, P. J.; Frye, S. V.; Arrowsmith, C. H.; Jin, J. A chemical probe selectively inhibits G9a and GLP methyltransferase activity in cells. *Nat. Chem. Biol.* **2011**, *7*, 566−574.
(92) Frye, S. V. The art of the chemical probe. *Nat. Chem. Biol.* **2010**, *6*, 159−161.
(93) Workman, P.; Collins, I. Probing the probes: fitness factors for small molecule tools. *Chem. Biol.* **2010**, *17*, 561−577.
(94) Bunnage, M. E.; Chekler, E. L.; Jones, L. H. Target validation using chemical probes. *Nat. Chem. Biol.* **2013**, *9*, 195−199.
(95) Liu, F.; Barsyte-Lovejoy, D.; Li, F.; Xiong, Y.; Korboukh, V.; Huang, X. P.; Allali-Hassani, A.; Janzen, W. P.; Roth, B. L.; Frye, S. V.; Arrowsmith, C. H.; Brown, P. J.; Vedadi, M.; Jin, J. Discovery of an in vivo chemical probe of the lysine methyltransferases G9a and GLP. *J. Med. Chem.* **2013**, *56*, 8931−8942.
(96) Konze, K. D.; Pattenden, S. G.; Liu, F.; Barsyte-Lovejoy, D.; Li, F.; Simon, J. M.; Davis, I. J.; Vedadi, M.; Jin, J. A chemical tool for in vitro and in vivo precipitation of lysine methyltransferase g9a. *ChemMedChem.* **2014**, *9*, 549−553.
(97) Yuan, Y.; Wang, Q.; Paulk, J.; Kubicek, S.; Kemp, M. M.; Adams, D. J.; Shamji, A. F.; Wagner, B. K.; Schreiber, S. L. A small-molecule probe of the histone methyltransferase G9a induces cellular senescence in pancreatic adenocarcinoma. *ACS Chem. Biol.* **2012**, *7*, 1152−1157.
(98) Sweis, R. F.; Pliushchev, M.; Brown, P. J.; Guo, J.; Li, F.; Maag, D.; Petros, A. M.; Soni, N. B.; Tse, C.; Vedadi, M.; Michaelides, M. R.; Chiang, G. G.; Pappano, W. N. Discovery and development of potent and selective inhibitors of histone methyltransferase G9a. *ACS Med. Chem. Lett.* **2014**, *5*, 205−209.
(99) O'Meara, M. M.; Simon, J. A. Inner workings and regulatory inputs that control polycomb repressive complex 2. *Chromosoma* **2012**, *121*, 221−234.
(100) Cao, R.; Wang, L.; Wang, H.; Xia, L.; Erdjument-Bromage, H.; Tempst, P.; Jones, R. S.; Zhang, Y. Role of histone H3 lysine 27 methylation in polycomb-group silencing. *Science* **2002**, *298*, 1039−1043.
(101) Kuzmichev, A.; Nishioka, K.; Erdjument-Bromage, H.; Tempst, P.; Reinberg, D. Histone methyltransferase activity associated with a human multiprotein complex containing the enhancer of zeste protein. *Genes Dev.* **2002**, *16*, 2893−2905.
(102) Margueron, R.; Reinberg, D. The polycomb complex PRC2 and its mark in life. *Nature* **2011**, *469*, 343−349.
(103) Czermin, B.; Melfi, R.; McCabe, D.; Seitz, V.; Imhof, A.; Pirrotta, V. *Drosophila* enhancer of Zeste/ESC complexes have a histone H3 methyltransferase activity that marks chromosomal polycomb sites. *Cell* **2002**, *111*, 185−196.
(104) Muller, J.; Hart, C. M.; Francis, N. J.; Vargas, M. L.; Sengupta, A.; Wild, B.; Miller, E. L.; O'Connor, M. B.; Kingston, R. E.; Simon, J. A. Histone methyltransferase activity of a *Drosophila* polycomb group repressor complex. *Cell* **2002**, *111*, 197−208.
(105) Joshi, P.; Carrington, E. A.; Wang, L.; Ketel, C. S.; Miller, E. L.; Jones, R. S.; Simon, J. A. Dominant alleles identify SET domain residues required for histone methyltransferase of polycomb repressive complex 2. *J. Biol. Chem.* **2008**, *283*, 27757−27766.
(106) Verma, S. K.; Tian, X.; LaFrance, L. V.; Duquenne, C.; Suarez, D. P.; Newlander, K. A.; Romeril, S. P.; Burgess, J. L.; Grant, S. W.; Brackley, J. A.; Graves, A. P.; Scherzer, D. A.; Shu, A.; Thompson, C.; Ott, H. M.; Aller, G. S. V.; Machutta, C. A.; Diaz, E.; Jiang, Y.; Johnson, N. W.; Knight, S. D.; Kruger, R. G.; McCabe, M. T.; Dhanak, D.; Tummino, P. J.; Creasy, C. L.; Miller, W. H. Identification of potent, selective, cell-active inhibitors of the histone lysine methyltransferase EZH2. *ACS Med. Chem. Lett.* **2012**, *3*, 1091−1096.
(107) Margueron, R.; Li, G.; Sarma, K.; Blais, A.; Zavadil, J.; Woodcock, C. L.; Dynlacht, B. D.; Reinberg, D. Ezh1 and Ezh2 maintain repressive chromatin through different mechanisms. *Mol. Cell* **2008**, *32*, 503−518.
(108) Shen, X.; Liu, Y.; Hsu, Y.-J.; Fujiwara, Y.; Kim, J.; Mao, X.; Yuan, G.-C.; Orkin, S. H. EZH1 mediates methylation on histone H3 lysine 27 and complements EZH2 in maintaining stem cell identity and executing pluripotency. *Mol. Cell* **2008**, *32*, 491−502.
(109) Zee, B. M.; Levin, R. S.; Xu, B.; LeRoy, G.; Wingreen, N. S.; Garcia, B. A. In vivo residue-specific histone methylation dynamics. *J. Biol. Chem.* **2010**, *285*, 3341−3350.
(110) Cao, R.; Zhang, Y. SUZ12 is required for both the histone methyltransferase activity and the silencing function of the EED−EZH2 complex. *Mol. Cell* **2004**, *15*, 57−67.
(111) Ketel, C. S.; Andersen, E. F.; Vargas, M. L.; Suh, J.; Strome, S.; Simon, J. A. Subunit contributions to histone methyltransferase activities of fly and worm polycomb group complexes. *Mol. Cell. Biol.* **2005**, *25*, 6857−6868.
(112) Pasini, D.; Bracken, A. P.; Jensen, M. R.; Lazzerini Denchi, E.; Helin, K. Suz12 is essential for mouse development and for EZH2 histone methyltransferase activity. *EMBO J.* **2004**, *23*, 4061−4071.
(113) Kim, H.; Kang, K.; Kim, J. AEBP2 as a potential targeting protein for polycomb repression complex PRC2. *Nucleic Acids Res.* **2009**, *37*, 2940−2950.
(114) Nekrasov, M.; Klymenko, T.; Fraterman, S.; Papp, B.; Oktaba, K.; Kocher, T.; Cohen, A.; Stunnenberg, H. G.; Wilm, M.; Muller, J. Pcl-PRC2 is needed to generate high levels of H3-K27 trimethylation at polycomb target genes. *EMBO J.* **2007**, *26*, 4078−4088.
(115) Walker, E.; Chang, W. Y.; Hunkapiller, J.; Cagney, G.; Garcha, K.; Torchia, J.; Krogan, N. J.; Reiter, J. F.; Stanford, W. L. Polycomb-like 2 associates with PRC2 and regulates transcriptional networks during mouse embryonic stem cell self-renewal and differentiation. *Cell Stem Cell* **2010**, *6*, 153−166.
(116) Li, G.; Margueron, R.; Ku, M. C.; Chambon, P.; Bernstein, B. E.; Reinberg, D. Jarid2 and PRC2, partners in regulating gene expression. *Genes Dev.* **2010**, *24*, 368−380.
(117) Morin, R. D.; Johnson, N. A.; Severson, T. M.; Mungall, A. J.; An, J.; Goya, R.; Paul, J. E.; Boyle, M.; Woolcock, B. W.; Kuchenbauer, F.; Yap, D.; Humphries, R. K.; Griffith, O. L.; Shah, S.; Zhu, H.; Kimbara, M.; Shashkin, P.; Charlot, J. F.; Tcherpakov, M.; Corbett, R.; Tam, A.; Varhol, R.; Smailus, D.; Moksa, M.; Zhao, Y.; Delaney, A.; Qian, H.; Birol, I.; Schein, J.; Moore, R.; Holt, R.; Horsman, D. E.; Connors, J. M.; Jones, S.; Aparicio, S.; Hirst, M.; Gascoyne, R. D.; Marra, M. A. Somatic mutations altering EZH2 (Tyr641) in follicular and diffuse large B-cell lymphomas of germinal-center origin. *Nat. Genet.* **2010**, *42*, 181−185.
(118) Morin, R. D.; Mendez-Lago, M.; Mungall, A. J.; Goya, R.; Mungall, K. L.; Corbett, R. D.; Johnson, N. A.; Severson, T. M.; Chiu, R.; Field, M.; Jackman, S.; Krzywinski, M.; Scott, D. W.; Trinh, D. L.; Tamura-Wells, J.; Li, S.; Firme, M. R.; Rogic, S.; Griffith, M.; Chan, S.; Yakovenko, O.; Meyer, I. M.; Zhao, E. Y.; Smailus, D.; Moksa, M.; Chittaranjan, S.; Rimsza, L.; Brooks-Wilson, A.; Spinelli, J. J.; Ben-Neriah, S.; Meissner, B.; Woolcock, B.; Boyle, M.; McDonald, H.; Tam, A.; Zhao, Y. J.; Delaney, A.; Zeng, T.; Tse, K.; Butterfield, Y.; Birol, I.; Holt, R.; Schein, J.; Horsman, D. E.; Moore, R.; Jones, S. J. M.; Connors, J. M.; Hirst, M.; Gascoyne, R. D.; Marra, M. A. Frequent mutation of histone-modifying genes in non-Hodgkin lymphoma. *Nature* **2011**, *476*, 298−303.

(119) Lohr, J. G.; Stojanov, P.; Lawrence, M. S.; Auclair, D.; Chapuy, B.; Sougnez, C.; Cruz-Gordillo, P.; Knoechel, B.; Asmann, Y. W.; Slager, S. L.; Novak, A. J.; Dogan, A.; Ansell, S. M.; Link, B. K.; Zou, L. H.; Gould, J.; Saksena, G.; Stransky, N.; Rangel-Escareno, C.; Fernandez-Lopez, J. C.; Hidalgo-Miranda, A.; Melendez-Zajgla, J.; Hernandez-Lemus, E.; Celis, A. S. C. Y.; Imaz-Rosshandler, I.; Ojesina, A. I.; Jung, J.; Pedamallu, C. S.; Lander, E. S.; Habermann, T. M.; Cerhan, J. R.; Shipp, M. A.; Getz, G.; Golub, T. R. Discovery and prioritization of somatic mutations in diffuse large B-cell lymphoma (DLBCL) by whole-exome sequencing. *Proc. Natl. Acad. Sci. U.S.A.* **2012**, *109*, 3879−3884.

(120) Yap, D. B.; Chu, J.; Berg, T.; Schapira, M.; Cheng, S. W.; Moradian, A.; Morin, R. D.; Mungall, A. J.; Meissner, B.; Boyle, M.; Marquez, V. E.; Marra, M. A.; Gascoyne, R. D.; Humphries, R. K.; Arrowsmith, C. H.; Morin, G. B.; Aparicio, S. A. Somatic mutations at EZH2 Y641 act dominantly through a mechanism of selectively altered PRC2 catalytic activity, to increase H3K27 trimethylation. *Blood* **2011**, *117*, 2451−2459.

(121) Sneeringer, C. J.; Scott, M. P.; Kuntz, K. W.; Knutson, S. K.; Pollock, R. M.; Richon, V. M.; Copeland, R. A. Coordinated activities of wild-type plus mutant EZH2 drive tumor-associated hyper-trimethylation of lysine 27 on histone H3 (H3K27) in human B-cell lymphomas. *Proc. Natl. Acad. Sci. U.S.A.* **2010**, *107*, 20980−20985.

(122) McCabe, M. T.; Graves, A. P.; Ganji, G.; Diaz, E.; Halsey, W. S.; Jiang, Y.; Smitheman, K. N.; Ott, H. M.; Pappalardi, M. B.; Allen, K. E.; Chen, S. B.; Della Pietra, A., 3rd; Dul, E.; Hughes, A. M.; Gilbert, S. A.; Thrall, S. H.; Tummino, P. J.; Kruger, R. G.; Brandt, M.; Schwartz, B.; Creasy, C. L. Mutation of A677 in histone methyltransferase EZH2 in human B-cell lymphoma promotes hypertrimethylation of histone H3 on lysine 27 (H3K27). *Proc. Natl. Acad. Sci. U.S.A.* **2012**, *109*, 2989−2994.

(123) Bracken, A. P.; Pasini, D.; Capra, M.; Prosperini, E.; Colli, E.; Helin, K. EZH2 is downstream of the pRB−E2F pathway, essential for proliferation and amplified in cancer. *EMBO J.* **2003**, *22*, 5323−5335.

(124) Simon, J. A.; Lange, C. A. Roles of the EZH2 histone methyltransferase in cancer epigenetics. *Mutat. Res.* **2008**, *647*, 21−29.

(125) Chi, P.; Allis, C. D.; Wang, G. G. Covalent histone modifications—miswritten, misinterpreted and mis-erased in human cancers. *Nat. Rev. Cancer* **2010**, *10*, 457−469.

(126) Kleer, C. G.; Cao, Q.; Varambally, S.; Shen, R.; Ota, I.; Tomlins, S. A.; Ghosh, D.; Sewalt, R. G.; Otte, A. P.; Hayes, D. F.; Sabel, M. S.; Livant, D.; Weiss, S. J.; Rubin, M. A.; Chinnaiyan, A. M. EZH2 is a marker of aggressive breast cancer and promotes neoplastic transformation of breast epithelial cells. *Proc. Natl. Acad. Sci. U.S.A.* **2003**, *100*, 11606−11611.

(127) Varambally, S.; Dhanasekaran, S. M.; Zhou, M.; Barrette, T. R.; Kumar-Sinha, C.; Sanda, M. G.; Ghosh, D.; Pienta, K. J.; Sewalt, R. G.; Otte, A. P.; Rubin, M. A.; Chinnaiyan, A. M. The polycomb group protein EZH2 is involved in progression of prostate cancer. *Nature* **2002**, *419*, 624−629.

(128) Velichutina, I.; Shaknovich, R.; Geng, H.; Johnson, N. A.; Gascoyne, R. D.; Melnick, A. M.; Elemento, O. EZH2-mediated epigenetic silencing in germinal center B cells contributes to proliferation and lymphomagenesis. *Blood* **2010**, *116*, 5247−5255.

(129) Shih, A. H.; Abdel-Wahab, O.; Patel, J. P.; Levine, R. L. The role of mutations in epigenetic regulators in myeloid malignancies. *Nat. Rev. Cancer* **2012**, *12*, 599−612.

(130) Knutson, S. K.; Wigle, T. J.; Warholic, N. M.; Sneeringer, C. J.; Allain, C. J.; Klaus, C. R.; Sacks, J. D.; Raimondi, A.; Majer, C. R.; Song, J.; Scott, M. P.; Jin, L.; Smith, J. J.; Olhava, E. J.; Chesworth, R.; Moyer, M. P.; Richon, V. M.; Copeland, R. A.; Keilhack, H.; Pollock, R. M.; Kuntz, K. W. A selective inhibitor of EZH2 blocks H3K27 methylation and kills mutant lymphoma cells. *Nat. Chem. Biol.* **2012**, *8*, 890−896.

(131) Richon, V. M.; Johnston, D.; Sneeringer, C. J.; Jin, L.; Majer, C. R.; Elliston, K.; Jerva, L. F.; Scott, M. P.; Copeland, R. A. Chemogenetic analysis of human protein methyltransferases. *Chem. Biol. Drug Des* **2011**, *78*, 199−210.

(132) Yonetani, T.; Theorell, H. Studies on liver alcohol hydrogenase complexes. 3. Multiple inhibition kinetics in the presence of two competitive inhibitors. *Arch. Biochem. Biophys.* **1964**, *106*, 243−251.

(133) McCabe, M. T.; Ott, H. M.; Ganji, G.; Korenchuk, S.; Thompson, C.; Van Aller, G. S.; Liu, Y.; Graves, A. P.; Iii, A. D.; Diaz, E.; Lafrance, L. V.; Mellinger, M.; Duquenne, C.; Tian, X.; Kruger, R. G.; McHugh, C. F.; Brandt, M.; Miller, W. H.; Dhanak, D.; Verma, S. K.; Tummino, P. J.; Creasy, C. L. EZH2 inhibition as a therapeutic strategy for lymphoma with EZH2-activating mutations. *Nature* **2012**, *492*, 108−112.

(134) Diaz, E.; Machutta, C. A.; Chen, S.; Jiang, Y.; Nixon, C.; Hofmann, G.; Key, D.; Sweitzer, S.; Patel, M.; Wu, Z.; Creasy, C. L.; Kruger, R. G.; LaFrance, L.; Verma, S.; Pappalardi, M. B.; Le, B.; Van Aller, G. S.; McCabe, M. T.; Tummino, P. J.; Pope, A. J.; Thrall, S. H.; Schwartz, B.; Brandt, M. Development and validation of reagents and assays for EZH2 peptide and nucleosome high-throughput screens. *J. Biomol. Screening* **2012**, *17*, 1279−1292.

(135) Beguelin, W.; Popovic, R.; Teater, M.; Jiang, Y.; Bunting, K. L.; Rosen, M.; Shen, H.; Yang, S. N.; Wang, L.; Ezponda, T.; Martinez-Garcia, E.; Zhang, H.; Zheng, Y.; Verma, S. K.; McCabe, M. T.; Ott, H. M.; Van Aller, G. S.; Kruger, R. G.; Liu, Y.; McHugh, C. F.; Scott, D. W.; Chung, Y. R.; Kelleher, N.; Shaknovich, R.; Creasy, C. L.; Gascoyne, R. D.; Wong, K. K.; Cerchietti, L.; Levine, R. L.; Abdel-Wahab, O.; Licht, J. D.; Elemento, O.; Melnick, A. M. EZH2 is required for germinal center formation and somatic EZH2 mutations promote lymphoid transformation. *Cancer Cell* **2013**, *23*, 677−692.

(136) *A study to investigate the safety, pharmacokinetics, pharmacodynamics and clinical activity of GSK2816126 in subjects with relapsed/refractory diffuse large B cell and transformed follicular lymphoma*; http://clinicaltrials.gov/ct2/show/NCT02082977?term=NCT02082977&=1.

(137) Qi, W.; Chan, H.; Teng, L.; Li, L.; Chuai, S.; Zhang, R.; Zeng, J.; Li, M.; Fan, H.; Lin, Y.; Gu, J.; Ardayfio, O.; Zhang, J.-H.; Yan, X.; Fang, J.; Mi, Y.; Zhang, M.; Zhou, T.; Feng, G.; Chen, Z.; Li, G.; Yang, T.; Zhao, K.; Liu, X.; Yu, Z.; Lu, C. X.; Atadja, P.; Li, E. Selective inhibition of Ezh2 by a small molecule inhibitor blocks tumor cells proliferation. *Proc. Natl. Acad. Sci. U.S.A.* **2012**, *109*, 21360−21365.

(138) Konze, K. D.; Ma, A.; Li, F.; Barsyte-Lovejoy, D.; Parton, T.; MacNevin, C. J.; Liu, F.; Gao, C.; Huang, X. P.; Kuznetsova, E.; Rougie, M.; Jiang, A.; Pattenden, S. G.; Norris, J. L.; James, L. I.; Roth, B. L.; Brown, P. J.; Frye, S. V.; Arrowsmith, C. H.; Hahn, K. M.; Wang, G. G.; Vedadi, M.; Jin, J. An orally bioavailable chemical probe of the lysine methyltransferases EZH2 and EZH1. *ACS Chem. Biol.* **2013**, *8*, 1324−1334.

(139) Knutson, S. K.; Warholic, N. M.; Wigle, T. J.; Klaus, C. R.; Allain, C. J.; Raimondi, A.; Porter Scott, M.; Chesworth, R.; Moyer, M. P.; Copeland, R. A.; Richon, V. M.; Pollock, R. M.; Kuntz, K. W.; Keilhack, H. Durable tumor regression in genetically altered malignant rhabdoid tumors by inhibition of methyltransferase EZH2. *Proc. Natl. Acad. Sci. U.S.A.* **2013**, *110*, 7922−7927.

(140) Wilson, B. G.; Roberts, C. W. SWI/SNF nucleosome remodellers and cancer. *Nat. Rev. Cancer* **2011**, *11*, 481−492.

(141) Wilson, B. G.; Wang, X.; Shen, X.; McKenna, E. S.; Lemieux, M. E.; Cho, Y. J.; Koellhoffer, E. C.; Pomeroy, S. L.; Orkin, S. H.; Roberts, C. W. Epigenetic antagonism between polycomb and SWI/SNF complexes during oncogenic transformation. *Cancer Cell* **2010**, *18*, 316−328.

(142) *Study of E7438 (EZH2 histone methyl transferase [HMT] inhibitor) as a single agent in subjects with advanced solid tumors or with B cell lymphomas*; http://clinicaltrials.gov/ct2/show/NCT01897571?term=NCT01897571&=1.

(143) Garapaty-Rao, S.; Nasveschuk, C.; Gagnon, A.; Chan, E. Y.; Sandy, P.; Busby, J.; Balasubramanian, S.; Campbell, R.; Zhao, F.; Bergeron, L.; Audia, J. E.; Albrecht, B. K.; Harmange, J. C.; Cummings, R.; Trojer, P. Identification of EZH2 and EZH1 small molecule inhibitors with selective impact on diffuse large B cell lymphoma cell growth. *Chem. Biol.* **2013**, *20*, 1329−1339.

(144) Nasveschuk, C. G.; Gagnon, A.; Garapaty-Rao, S.; Balasubramanian, S.; Campbell, R.; Lee, C.; Zhao, F.; Bergeron, L.;

Cummings, R.; Trojer, P.; Audia, J. E.; Albrecht, B. K.; Harmange, J. C. Discovery and optimization of tetramethylpiperidinyl benzamides as inhibitors of EZH2. *ACS Med. Chem. Lett.* **2014**, *5*, 378−383.
(145) Ruthenburg, A. J.; Allis, C. D.; Wysocka, J. Methylation of lysine 4 on histone H3: intricacy of writing and reading a single epigenetic mark. *Mol. Cell* **2007**, *25*, 15−30.
(146) Brown, M. A.; Sims, R. J., III; Gottlieb, P. D.; Tucker, P. W. Identification and characterization of Smyd2: a split SET/MYND domain-containing histone H3 lysine 36-specific methyltransferase that interacts with the Sin3 histone deacetylase complex. *Mol. Cancer* **2006**, *5*, 26.
(147) Dillon, S. C.; Zhang, X.; Trievel, R. C.; Cheng, X. The SET-domain protein superfamily: protein lysine methyltransferases. *Genome Biol.* **2005**, *6*, 227.
(148) Avdic, V.; Zhang, P.; Lanouette, S.; Groulx, A.; Tremblay, V.; Brunzelle, J.; Couture, J. F. Structural and biochemical insights into MLL1 core complex assembly. *Structure* **2011**, *19*, 101−108.
(149) Krivtsov, A. V.; Armstrong, S. A. MLL translocations, histone modifications and leukaemia stem-cell development. *Nat. Rev. Cancer* **2007**, *7*, 823−833.
(150) Albert, M.; Helin, K. Histone methyltransferases in cancer. *Semin. Cell Dev. Biol.* **2010**, *21*, 209−220.
(151) Kohlmann, A.; Schoch, C.; Dugas, M.; Schnittger, S.; Hiddemann, W.; Kern, W.; Haferlach, T. New insights into MLL gene rearranged acute leukemias using gene expression profiling: shared pathways, lineage commitment, and partner genes. *Leukemia* **2005**, *19*, 953−964.
(152) Hess, J. L. MLL: a histone methyltransferase disrupted in leukemia. *Trends Mol. Med.* **2004**, *10*, 500−507.
(153) Yu, B. D.; Hess, J. L.; Horning, S. E.; Brown, G. A.; Korsmeyer, S. J. Altered Hox expression and segmental identity in Mll-mutant mice. *Nature* **1995**, *378*, 505−508.
(154) Karatas, H.; Townsend, E. C.; Cao, F.; Chen, Y.; Bernard, D.; Liu, L.; Lei, M.; Dou, Y.; Wang, S. High-affinity, small-molecule peptidomimetic inhibitors of MLL1/WDR5 protein−protein interaction. *J. Am. Chem. Soc.* **2013**, *135*, 669−682.
(155) Senisterra, G.; Wu, H.; Allali-Hassani, A.; Wasney, G. A.; Barsyte-Lovejoy, D.; Dombrovski, L.; Dong, A.; Nguyen, K. T.; Smil, D.; Bolshan, Y.; Hajian, T.; He, H.; Seitova, A.; Chau, I.; Li, F.; Poda, G.; Couture, J. F.; Brown, P. J.; Al-Awar, R.; Schapira, M.; Arrowsmith, C. H.; Vedadi, M. Small-molecule inhibition of MLL activity by disruption of its interaction with WDR5. *Biochem. J.* **2013**, *449*, 151−159.
(156) Pradhan, S.; Chin, H. G.; Esteve, P. O.; Jacobsen, S. E. SET7/9 mediated methylation of non-histone proteins in mammalian cells. *Epigenetics* **2009**, *4*, 383−387.
(157) Siebel, A. L.; Fernandez, A. Z.; El-Osta, A. Glycemic memory associated epigenetic changes. *Biochem. Pharmacol.* **2010**, *80*, 1853−1859.
(158) Barsyte-Lovejoy, D.; Li, F.; Oudhoff, M. J.; Tatlock, J. H.; Dong, A.; Zeng, H.; Wu, H.; Freeman, S. A.; Schapira, M.; Senisterra, G. A.; Kuznetsova, E.; Marcellus, R.; Allali-Hassani, A.; Kennedy, S.; Lambert, J. P.; Couzens, A. L.; Aman, A.; Gingras, A. C.; Al-Awar, R.; Fish, P. V.; Gerstenberger, B. S.; Roberts, L.; Benn, C. L.; Grimley, R. L.; Braam, M. J.; Rossi, F. M.; Sudol, M.; Brown, P. J.; Bunnage, M. E.; Owen, D. R.; Zaph, C.; Vedadi, M.; Arrowsmith, C. H. (*R*)-PFI-2 is a potent and selective inhibitor of SETD7 methyltransferase activity in cells. *Proc. Natl. Acad. Sci. U.S.A.* **2014**, *111*, 12853−12858.
(159) Gottlieb, P. D.; Pierce, S. A.; Sims, R. J.; Yamagishi, H.; Weihe, E. K.; Harriss, J. V.; Maika, S. D.; Kuziel, W. A.; King, H. L.; Olson, E. N.; Nakagawa, O.; Srivastava, D. Bop encodes a muscle-restricted protein containing MYND and SET domains and is essential for cardiac differentiation and morphogenesis. *Nat. Genet.* **2002**, *31*, 25−32.
(160) Hamamoto, R.; Furukawa, Y.; Morita, M.; Iimura, Y.; Silva, F. P.; Li, M.; Yagyu, R.; Nakamura, Y. SMYD3 encodes a histone methyltransferase involved in the proliferation of cancer cells. *Nat. Cell Biol.* **2004**, *6*, 731−740.
(161) Hamamoto, R.; Silva, F. P.; Tsuge, M.; Nishidate, T.; Katagiri, T.; Nakamura, Y.; Furukawa, Y. Enhanced SMYD3 expression is essential for the growth of breast cancer cells. *Cancer Sci.* **2006**, *97*, 113−118.
(162) Mazur, P. K.; Reynoird, N.; Khatri, P.; Jansen, P. W. T. C.; Wilkinson, A. W.; Liu, S. C.; Barbash, O.; Van Aller, G. S.; Huddleston, M.; Dhanak, D.; Tummino, P. J.; Kruger, R. G.; Garcia, B. A.; Butte, A. J.; Vermeulen, M.; Sage, J.; Gozani, O. SMYD3 links lysine methylation of MAP3K2 to Ras-driven cancer. *Nature* **2014**, *510*, 283−287.
(163) Abu-Farha, M.; Lambert, J. P.; Al-Madhoun, A. S.; Elisma, F.; Skerjanc, I. S.; Figeys, D. The tale of two domains: proteomics and genomics analysis of SMYD2, a new histone methyltransferase. *Mol. Cell. Proteomics* **2008**, *7*, 560−572.
(164) Huang, J.; Perez-Burgos, L.; Placek, B. J.; Sengupta, R.; Richter, M.; Dorsey, J. A.; Kubicek, S.; Opravil, S.; Jenuwein, T.; Berger, S. L. Repression of p53 activity by Smyd2-mediated methylation. *Nature* **2006**, *444*, 629−632.
(165) Saddic, L. A.; West, L. E.; Aslanian, A.; Yates, J. R., III; Rubin, S. M.; Gozani, O.; Sage, J. Methylation of the retinoblastoma tumor suppressor by SMYD2. *J. Biol. Chem.* **2010**, *285*, 37733−37740.
(166) Sakamoto, L. H.; Andrade, R. V.; Felipe, M. S.; Motoyama, A. B.; Pittella Silva, F. SMYD2 is highly expressed in pediatric acute lymphoblastic leukemia and constitutes a bad prognostic factor. *Leuk. Res.* **2014**, *38*, 496−502.
(167) Komatsu, S.; Imoto, I.; Tsuda, H.; Kozaki, K. I.; Muramatsu, T.; Shimada, Y.; Aiko, S.; Yoshizumi, Y.; Ichikawa, D.; Otsuji, E.; Inazawa, J. Overexpression of SMYD2 relates to tumor cell proliferation and malignant outcome of esophageal squamous cell carcinoma. *Carcinogenesis* **2009**, *30*, 1139−1146.
(168) Ferguson, A. D.; Larsen, N. A.; Howard, T.; Pollard, H.; Green, I.; Grande, C.; Cheung, T.; Garcia-Arenas, R.; Cowen, S.; Wu, J.; Godin, R.; Chen, H.; Keen, N. Structural basis of substrate methylation and inhibition of SMYD2. *Structure* **2011**, *19*, 1262−1273.
(169) *LLY-507: A chemical probe for SMYD2 protein lysine methyltransferase*; http://www.thesgc.org/chemical-probes/LLY-507.
(170) de Almeida, S. F.; Grosso, A. R.; Koch, F.; Fenouil, R.; Carvalho, S.; Andrade, J.; Levezinho, H.; Gut, M.; Eick, D.; Gut, I.; Andrau, J. C.; Ferrier, P.; Carmo-Fonseca, M. Splicing enhances recruitment of methyltransferase HYPB/Setd2 and methylation of histone H3 Lys36. *Nat. Struct. Mol. Biol.* **2011**, *18*, 977−983.
(171) Newbold, R. F.; Mokbel, K. Evidence for a tumour suppressor function of SETD2 in human breast cancer: a new hypothesis. *Anticancer Res.* **2010**, *30*, 3309−3311.
(172) Hu, M.; Sun, X. J.; Zhang, Y. L.; Kuang, Y.; Hu, C. Q.; Wu, W. L.; Shen, S. H.; Du, T. T.; Li, H.; He, F.; Xiao, H. S.; Wang, Z. G.; Liu, T. X.; Lu, H.; Huang, Q. H.; Chen, S. J.; Chen, Z. Histone H3 lysine 36 methyltransferase Hypb/Setd2 is required for embryonic vascular remodeling. *Proc. Natl. Acad. Sci. U.S.A.* **2010**, *107*, 2956−2961.
(173) Zhu, X.; He, F.; Zeng, H.; Ling, S.; Chen, A.; Wang, Y.; Yan, X.; Wei, W.; Pang, Y.; Cheng, H.; Hua, C.; Zhang, Y.; Yang, X.; Lu, X.; Cao, L.; Hao, L.; Dong, L.; Zou, W.; Wu, J.; Li, X.; Zheng, S.; Yan, J.; Zhou, J.; Zhang, L.; Mi, S.; Wang, X.; Zhang, L.; Zou, Y.; Chen, Y.; Geng, Z.; Wang, J.; Zhou, J.; Liu, X.; Wang, J.; Yuan, W.; Huang, G.; Cheng, T.; Wang, Q. F. Identification of functional cooperative mutations of SETD2 in human acute leukemia. *Nat. Genet.* **2014**, *46*, 287−293.
(174) Fontebasso, A. M.; Schwartzentruber, J.; Khuong-Quang, D. A.; Liu, X. Y.; Sturm, D.; Korshunov, A.; Jones, D. T.; Witt, H.; Kool, M.; Albrecht, S.; Fleming, A.; Hadjadj, D.; Busche, S.; Lepage, P.; Montpetit, A.; Staffa, A.; Gerges, N.; Zakrzewska, M.; Zakrzewski, K.; Liberski, P. P.; Hauser, P.; Garami, M.; Klekner, A.; Bognar, L.; Zadeh, G.; Faury, D.; Pfister, S. M.; Jabado, N.; Majewski, J. Mutations in SETD2 and genes affecting histone H3K36 methylation target hemispheric high-grade gliomas. *Acta Neuropathol.* **2013**, *125*, 659−669.
(175) Zheng, W.; Ibáñez, G.; Wu, H.; Blum, G.; Zeng, H.; Dong, A.; Li, F.; Hajian, T.; Allali-Hassani, A.; Amaya, M. F.; Siarheyeva, A.; Yu, W.; Brown, P. J.; Schapira, M.; Vedadi, M.; Min, J.; Luo, M. Sinefungin

derivatives as inhibitors and structure probes of protein lysine methyltransferase SETD2. *J. Am. Chem. Soc.* **2012**, *134*, 18004−18014.
(176) Beck, D. B.; Oda, H.; Shen, S. S.; Reinberg, D. PR-Set7 and H4K20me1: at the crossroads of genome integrity, cell cycle, chromosome condensation, and transcription. *Genes Dev.* **2012**, *26*, 325−337.
(177) Nishioka, K.; Rice, J. C.; Sarma, K.; Erdjument-Bromage, H.; Werner, J.; Wang, Y.; Chuikov, S.; Valenzuela, P.; Tempst, P.; Steward, R.; Lis, J. T.; Allis, C. D.; Reinberg, D. PR-Set7 is a nucleosome-specific methyltransferase that modifies lysine 20 of histone H4 and is associated with silent chromatin. *Mol. Cell* **2002**, *9*, 1201−1213.
(178) Fang, J.; Feng, Q.; Ketel, C. S.; Wang, H.; Cao, R.; Xia, L.; Erdjument-Bromage, H.; Tempst, P.; Simon, J. A.; Zhang, Y. Purification and functional characterization of SET8, a nucleosomal histone H4-lysine 20-specific methyltransferase. *Curr. Biol.* **2002**, *12*, 1086−1099.
(179) Takawa, M.; Cho, H. S.; Hayami, S.; Toyokawa, G.; Kogure, M.; Yamane, Y.; Iwai, Y.; Maejima, K.; Ueda, K.; Masuda, A.; Dohmae, N.; Field, H. I.; Tsunoda, T.; Kobayashi, T.; Akasu, T.; Sugiyama, M.; Ohnuma, S.; Atomi, Y.; Ponder, B. A. J.; Nakamura, Y.; Hamamoto, R. Histone lysine methyltransferase SETD8 promotes carcinogenesis by deregulating PCNA expression. *Cancer Res.* **2012**, *72*, 3217−3227.
(180) Williams, D. E.; Dalisay, D. S.; Li, F.; Amphlett, J.; Maneerat, W.; Chavez, M. A. G.; Wang, Y. A.; Matainaho, T.; Yu, W.; Brown, P. J.; Arrowsmith, C. H.; Vedadi, M.; Andersen, R. J. Nahuoic acid A produced by a *Streptomyces* sp. isolated from a marine sediment is a selective SAM-competitive inhibitor of the histone methyltransferase SETD8. *Org. Lett.* **2013**, *15*, 414−417.
(181) Ma, A.; Yu, W.; Li, F.; Bleich, R. M.; Herold, J. M.; Butler, K. V.; Norris, J. L.; Korboukh, V.; Tripathy, A.; Janzen, W. P.; Arrowsmith, C. H.; Frye, S. V.; Vedadi, M.; Brown, P. J.; Jin, J. Discovery of a selective, substrate-competitive inhibitor of the lysine methyltransferase SETD8. *J. Med. Chem.* **2014**, *57*, 6822−6833.
(182) Ma, A.; Yu, W.; Xiong, Y.; Butler, K. V.; Brown, P. J.; Jin, J. Structure−activity relationship studies of SETD8 inhibitors. *Med. Chem. Comm* **2014**, *5*, 1892−1898.
(183) Blum, G.; Ibanez, G.; Rao, X.; Shum, D.; Radu, C.; Djaballah, H.; Rice, J. C.; Luo, M. Small-molecule inhibitors of SETD8 with cellular activity. *ACS Chem. Biol.* **2014**, *9*, 2471−2478.
(184) Feng, Q.; Wang, H.; Ng, H. H.; Erdjument-Bromage, H.; Tempst, P.; Struhl, K.; Zhang, Y. Methylation of H3-lysine 79 is mediated by a new family of HMTases without a SET domain. *Curr. Biol.* **2002**, *12*, 1052−1058.
(185) Min, J.; Feng, Q.; Li, Z.; Zhang, Y.; Xu, R. M. Structure of the catalytic domain of human DOT1L, a non-SET domain nucleosomal histone methyltransferase. *Cell* **2003**, *112*, 711−723.
(186) Schubert, H. L.; Blumenthal, R. M.; Cheng, X. D. Many paths to methyltransfer: a chronicle of convergence. *Trends Biochem. Sci.* **2003**, *28*, 329−335.
(187) Frederiks, F.; Tzouros, M.; Oudgenoeg, G.; van Welsem, T.; Fornerod, M.; Krijgsveld, J.; van Leeuwen, F. Nonprocessive methylation by Dot1 leads to functional redundancy of histone H3K79 methylation states. *Nat. Struct. Mol. Biol.* **2008**, *15*, 550−557.
(188) Nguyen, A. T.; Zhang, Y. The diverse functions of Dot1 and H3K79 methylation. *Genes Dev.* **2011**, *25*, 1345−1358.
(189) Nguyen, A. T.; He, J.; Taranova, O.; Zhang, Y. Essential role of DOT1L in maintaining normal adult hematopoiesis. *Cell Res.* **2011**, *21*, 1370−1373.
(190) Nguyen, A. T.; Xiao, B.; Neppl, R. L.; Kallin, E. M.; Li, J. A.; Chen, T. P.; Wang, D. Z.; Xiao, X. A.; Zhang, Y. DOT1L regulates dystrophin expression and is critical for cardiac function. *Genes Dev.* **2011**, *25*, 263−274.
(191) Nguyen, A. T.; Taranova, O.; He, J.; Zhang, Y. DOT1L, the H3K79 methyltransferase, is required for MLL-AF9-mediated leukemogenesis. *Blood* **2011**, *117*, 6912−6922.
(192) Bitoun, E.; Oliver, P. L.; Davies, K. E. The mixed-lineage leukemia fusion partner AF4 stimulates RNA polymerase II transcriptional elongation and mediates coordinated chromatin remodeling. *Hum. Mol. Genet.* **2007**, *16*, 92−106.
(193) Mueller, D.; Bach, C.; Zeisig, D.; Garcia-Cuellar, M. P.; Monroe, S.; Sreekumar, A.; Zhou, R.; Nesvizhskii, A.; Chinnaiyan, A.; Hess, J. L.; Slany, R. K. A role for the MLL fusion partner ENL in transcriptional elongation and chromatin modification. *Blood* **2007**, *110*, 4445−4454.
(194) Yokoyama, A.; Lin, M.; Naresh, A.; Kitabayashi, I.; Cleary, M. L. A higher-order complex containing AF4 and ENL family proteins with P-TEFb facilitates oncogenic and physiologic MLL-dependent transcription. *Cancer Cell* **2010**, *17*, 198−212.
(195) Biswas, D.; Milne, T. A.; Basrur, V.; Kim, J.; Elenitoba-Johnson, K. S. J.; Allis, C. D.; Roeder, R. G. Function of leukemogenic mixed lineage leukemia 1 (MLL) fusion proteins through distinct partner protein complexes. *Proc. Natl. Acad. Sci. U.S.A.* **2011**, *108*, 15751−15756.
(196) Anglin, J. L.; Song, Y. A medicinal chemistry perspective for targeting histone H3 lysine-79 methyltransferase DOT1L. *J. Med. Chem.* **2013**, *56*, 8972−8983.
(197) Daigle, S. R.; Olhava, E. J.; Therkelsen, C. A.; Majer, C. R.; Sneeringer, C. J.; Song, J.; Johnston, L. D.; Scott, M. P.; Smith, J. J.; Xiao, Y.; Jin, L.; Kuntz, K. W.; Chesworth, R.; Moyer, M. P.; Bernt, K. M.; Tseng, J. C.; Kung, A. L.; Armstrong, S. A.; Copeland, R. A.; Richon, V. M.; Pollock, R. M. Selective killing of mixed lineage leukemia cells by a potent small-molecule DOT1L inhibitor. *Cancer Cell* **2011**, *20*, 53−65.
(198) Basavapathruni, A.; Jin, L.; Daigle, S. R.; Majer, C. R.; Therkelsen, C. A.; Wigle, T. J.; Kuntz, K. W.; Chesworth, R.; Pollock, R. M.; Scott, M. P.; Moyer, M. P.; Richon, V. M.; Copeland, R. A.; Olhava, E. J. Conformational adaptation drives potent, selective and durable inhibition of the human protein methyltransferase DOT1L. *Chem. Biol. Drug Des.* **2012**, *80*, 971−980.
(199) Yu, W.; Chory, E. J.; Wernimont, A. K.; Tempel, W.; Scopton, A.; Federation, A.; Marineau, J. J.; Qi, J.; Barsyte-Lovejoy, D.; Yi, J.; Marcellus, R.; Iacob, R. E.; Engen, J. R.; Griffin, C.; Aman, A.; Wienholds, E.; Li, F.; Pineda, J.; Estiu, G.; Shatseva, T.; Hajian, T.; Al-awar, R.; Dick, J. E.; Vedadi, M.; Brown, P. J.; Arrowsmith, C. H.; Bradner, J. E.; Schapira, M. Catalytic site remodelling of the DOT1L methyltransferase by selective inhibitors. *Nat. Commun.* **2012**, *3*, 1288.
(200) Bernt, K. M.; Zhu, N.; Sinha, A. U.; Vempati, S.; Faber, J.; Krivtsov, A. V.; Feng, Z. H.; Punt, N.; Daigle, A.; Bullinger, L.; Pollock, R. M.; Richon, V. M.; Kung, A. L.; Armstrong, S. A. MLL-rearranged leukemia is dependent on aberrant H3K79 methylation by DOT1L. *Cancer Cell* **2011**, *20*, 66−78.
(201) Yao, Y.; Chen, P.; Diao, J.; Cheng, G.; Deng, L.; Anglin, J. L.; Prasad, B. V. V; Song, Y. Selective inhibitors of histone methyltransferase DOT1L: design, synthesis and crystallographic studies. *J. Am. Chem. Soc.* **2011**, *133*, 16746−16749.
(202) Anglin, J. L.; Deng, L.; Yao, Y.; Cai, G.; Liu, Z.; Jiang, H.; Cheng, G.; Chen, P.; Dong, S.; Song, Y. Synthesis and structure−activity relationship investigation of adenosine-containing inhibitors of histone methyltransferase DOT1L. *J. Med. Chem.* **2012**, *55*, 8066−8074.
(203) Daigle, S. R.; Olhava, E. J.; Therkelsen, C. A.; Basavapathruni, A.; Jin, L.; Boriack-Sjodin, P. A.; Allain, C. J.; Klaus, C. R.; Raimondi, A.; Scott, M. P.; Waters, N. J.; Chesworth, R.; Moyer, M. P.; Copeland, R. A.; Richon, V. M.; Pollock, R. M. Potent inhibition of DOT1L as treatment of MLL-fusion leukemia. *Blood* **2013**, *122*, 1017−1025.
(204) Chen, L.; Deshpande, A. J.; Banka, D.; Bernt, K. M.; Dias, S.; Buske, C.; Olhava, E. J.; Daigle, S. R.; Richon, V. M.; Pollock, R. M.; Armstrong, S. A. Abrogation of MLL-AF10 and CALM-AF10-mediated transformation through genetic inactivation or pharmacological inhibition of the H3K79 methyltransferase Dot1l. *Leukemia* **2013**, *27*, 813−822.
(205) Deshpande, A. J.; Chen, L.; Fazio, M.; Sinha, A. U.; Bernt, K. M.; Banka, D.; Dias, S.; Chang, J.; Olhava, E. J.; Daigle, S. R.; Richon, V. M.; Pollock, R. M.; Armstrong, S. A. Leukemic transformation by the MLL−AF6 fusion oncogene requires the H3K79 methyltransferase Dot1l. *Blood* **2013**, *121*, 2533−2541.

(206) *Dose escalation study of EPZ-5676 in pediatric patients with leukemias bearing a rearrangement of the MLL gene*; http://clinicaltrials.gov/ct2/show/NCT02141828?term=NCT02141828&=1.
(207) *A first-in-human phase 1 and expanded cohort study of EPZ-5676 in advanced hematologic malignancies, including acute leukemia with rearrangement of the MLL gene*; http://clinicaltrials.gov/ct2/show/NCT01684150?term=NCT01684150&=1.
(208) Bedford, M. T.; Clarke, S. G. Protein arginine methylation in mammals: who, what, and why. *Mol. Cell* **2009**, *33*, 1−13.
(209) Najbauer, J.; Johnson, B. A.; Young, A. L.; Aswad, D. W. Peptides with sequences similar to glycine, arginine-rich motifs in proteins interacting with RNA are efficiently recognized by methyltransferase(s) modifying arginine in numerous proteins. *J. Biol. Chem.* **1993**, *268*, 10501−10509.
(210) Boffa, L. C.; Karn, J.; Vidali, G.; Allfrey, V. G. Distribution of N^G,N^G-dimethylarginine in nuclear protein fractions. *Biochem. Biophys. Res. Commun.* **1977**, *74*, 969−976.
(211) Hughes, R. M.; Waters, M. L. Arginine methylation in a beta-hairpin peptide: implications for Arg−π interactions, ΔC_p°, and the cold denatured state. *J. Am. Chem. Soc.* **2006**, *128*, 12735−12742.
(212) Bedford, M. T.; Richard, S. Arginine methylation an emerging regulator of protein function. *Mol. Cell* **2005**, *18*, 263−272.
(213) Yang, Y.; Bedford, M. T. Protein arginine methyltransferases and cancer. *Nat. Rev. Cancer* **2013**, *13*, 37−50.
(214) Zhang, X.; Zhou, L.; Cheng, X. Crystal structure of the conserved core of protein arginine methyltransferase PRMT3. *EMBO J.* **2000**, *19*, 3509−3519.
(215) Zhang, X.; Cheng, X. Structure of the predominant protein arginine methyltransferase PRMT1 and analysis of its binding to substrate peptides. *Structure* **2003**, *11*, 509−520.
(216) Lee, J.; Bedford, M. T. PABP1 identified as an arginine methyltransferase substrate using high-density protein arrays. *EMBO Rep.* **2002**, *3*, 268−273.
(217) Cheng, D.; Cote, J.; Shaaban, S.; Bedford, M. T. The arginine methyltransferase CARM1 regulates the coupling of transcription and mRNA processing. *Mol. Cell* **2007**, *25*, 71−83.
(218) Branscombe, T. L.; Frankel, A.; Lee, J. H.; Cook, J. R.; Yang, Z.; Pestka, S.; Clarke, S. PRMT5 (Janus kinase-binding protein 1) catalyzes the formation of symmetric dimethylarginine residues in proteins. *J. Biol. Chem.* **2001**, *276*, 32971−32976.
(219) Jansson, M.; Durant, S. T.; Cho, E. C.; Sheahan, S.; Edelmann, M.; Kessler, B.; La Thangue, N. B. Arginine methylation regulates the p53 response. *Nat. Cell Biol.* **2008**, *10*, 1431−1439.
(220) Lin, W. J.; Gary, J. D.; Yang, M. C.; Clarke, S.; Herschman, H. R. The mammalian immediate-early TIS21 protein and the leukemia-associated BTG1 protein interact with a protein-arginine N-methyltransferase. *J. Biol. Chem.* **1996**, *271*, 15034−15044.
(221) Tang, J.; Frankel, A.; Cook, R. J.; Kim, S.; Paik, W. K.; Williams, K. R.; Clarke, S.; Herschman, H. R. PRMT1 is the predominant type I protein arginine methyltransferase in mammalian cells. *J. Biol. Chem.* **2000**, *275*, 7723−7730.
(222) Wang, H.; Huang, Z. Q.; Xia, L.; Feng, Q.; Erdjument-Bromage, H.; Strahl, B. D.; Briggs, S. D.; Allis, C. D.; Wong, J.; Tempst, P.; Zhang, Y. Methylation of histone H4 at arginine 3 facilitating transcriptional activation by nuclear hormone receptor. *Science* **2001**, *293*, 853−857.
(223) Strahl, B. D.; Briggs, S. D.; Brame, C. J.; Caldwell, J. A.; Koh, S. S.; Ma, H.; Cook, R. G.; Shabanowitz, J.; Hunt, D. F.; Stallcup, M. R.; Allis, C. D. Methylation of histone H4 at arginine 3 occurs in vivo and is mediated by the nuclear receptor coactivator PRMT1. *Curr. Biol.* **2001**, *11*, 996−1000.
(224) Goulet, I.; Gauvin, G.; Boisvenue, S.; Cote, J. Alternative splicing yields protein arginine methyltransferase 1 isoforms with distinct activity, substrate specificity, and subcellular localization. *J. Biol. Chem.* **2007**, *282*, 33009−33021.
(225) Baldwin, R. M.; Morettin, A.; Paris, G.; Goulet, I.; Cote, J. Alternatively spliced protein arginine methyltransferase 1 isoform PRMT1v2 promotes the survival and invasiveness of breast cancer cells. *Cell Cycle* **2012**, *11*, 4597−4612.
(226) Seligson, D. B.; Horvath, S.; Shi, T.; Yu, H.; Tze, S.; Grunstein, M.; Kurdistani, S. K. Global histone modification patterns predict risk of prostate cancer recurrence. *Nature* **2005**, *435*, 1262−1266.
(227) Teyssier, C.; Le Romancer, M.; Sentis, S.; Jalaguier, S.; Corbo, L.; Cavailles, V. Protein arginine methylation in estrogen signaling and estrogen-related cancers. *Trends Endocrinol. Metab.* **2010**, *21*, 181−189.
(228) Le Romancer, M.; Treilleux, I.; Bouchekioua-Bouzaghou, K.; Sentis, S.; Corbo, L. Methylation, a key step for nongenomic estrogen signaling in breast tumors. *Steroids* **2010**, *75*, 560−564.
(229) Cheung, N.; Chan, L. C.; Thompson, A.; Cleary, M. L.; So, C. W. Protein arginine-methyltransferase-dependent oncogenesis. *Nat. Cell Biol.* **2007**, *9*, 1208−1215.
(230) Shia, W. J.; Okumura, A. J.; Yan, M.; Sarkeshik, A.; Lo, M. C.; Matsuura, S.; Komeno, Y.; Zhao, X.; Nimer, S. D.; Yates, J. R., III; Zhang, D. E. PRMT1 interacts with AML1-ETO to promote its transcriptional activation and progenitor cell proliferative potential. *Blood* **2012**, *119*, 4953−4962.
(231) Yoshimatsu, M.; Toyokawa, G.; Hayami, S.; Unoki, M.; Tsunoda, T.; Field, H. I.; Kelly, J. D.; Neal, D. E.; Maehara, Y.; Ponder, B. A.; Nakamura, Y.; Hamamoto, R. Dysregulation of PRMT1 and PRMT6, Type I arginine methyltransferases, is involved in various types of human cancers. *Int. J. Cancer* **2011**, *128*, 562−573.
(232) Mathioudaki, K.; Papadokostopoulou, A.; Scorilas, A.; Xynopoulos, D.; Agnanti, N.; Talieri, M. The PRMT1 gene expression pattern in colon cancer. *Br. J. Cancer* **2008**, *99*, 2094−2099.
(233) Mathioudaki, K.; Scorilas, A.; Ardavanis, A.; Lymberi, P.; Tsiambas, E.; Devetzi, M.; Apostolaki, A.; Talieri, M. Clinical evaluation of PRMT1 gene expression in breast cancer. *Tumour Biol.* **2011**, *32*, 575−582.
(234) Papadokostopoulou, A.; Mathioudaki, K.; Scorilas, A.; Xynopoulos, D.; Ardavanis, A.; Kouroumalis, E.; Talieri, M. Colon cancer and protein arginine methyltransferase 1 gene expression. *Anticancer Res.* **2009**, *29*, 1361−1366.
(235) Wang, S.; Tan, X.; Yang, B.; Yin, B.; Yuan, J.; Qiang, B.; Peng, X. The role of protein arginine-methyltransferase 1 in gliomagenesis. *BMB Rep.* **2012**, *45*, 470−475.
(236) Mitchell, T. R.; Glenfield, K.; Jeyanthan, K.; Zhu, X. D. Arginine methylation regulates telomere length and stability. *Mol. Cell. Biol.* **2009**, *29*, 4918−4934.
(237) Sakamaki, J.; Daitoku, H.; Ueno, K.; Hagiwara, A.; Yamagata, K.; Fukamizu, A. Arginine methylation of BCL-2 antagonist of cell death (BAD) counteracts its phosphorylation and inactivation by Akt. *Proc. Natl. Acad. Sci. U.S.A.* **2011**, *108*, 6085−6090.
(238) Yamagata, K.; Daitoku, H.; Takahashi, Y.; Namiki, K.; Hisatake, K.; Kako, K.; Mukai, H.; Kasuya, Y.; Fukamizu, A. Arginine methylation of FOXO transcription factors inhibits their phosphorylation by Akt. *Mol. Cell* **2008**, *32*, 221−231.
(239) Yu, Z.; Vogel, G.; Coulombe, Y.; Dubeau, D.; Spehalski, E.; Hebert, J.; Ferguson, D. O.; Masson, J. Y.; Richard, S. The MRE11 GAR motif regulates DNA double-strand break processing and ATR activation. *Cell Res.* **2012**, *22*, 305−320.
(240) Boisvert, F. M.; Rhie, A.; Richard, S.; Doherty, A. J. The GAR motif of 53BP1 is arginine methylated by PRMT1 and is necessary for 53BP1 DNA binding activity. *Cell Cycle* **2005**, *4*, 1834−1841.
(241) Butler, J. S.; Zurita-Lopez, C. I.; Clarke, S. G.; Bedford, M. T.; Dent, S. Y. Protein-arginine methyltransferase 1 (PRMT1) methylates Ash2L, a shared component of mammalian histone H3K4 methyltransferase complexes. *J. Biol. Chem.* **2011**, *286*, 12234−12244.
(242) Guendel, I.; Carpio, L.; Pedati, C.; Schwartz, A.; Teal, C.; Kashanchi, F.; Kehn-Hall, K. Methylation of the tumor suppressor protein, BRCA1, influences its transcriptional cofactor function. *PLoS One* **2010**, *5*, e11379.
(243) Cheng, D.; Yadav, N.; King, R. W.; Swanson, M. S.; Weinstein, E. J.; Bedford, M. T. Small molecule regulators of protein arginine methyltransferases. *J. Biol. Chem.* **2004**, *279*, 23892−23899.
(244) Ragno, R.; Simeoni, S.; Castellano, S.; Vicidomini, C.; Mai, A.; Caroli, A.; Tramontano, A.; Bonaccini, C.; Trojer, P.; Bauer, I.; Brosch, G.; Sbardella, G. Small molecule inhibitors of histone arginine methyltransferases: homology modeling, molecular docking, binding

mode analysis, and biological evaluations. *J. Med. Chem.* **2007**, *50*, 1241−1253.
(245) Sams-Dodd, F. Target-based drug discovery: is something wrong? *Drug Discovery Today* **2005**, *10*, 139−147.
(246) Spannhoff, A.; Heinke, R.; Bauer, I.; Trojer, P.; Metzger, E.; Gust, R.; Schule, R.; Brosch, G.; Sippl, W.; Jung, M. Target-based approach to inhibitors of histone arginine methyltransferases. *J. Med. Chem.* **2007**, *50*, 2319−2325.
(247) Spannhoff, A.; Machmur, R.; Heinke, R.; Trojer, P.; Bauer, I.; Brosch, G.; Schule, R.; Hanefeld, W.; Sippl, W.; Jung, M. A novel arginine methyltransferase inhibitor with cellular activity. *Bioorg. Med. Chem. Lett.* **2007**, *17*, 4150−4153.
(248) Heinke, R.; Spannhoff, A.; Meier, R.; Trojer, P.; Bauer, I.; Jung, M.; Sippl, W. Virtual screening and biological characterization of novel histone arginine methyltransferase PRMT1 inhibitors. *ChemMedChem* **2009**, *4*, 69−77.
(249) Bonham, K.; Hemmers, S.; Lim, Y. H.; Hill, D. M.; Finn, M. G.; Mowen, K. A. Effects of a novel arginine methyltransferase inhibitor on T-helper cell cytokine production. *FEBS J.* **2010**, *277*, 2096−2108.
(250) Feng, Y.; Li, M.; Wang, B.; Zheng, Y. G. Discovery and mechanistic study of a class of protein arginine methylation inhibitors. *J. Med. Chem.* **2010**, *53*, 6028−6039.
(251) Dowden, J.; Pike, R. A.; Parry, R. V.; Hong, W.; Muhsen, U. A.; Ward, S. G. Small molecule inhibitors that discriminate between protein arginine N-methyltransferases PRMT1 and CARM1. *Org. Biomol. Chem.* **2011**, *9*, 7814−7821.
(252) Dillon, M. B. C.; Bachovchin, D. A.; Brown, S. J.; Finn, M. G.; Rosen, H.; Cravatt, B. F.; Mowen, K. A. Novel inhibitors for PRMT1 discovered by high-throughput screening using activity-based fluorescence polarization. *ACS Chem. Biol.* **2012**, *7*, 1198−1204.
(253) Wang, J.; Chen, L.; Sinha, S. H.; Liang, Z.; Chai, H.; Muniyan, S.; Chou, Y. W.; Yang, C.; Yan, L.; Feng, Y.; Kathy, L. K.; Lin, M. F.; Jiang, H.; George Zheng, Y.; Luo, C. Pharmacophore-based virtual screening and biological evaluation of small molecule inhibitors for protein arginine methylation. *J. Med. Chem.* **2012**, *55*, 7978−7987.
(254) Yan, L.; Yan, C.; Qian, K.; Su, H.; Kofsky-Wofford, S. A.; Lee, W. C.; Zhao, X.; Ho, M. C.; Ivanov, I.; Zheng, Y. G. Diamidine compounds for selective inhibition of protein arginine methyltransferase 1. *J. Med. Chem.* **2014**, *57*, 2611−2622.
(255) Tang, J.; Gary, J. D.; Clarke, S.; Herschman, H. R. PRMT 3, a type I protein arginine N-methyltransferase that differs from PRMT1 in its oligomerization, subcellular localization, substrate specificity, and regulation. *J. Biol. Chem.* **1998**, *273*, 16935−16945.
(256) Bachand, F.; Silver, P. A. PRMT3 is a ribosomal protein methyltransferase that affects the cellular levels of ribosomal subunits. *EMBO J.* **2004**, *23*, 2641−2650.
(257) Swiercz, R.; Person, M. D.; Bedford, M. T. Ribosomal protein S2 is a substrate for mammalian PRMT3 (protein arginine methyltransferase 3). *Biochem. J.* **2005**, *386*, 85−91.
(258) Di Lorenzo, A.; Bedford, M. T. Histone arginine methylation. *FEBS Lett.* **2011**, *585*, 2024−2031.
(259) Swiercz, R.; Cheng, D.; Kim, D.; Bedford, M. T. Ribosomal protein rpS2 is hypomethylated in PRMT3-deficient mice. *J. Biol. Chem.* **2007**, *282*, 16917−16923.
(260) Smith, J. J.; Rucknagel, K. P.; Schierhorn, A.; Tang, J.; Nemeth, A.; Linder, M.; Herschman, H. R.; Wahle, E. Unusual sites of arginine methylation in poly(A)-binding protein II and in vitro methylation by protein arginine methyltransferases PRMT1 and PRMT3. *J. Biol. Chem.* **1999**, *274*, 13229−13234.
(261) Fronz, K.; Otto, S.; Kolbel, K.; Kuhn, U.; Friedrich, H.; Schierhorn, A.; Beck-Sickinger, A. G.; Ostareck-Lederer, A.; Wahle, E. Promiscuous modification of the nuclear poly(A)-binding protein by multiple protein-arginine methyltransferases does not affect the aggregation behavior. *J. Biol. Chem.* **2008**, *283*, 20408−20420.
(262) Tavanez, J. P.; Bengoechea, R.; Berciano, M. T.; Lafarga, M.; Carmo-Fonseca, M.; Enguita, F. J. Hsp70 chaperones and type I PRMTs are sequestered at intranuclear inclusions caused by polyalanine expansions in PABPN1. *PLoS One* **2009**, *4*, e6418.
(263) Allali-Hassani, A.; Wasney, G. A.; Siarheyeva, A.; Hajian, T.; Arrowsmith, C. H.; Vedadi, M. Fluorescence-based methods for screening writers and readers of histone methyl marks. *J. Biomol. Screening* **2012**, *17*, 71−84.
(264) Lai, Y.; Song, M.; Hakala, K.; Weintraub, S. T.; Shiio, Y. Proteomic dissection of the von Hippel-Lindau (VHL) interactome. *J. Proteome Res.* **2011**, *10*, 5175−5182.
(265) Singh, V.; Miranda, T. B.; Jiang, W.; Frankel, A.; Roemer, M. E.; Robb, V. A.; Gutmann, D. H.; Herschman, H. R.; Clarke, S.; Newsham, I. F. DAL-1/4.1B tumor suppressor interacts with protein arginine N-methyltransferase 3 (PRMT3) and inhibits its ability to methylate substrates in vitro and in vivo. *Oncogene* **2004**, *23*, 7761−7771.
(266) Takahashi, Y.; Iwai, M.; Kawai, T.; Arakawa, A.; Ito, T.; Sakurai-Yageta, M.; Ito, A.; Goto, A.; Saito, M.; Kasumi, F.; Murakami, Y. Aberrant expression of tumor suppressors CADM1 and 4.1B in invasive lesions of primary breast cancer. *Breast Cancer* **2012**, *19*, 242−252.
(267) Alexiou, G. A.; Markoula, S.; Gogou, P.; Kyritsis, A. P. Genetic and molecular alterations in meningiomas. *Clin. Neurol. Neurosurg.* **2011**, *113*, 261−267.
(268) Heller, G.; Geradts, J.; Ziegler, B.; Newsham, I.; Filipits, M.; Markis-Ritzinger, E. M.; Kandioler, D.; Berger, W.; Stiglbauer, W.; Depisch, D.; Pirker, R.; Zielinski, C. C.; Zochbauer-Muller, S. Downregulation of TSLC1 and DAL-1 expression occurs frequently in breast cancer. *Breast Cancer Res. Treat.* **2007**, *103*, 283−291.
(269) Chen, X.; Niroomand, F.; Liu, Z.; Zankl, A.; Katus, H. A.; Jahn, L.; Tiefenbacher, C. P. Expression of nitric oxide related enzymes in coronary heart disease. *Basic Res. Cardiol.* **2006**, *101*, 346−353.
(270) Miyata, S.; Mori, Y.; Tohyama, M. PRMT3 is essential for dendritic spine maturation in rat hippocampal neurons. *Brain Res.* **2010**, *1352*, 11−20.
(271) Siarheyeva, A.; Senisterra, G.; Allali-Hassani, A.; Dong, A.; Dobrovetsky, E.; Wasney, G. A.; Chau, I.; Marcellus, R.; Hajian, T.; Liu, F.; Korboukh, I.; Smil, D.; Bolshan, Y.; Min, J.; Wu, H.; Zeng, H.; Loppnau, P.; Poda, G.; Griffin, C.; Aman, A.; Brown, P. J.; Jin, J.; Al-awar, R.; Arrowsmith, C. H.; Schapira, M.; Vedadi, M. An allosteric inhibitor of protein arginine methyltransferase 3. *Structure* **2012**, *20*, 1425−1435.
(272) Liu, F.; Li, F.; Ma, A.; Dobrovetsky, E.; Dong, A.; Gao, C.; Korboukh, I.; Liu, J.; Smil, D.; Brown, P. J.; Frye, S. V.; Arrowsmith, C. H.; Schapira, M.; Vedadi, M.; Jin, J. Exploiting an allosteric binding site of PRMT3 yields potent and selective inhibitors. *J. Med. Chem.* **2013**, *56*, 2110−2124.
(273) Chen, D.; Ma, H.; Hong, H.; Koh, S. S.; Huang, S. M.; Schurter, B. T.; Aswad, D. W.; Stallcup, M. R. Regulation of transcription by a protein methyltransferase. *Science* **1999**, *284*, 2174−2177.
(274) Bauer, U. M.; Daujat, S.; Nielsen, S. J.; Nightingale, K.; Kouzarides, T. Methylation at arginine 17 of histone H3 is linked to gene activation. *EMBO Rep.* **2002**, *3*, 39−44.
(275) Yadav, N.; Lee, J.; Kim, J.; Shen, J. J.; Hu, M. C. T.; Aldaz, C. M.; Bedford, M. T. Specific protein methylation defects and gene expression perturbations in coactivator-associated arginine methyltransferase 1-deficient mice. *Proc. Natl. Acad. Sci. U.S.A.* **2003**, *100*, 6464−6468.
(276) Cheng, D. H.; Cote, J.; Shaaban, S.; Bedford, M. T. The arginine methyltransferase CARM1 regulates the coupling of transcription and mRNA processing. *Mol. Cell* **2007**, *25*, 71−83.
(277) El Messaoudi, S.; Fabbrizio, E.; Rodriguez, C.; Chuchana, P.; Fauquier, L.; Cheng, D. H.; Theillet, C.; Vandel, L.; Bedford, M. T.; Sardet, C. Coactivator-associated arginine methyltransferase 1 (CARM1) is a positive regulator of the Cyclin E1 gene. *Proc. Natl. Acad. Sci. U.S.A.* **2006**, *103*, 13351−13356.
(278) Lee, Y. H.; Stallcup, M. R. Roles of protein arginine methylation in DNA damage signaling pathways Is CARM1 a life-or-death decision point? *Cell Cycle* **2011**, *10*, 1343−1344.
(279) Fujiwara, T.; Mori, Y.; Chu, D. L.; Koyama, Y.; Miyata, S.; Tanaka, H.; Yachi, K.; Kubo, T.; Yoshikawa, H.; Tohyama, M. CARM1

regulates proliferation of PC12 cells by methylating HuD. *Mol. Cell. Biol.* **2006**, *26*, 2273−2285.
(280) Li, H. W.; Park, S. M.; Kilburn, B.; Jelinek, M. A.; Henschen-Edman, A.; Aswad, D. W.; Stallcup, M. R.; Laird-Offringa, I. A. Lipopolysaccharide-induced methylation of HuR, an mRNA-stabilizing protein, by CARM1. *J. Biol. Chem.* **2002**, *277*, 44623−44630.
(281) Xu, W.; Chen, H. W.; Du, K. Y.; Asahara, H.; Tini, M.; Emerson, B. M.; Montminy, M.; Evans, R. M. A transcriptional switch mediated by cofactor methylation. *Science* **2001**, *294*, 2507−2511.
(282) Chevillard-Briet, M.; Trouche, D.; Vandel, L. Control of CBP co-activating activity by arginine methylation. *EMBO J.* **2002**, *21*, 5457−5466.
(283) Hong, H.; Kao, C.; Jeng, M. H.; Eble, J. N.; Koch, M. O.; Gardner, T. A.; Zhang, S.; Li, L.; Pan, C. X.; Hu, Z.; MacLennan, G. T.; Cheng, L. Aberrant expression of CARM1, a transcriptional coactivator of androgen receptor, in the development of prostate carcinoma and androgen-independent status. *Cancer* **2004**, *101*, 83−89.
(284) Majumder, S.; Liu, Y.; Ford, O. H., III; Mohler, J. L.; Whang, Y. E. Involvement of arginine methyltransferase CARM1 in androgen receptor function and prostate cancer cell viability. *Prostate* **2006**, *66*, 1292−1301.
(285) Huynh, T.; Chen, Z.; Pang, S. H.; Geng, J. P.; Bandiera, T.; Bindi, S.; Vianello, P.; Roletto, F.; Thieffine, S.; Galvani, A.; Vaccaro, W.; Poss, M. A.; Trainor, G. L.; Lorenzi, M. V.; Gottardis, M.; Jayaraman, L.; Purandare, A. V. Optimization of pyrazole inhibitors of coactivator associated arginine methyltransferase 1 (CARM1). *Bioorg. Med. Chem. Lett.* **2009**, *19*, 2924−2927.
(286) Purandare, A. V.; Chen, Z.; Huynh, T.; Pang, S.; Geng, J.; Vaccaro, W.; Poss, M. A.; Oconnell, J.; Nowak, K.; Jayaraman, L. Pyrazole inhibitors of coactivator associated arginine methyltransferase 1 (CARM1). *Bioorg. Med. Chem. Lett.* **2008**, *18*, 4438−4441.
(287) Wan, H. H.; Huynh, T.; Pang, S. H.; Geng, J. P.; Vaccaro, W.; Poss, M. A.; Trainor, G. L.; Lorenzi, M. V.; Gottardis, M.; Jayaraman, L.; Purandare, A. V. Benzo[*d*]imidazole inhibitors of coactivator associated arginine methyltransferase 1 (CARM1)—hit to lead studies. *Bioorg. Med. Chem. Lett.* **2009**, *19*, 5063−5066.
(288) Therrien, E.; Larouche, G.; Manku, S.; Allan, M.; Nguyen, N.; Styhler, S.; Robert, M. F.; Goulet, A. C.; Besterman, J. M.; Nguyen, H.; Wahhab, A. 1,2-Diamines as inhibitors of co-activator associated arginine methyltransferase 1 (CARM1). *Bioorg. Med. Chem. Lett.* **2009**, *19*, 6725−6732.
(289) Allan, M.; Manku, S.; Therrien, E.; Nguyen, N.; Styhler, S.; Robert, M. F.; Goulet, A. C.; Petschner, A. J.; Rahil, G.; MacLeod, A. R.; Deziel, R.; Besterman, J. M.; Nguyen, H.; Wahhab, A. *N*-Benzyl-1-heteroaryl-3-(trifluoromethyl)-1*H*-pyrazole-5-carboxamides as inhibitors of co-activator associated arginine methyltransferase 1 (CARM1). *Bioorg. Med. Chem. Lett.* **2009**, *19*, 1218−1223.
(290) Selvi, B. R.; Batta, K.; Kishore, A. H.; Mantelingu, K.; Varier, R. A.; Balasubramanyam, K.; Pradhan, S. K.; Dasgupta, D.; Sriram, S.; Agrawal, S.; Kundu, T. K. Identification of a novel inhibitor of coactivator-associated arginine methyltransferase 1 (CARM1)-mediated methylation of histone H3 Arg-17. *J. Biol. Chem.* **2010**, *285*, 7143−7152.